LABORATORY SCALE EVALUATION OF THE FEASIBILITY OF USING GUANIDINIUM SALTS AS A MEANS OF INSITU SOIL STRENGTHENING FOR WEAK CLAYS

A Thesis Submitted to the

College of Graduate and Postdoctoral Studies

In Partial Fulfillment of the Requirements

For the Degree of Master of Science

In the of Department of Civil, Geological, and Environmental Engineering

University of Saskatchewan

Saskatoon

By

Adam Benjamin Leik

Permission to Use

In presenting this thesis/dissertation in partial fulfillment of the requirements for a Postgraduate degree from the University of Saskatchewan, I agree that the Libraries of this University may make it freely available for inspection. I further agree that permission for copying of this thesis/dissertation in any manner, in whole or in part, for scholarly purposes may be granted by the professor or professors who supervised my thesis/dissertation work or, in their absence, by the Head of the Department or the Dean of the College in which my thesis work was done. It is understood that any copying or publication or use of this thesis/dissertation or parts thereof for financial gain shall not be allowed without my written permission. It is also understood that due recognition shall be given to me and to the University of Saskatchewan in any scholarly use which may be made of any material in my thesis/dissertation.

Requests for permission to copy or to make other uses of materials in this thesis/dissertation in whole or part should be addressed to:

Head of the Department of Civil, Geological, and Environmental Engineering
57 Campus Drive
University of Saskatchewan
Saskatoon, Saskatchewan S7N 5A9 Canada

OR

Dean
College of Graduate and Postdoctoral Studies
University of Saskatchewan
116 Thorvaldson Building, 110 Science Place
Saskatoon, Saskatchewan S7N 5C9 Canada

Abstract

Deep-seated, slow moving landslides are widespread throughout the prairie provinces of Canada, especially in Saskatchewan and eastern Alberta. These landslides are characterized by a thick deposit of glacial drift underlain by poorly lithified cretaceous shale (Bearpaw, Lea Park formations). Multiple thin layers of extremely weak, smectite rich, clayey soils are often found within the upper portions of these cretaceous shale formations. The interfaces of these smectitic clay lenses typically produce a pronounced shear plane, turning the overlying soils into a large slump block. Landslides of this nature can span several hundred meters in length, which provides a threat to infrastructure such as roads, bridges, and pipelines.

Due to the depth of these shear zones, and the scale of these types of creeping failures, remediation via traditional geotechnical engineering solutions is either not feasible or extremely costly to pursue. The lack of available solutions for this common problem has prompted research that stems from a multi-disciplinary approach. The current research is intended to evaluate the feasibility of modifying the porewater chemistry of these smectitic shear zones by using guanidinium chloride to propagate mineralogical alteration through ion exchange, as a means of insitu soil strengthening.

This study was limited to laboratory scale testing. The specific objectives for this research were to: i.) characterise the mechanism by which guanidinium salts can alter the mineralogical and macroscopically observable properties of natural expansive clay soils; and, ii.) assess fundamental questions pertaining to the full-scale implementation of the proposed insitu strengthening technique.

A local prairie soil, Regina Clay, was used for the majority of testing procedures, as it is readily available and is representative of the types of soils associated with the problem that this research aimed to address. The results from a series of batch-style geotechnical and mineralogical testing procedures contributed to a clearer understanding of the mechanisms associated with this treatment, the required strengths of saline solution for treatment, quantified the effects of treatment, and the permanence of the effects associated with this treatment.

Treating expansive soils with concentrations of 0.1 molar guanidinium chloride saline solutions were found to cause permanent alterations to the smectite mineral's basal spacing and soil fabric, increase the permeability by half an order of magnitude, and increase the residual shear strength by up to 100%, all without reducing the oedometric stiffness.

As the present study is limited to laboratory-scale trials, a full-scale test site is recommended to further validate the effects found in this research. However, despite the limitations of this work, the potential for insitu soil strengthening via guanidinium salts appears to be significant.

Acknowledgements

Becoming an author of a thesis is an accomplishment I never thought I would claim when I began my post-secondary education as an undergraduate student. There are an insurmountable number of people to thank for helping me reach this point. I would like to take this moment to reflect upon just a few of the amazing people who helped me get here.

Firstly, I would like to thank my academic committee. Your guidance throughout my research program was greatly appreciated. Matt, your knowledge of geochemistry and mineralogy was a great resource to have. Dave, thank you for all the long discussions and critical assessments of my work. I hope that you are aware of just how greatly you have impacted my young career.

Ian, thank you for giving me an opportunity to be a graduate student. Your ability to lead me down a path I didn't know I was on is a skill that all academic supervisors should be jealous of. Every time I left your office, I felt a new fire inside of me to push harder on my academic journey. Your one-liner statements of advice will stick with me for the rest of my life.

Adam Sr., thanks for being a great role model for all of us in the geotechnical lab. Your trust to let me deliver lectures to undergraduate students helped me develop a skill that is hard to practice; impromptu lecturing.

To the lab, you guys truly made my time as a graduate student special. It is rare to get such a large group of cohesive, intelligent, and great people together. I will miss you guys and remember my time as part of the "Dirt Nerds" fondly.

I would like to give a special shoutout to one of my fellow graduate students, Bryce. You were essentially a second supervisor for me. You took notice of my interest in geotechnics when I was a third-year undergraduate student. In all honesty, you were responsible for making me consider graduate school in the first place. You are an unbelievably intelligent individual, a leader among the "Dirt Nerds", and I have no doubt that you will accomplish great things. I am happy to have you as one of my good friends.

To my family, thank you for the support you have given me throughout my life. I am grateful to be surrounded by such wonderful people.

Lastly, I would like to thank my wife, Kelsey. Pursuing a graduate degree is taxing on the student, but perhaps even more of a burden of their partner. Thank you for understanding my complete lack of time awareness. Thank you for listening to me talk about clay every day for 20 months. Thank you for picking me up and dusting me off on a weekly basis. Thank you for affording me the opportunity to go back to school. Thank you for everything. You are the glue that holds me together, I love you.

Table of Contents

Permission to Use i
Abstract ii
Acknowledgements iv
List of Figures ix
List of Tables xii
Chapter 1 Introduction 1
1.1 Background 1
1.2 Research Objectives 2
1.3 Scope 3
1.4 Organization of Thesis 4
Chapter 2 Literature Review 5
2.1 Introduction 5
2.2 Clay Minerals 5
2.3 The Role of Isomorphic Substitution and Cation Exchange Capacity 9
2.4 Clay-Water-Electrolyte Interaction 11
2.4.1 Interlayer Swelling 11
2.4.2 Diffused Double Layer Swelling 14
2.5 Concept of True Effective Stress 18
2.5.1 Measuring Repulsive and Attractive Stresses 21
2.6 Residual Shear Strength 23
2.7 Effect of Ion Species 26
2.8 Previous Research with the Guanidinium Ion in Geotechnics 27
Chapter 3 Methodology 29
3.1 Introduction 29
3.1.1 General Soil Characterization 29
3.1.1 Quantitative X-ray Diffraction (XRD) 30
3.1.2 Cation Exchange Capacity (CEC) 30
3.1.3 Porewater Analysis 32
3.2 Investigating the Mechanism 34
3.2.1 Qualitative XRD 34
3.2.2 Batch Ion Exchange Testing 37
3.2.3 Scanning Electron Microscopy and Environmental Scanning Electron Microscopy 37

3.3 Quantifying the Effects and Assessing Potential Implications of GuCl Treatment 40
3.3.1 Liquid Limit Testing 40
3.3.2 Ring Shear Testing 40
3.3.3 Free Swell Testing 44
3.3.4 Oedometer Testing of Regina Clay 45
3.3.4.1 Assessment of Permeability and Stiffness 45
3.3.4.2 Osmotic Consolidation 45
Chapter 4 Results and Discussion 49
4.1 Introduction 49
4.1.1 General Soil Characterization 49
4.1.2 Porewater Analysis 50
4.1.3 Summary of General Soil Characterisation 50
4.2 Investigating the Mechanism Results 53
4.2.1 Qualitative XRD 53
4.2.2 Batch Ion Exchange 56
4.2.3 SEM and eSEM 60
4.3 Quantifying the Effects and Assessing Potential Implications of GuCl Treatment 65
4.3.1 Liquid Limit Testing and Free Swell Testing 65
4.3.2 Ring Shear Testing 67
4.3.3 Oedometer Testing 72
4.3.3.1 Permeability 72
4.3.3.2 Stiffness 73
4.3.3.3 Osmotic Consolidation 76
4.3.4 Comparing experimental and theoretical changes in R-A stresses for Regina Clay 80
Chapter 5 Conclusion 83
5.1 Study Objectives 83
5.2 Summary of Results from General Soil Characterisation 83
5.3 Summary of Results from Investigating the Mechanism 84
5.4 Summary of Quantified Effects and Assessment of Field-Scale Implications 85
5.5 Future Research 88
References 90
APPENDIX SYNTHETIC POREWATER CONSTITUENTS 96

List of Figures

Figure 2.1: The three building blocks of clay minerals: a.) typical octahedral, b.) the lattice structure of gibbsite and brucite sheets, c.) a typical silica tetrahedral lattice structure. 6
Figure 2.2: a.) The structure of a kaolinite mineral. b.) The structure of an illite mineral. c.) The structure of a montmorillonite mineral. 8
Figure 2.3: Interlayer selectivity feedback loop (Laird, 1996; Laird & Shang, 1997)..... 13
Figure 2.4: The distribution of cations and anions within the DDL as proposed by Gouy-Chapman-Stern theory. Adapted from Mitchell & Soga (2005). 16
Figure 2.5: Conceptual image of the different forces present within a fine-grained soil. 20
Figure 2.6: Three-dimensional constitutive surface for montmorillonite as proposed by Barbour (1987), data taken from Mesri & Olson (1971). 22
Figure 2.7: a.) Chemical formula for guanidinium chloride; b.) the structure of a single guanidinium ion. 28
Figure 3.1: The experimental setup used for CEC testing. 31
Figure 3.2: An example of the blue halo that forms at the end point of a methylene blue spot test. 32
Figure 3.3: The apparatus used to collect porewater samples. Each tube connects to a sample of the same soil. The porewater collected from each tube was combined in a single beaker to create a single porewater sample. 33
Figure 3.4: a.) Depositing a sample onto a 0.45 μm filter via a Millipore apparatus; b.) a sample deposited onto a glass slide; c.) a sample mounted in the XRD sample holder. 36
Figure 3.5: a.) Sputter coated and mounted SEM samples; b.) Hitachi SU8000 SEM device. 38
Figure 3.6: A sample used for eSEM. Note the clearly defined shear plane between the two pieces of clay. 39
Figure 3.7: Work-flow for the different types of ring shear testing. 42
Figure 3.9: The Bromhead Ring Shear Apparatus used for testing. 43
Figure 3.8: a.) The EC probe; and, b.) the peristaltic pump set-up for ring shear testing. 43
Figure 3.10: Experimental setup of all free swell index tests. 44
Figure 3.11: Typical Oedometer used for testing. 46
Figure 3.12: Typical image assessing the volume change due to osmotic consolidation. Adapted from Barbour (1987). 47
Figure 3.13: Workflow for osmotic consolidation testing. 48
Figure 4.1: Grainsize analysis for the four natural soils. 49

Figure 4.2: Piper (trilinear) plot of the insitu porewater ionic compositions. 51
Figure 4.3: Regina Clay XRD traces. 53
Figure 4.4: Whitecourt Clay XRD traces. 55
Figure 4.5: Floral Till XRD traces. 55
Figure 4.6: Battleford Till XRD traces. 56
Figure 4.7: Cationic composition of Regina Clay free porewater with addition of $CaCl_2$. 58
Figure 4.8: Cationic composition of Regina Clay free porewater with addition of NaCl. 58
Figure 4.9: Cationic composition of Regina Clay free porewater with addition of KCl. 59
Figure 4.10: Cationic composition of Regina Clay free porewater with addition of GuCl. 59
Figure 4.11: SEM image of an untreated Regina Clay sample at 6000x magnification. 61
Figure 4.12: SEM image of an 0.1 M treated Regina Clay sample at 6000x magnification. 61
Figure 4.13: eSEM image of the shear plane of an untreated Regina Clay sample at 100x magnification. Note the vertical lineaments (micro striations) in the sample, and the “smooth” surface. 63
Figure 4.14: eSEM image of the shear plane of a 0.1 M treated Regina Clay sample at 100x magnification. Note the “rough” surface with rotund looking particles. 64
Figure 4.15: Liquid limit test results for the four natural soils when GuCl solutions were used as the wetting fluid. Regina Clay was also tested using a KCl solution to compare the effects of KCl to GuCl. 66
Figure 4.16 Residual failure envelopes of Regina Clay determined using DDI water, a synthetic porewater solution, and a 0.1 M GuCl solution. 68
Figure 4.17: Evaluating the permanence of GuCl treatment for Regina Clay with DDI water as the initial wetting fluid. 71
Figure 4.18: Evaluating the permanence of GuCl treatment for Regina Clay with a synthetic porewater solution as the initial wetting fluid. 71
Figure 4.19: The hydraulic conductivity of 0.1 M GuCl treated Regina Clay remains approximately half an order of magnitude larger across load steps to 800 kPa. 72
Figure 4.20: A comparison of oedometric stiffness between untreated and treated Regina Clay samples. 74
Figure 4.21: Semi-log plot of void ratio versus effective stress for RC1 (GuCl introduced at 45 kPa). ... 75
Figure 4.22: Semi-log plot of void ratio versus effective stress for RC2 (GuCl introduced at 100 kPa). .. 75
Figure 4.23: Time versus displacement for RC1: Osmotic consolidation test at 45 kPa mechanical stress. 77
Figure 4.24: Time versus displacement for RC2: Osmotic consolidation test at 100 kPa mechanical stress. 78

Figure 4.25: Time versus displacement for RC3: Osmotic consolidation test at 200 kPa mechanical stress. 78
Figure 4.26: Time versus displacement for RC4: Osmotic consolidation test at 400 kPa mechanical stress. 79
Figure 4.27: Indirect assessment of changes in the R-A stress state for a Regina Clay sample treated with a 0.1 M GuCl solution. 79
Figure 4.28: Comparison of repulsive stresses as predicted from osmotic pressure theory and back analyzed values from the ring shear testing. 81
Figure 5.1: Conceptual image of the insitu soil strengthening technique. 89

List of Tables

Table 2.1: Summary of common clay mineral characteristics 10
Table 4.1: Clay Fraction, Quantitative XRD, CEC, and Exchangeable Sodium Percentage 52
Table 4.2: Insitu Porewater Major Ion Compositions 52
Table 4.3: Insitu Porewater Major Ion Compositions 67
Table 4.4: Stiffness Parameters Obtained from Oedometric Testing 73
Table A.1: Regina Clay Synthetic Porewater Constituents 97
Table A.2: Whitecourt Clay Synthetic Porewater Constituents 97
Table A.3: Floral Till Synthetic Porewater Constituents 98
Table A.4: Battleford Till Synthetic Porewater Constituents 98

Chapter 1 Introduction

1.1 Background

Deep-seated, slow moving landslides are common throughout the prairie provinces of Canada, especially in Saskatchewan and eastern Alberta. These landslides are characterized by a thick deposit of glacial drift underlain by poorly lithified cretaceous shale (Bearpaw, Lea Park formations). These materials are known for their high slaking nature and lack of significant lithification or cementation. Multiple thin layers of extremely weak, smectite rich, clayey soils are often found within the upper portions of these cretaceous shale formations. These weak layers of highly active clay are often underlain by a thick deposit of cretaceous clay shale (Christiansen, 1983; Sauer, 1984). The smectitic clay lenses in these formations are often the location of a pronounced shear plane, which turns the overlying glacial drift into a slump block. Landslides of this nature can span several hundred metres in length, which provides a threat to infrastructure such as roads, bridges, and pipelines. Figure 1.1 shows an image taken from Eckel et al (1987) that details the stratigraphy of a landslide that is an excellent example of this type of slope failure.

Due to the depth of the shear zone, and the magnitude of these creeping failures, remediation via traditional geotechnical engineering solutions is either impractical or very expensive. The lack of available solutions for this widespread problem has prompted research towards a solution that stems from a multi-disciplinary approach. This research evaluates the feasibility of modifying the porewater chemistry of these smectitic shear zones by using guanidinium chloride (GuCl) to effect mineralogical alteration through ion exchange, as a means of insitu soil strengthening.

Guanidinium is a thin, flat, organic ion that biodegrades in naturally occurring surface water (Marcus, 2012; Mitchell, 1987). To date, research pertaining to the effects that guanidinium salts have on highly smectitic soils is limited, particularly with natural soils. Plötze & Kahr (2008) are the first researchers to document using guanidinium salts with smectitic soils. Their research pertained to x-ray diffraction (XRD), as they used the guanidinium ion to induce a long-lasting collapse of the interlayer spacing of smectites. This effect made the guanidinium ion a useful XRD peak diagnostic tool. Subsequently, Minder (2016) provided an excellent basis for using

guanidinium salts in geotechnics. Minder demonstrated that guanidinium salts caused a reduction in swell index, and increases in permeability, shear strength and pore size for a manufactured bentonite.

The objectives of this study (listed in Section 1.2) were achieved through a series of laboratory-scale tests. A general characterisation of the interaction of guanidinium salts and natural smectitic clays was performed. Real-world concerns were also addressed, such as the permanence of this insitu strengthening technique and the possibility of volume change induced by osmotic consolidation.

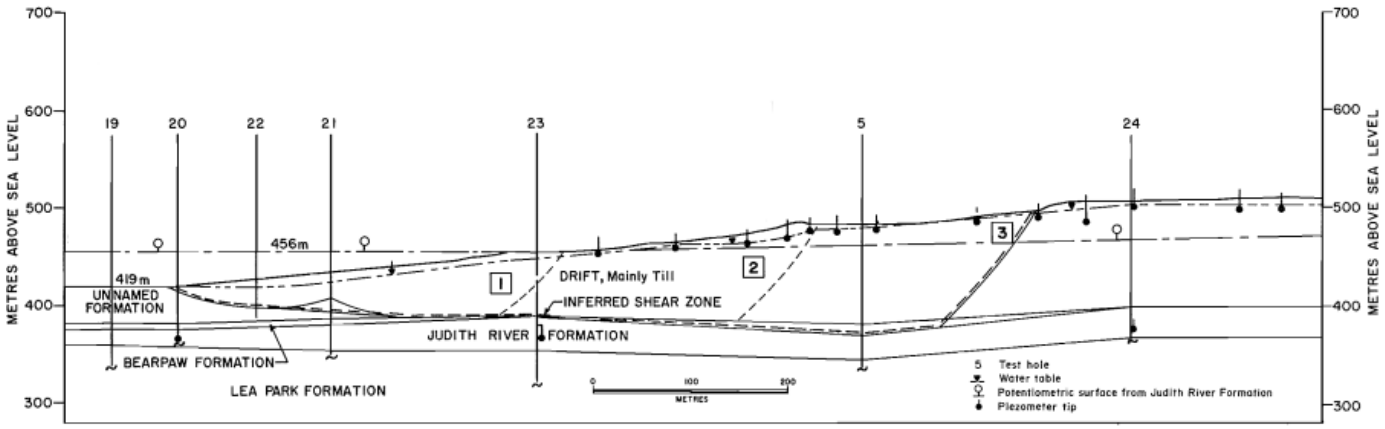

Figure 1.1: Cross-section showing the geometry of the Petrofka landslide in Saskatchewan. Note the thin shear zone within the bearpaw formation and the three distinct slump blocks that form. Taken from Eckel et al (1987).

1.2 Research Objectives

Minder (2016) demonstrated that guanidinium salts were capable of increasing the hydraulic conductivity and shear strength of smectitic soils; however, his work was limited to commercially available clay materials. Due to the complexity of ion exchange within natural soils and the potential for interaction or competition of ions that exist in natural porewater, it seemed a prudent next step to investigate whether the findings of Minder (2016) could be reproduced for natural soils. Furthermore, the identification of the mechanism at the mineralogical scale remained to be clearly defined.

The present research will look to fill this knowledge gap, and to further contribute to this novel engineering solution by completing the two following objectives:

1. Clearly identify the mechanism at a mineralogical scale by which guanidinium salts can alter the properties of expansive clay soils; and,
2. Assess and quantify potential implications associated with full-scale use of this insitu soil strengthening technique.

The following two tasks were completed to fulfill Objective One:

I. Conduct microscopic testing procedures such as environmental scanning electron microscopy (eSEM), scanning electron microscopy (SEM), and X-Ray Diffraction (XRD) testing to investigate alterations to the smectitic clay mineral, and;
II. Assess the montmorillonite mineral's affinity for the guanidinium ion relative to other major cations found in the soil's porewater.

The following three tasks were performed to achieve Objective Two:

III. Characterise a group of four natural prairie soils;
IV. Subject this group of soils to chemical treatments using guanidinium salts with varying delivery methods with the intent of evaluating key geotechnical parameters, and;
V. Quantify the impact that guanidinium salts on the four different soils.

The terms "mineralogical/chemical" and "macroscopically observable" changes will be used throughout this thesis. Mineralogical/chemical changes will refer to changes in the soil that are not apparent to the naked eye (i.e. a change in soil fabric), while the term macroscopically observable will refer to changes in the visible, physical behavior of a soil.

1.3 Scope

The work presented in this document is limited to laboratory-scale testing conditions. The intent of the research was to focus on the feasibility of using guanidinium salts as a means of an insitu strengthening technique for natural soils. There will be several references to clay minerals throughout this document, particularly the mineral smectite. Although the term "smectite" encompasses a variety of 2:1 phyllosilicates, its use herein will refer exclusively to the clay mineral montmorillonite unless explicitly stated.

1.4 Organization of Thesis

This thesis consists of five main chapters:

- Chapter 1 introduces the purpose of the research project;
- Chapter 2 consists of a review of the literature pertinent to the problem and intended research objectives;
- Chapter 3 will describe the methodology and procedures for the laboratory testing program;
- Chapter 4 presents the results obtained through the completion of the laboratory program; and,
- Chapter 5 summarizes the laboratory program findings, draws conclusions from the research and makes recommendations for future work.

Chapter 2 Literature Review

2.1 Introduction

Chapter 2 outlines the importance of clay mineralogy as it relates to the macroscopically observable behaviour of clayey soils. Firstly, focus will be drawn to the clay-water interaction and the various phenomena associated with the hydration of clay particles; namely interlayer and diffused double layer (DDL) swelling. Next, the concept of the True Effective Stress will be presented. Then, the effects that porewater constituency have on the residual shear strength of expansive soils will be discussed. Lastly, the previous work regarding the use of guanidinium salts in geotechnics will be summarized.

2.2 Clay Minerals

The particle size of a natural soil typically varies by several orders of magnitude across the three most common soil types: sand, silt, and clay. The grain-size distribution of a soil is divided into two different categories - the coarse grained and fine grained fractions. The “coarse grained” fraction of a soil is comprised of any particles larger than 0.0075 mm in diameter, leaving the latter as “fine grained”. The fine grained fraction of a soil is usually composed of both silt and clay.

Clay particles are defined as finer than 2 μm in diameter (Mitchell & Soga, 2005). There are some exceptions to this statement, as some clay particles are larger than 2 μm in diameter. Mitchell & Soga (2005) and Mackenzie & Mitchell (1966) have therefore declared two separate terms to be used when referring to clays: clay minerals and clay sized particles. Clay minerals are defined as having the following characteristics:

(1) Small particle size;
(2) Net negative surface charge;
(3) Plasticity when mixed with water; and,
(4) High resistance to weathering.

Clay minerals are comprised of cationic octahedral and tetrahedral sheets. The octahedral sheets may vary in their composition but are most notably dominated by either aluminum or magnesium cation. Aluminum and Magnesium dominated octahedral sheets are referred to as Gibbsite and Brucite sheets, respectively (Mackenzie & Mitchell, 1966; Mitchell & Soga, 2005).The tetrahedral portion of a clay mineral is almost invariably made up of silica and oxygen (Mitchell & Soga, 2005). Figure 2.1 provides an illustration of each of the three aforementioned clay building blocks just described.

Measuring the basal spacing of a clay mineral is a common technique used to distinguish clay minerals from one another (Mitchell & Soga, 2005). The basal spacing (dimension shown in Figure 2.2) of a clay mineral refers to the "001" or "d-spacing" of the crystalline structure.

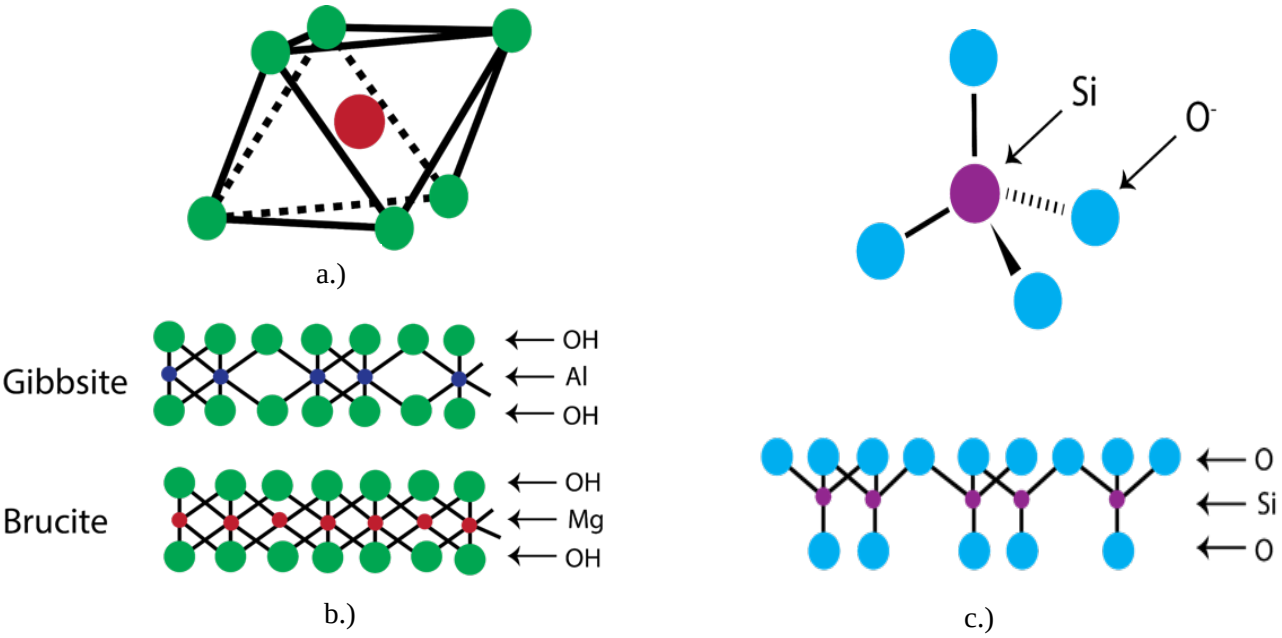

Figure 2.1: The three building blocks of clay minerals: a.) typical octahedral, b.) the lattice structure of gibbsite and brucite sheets, c.) a typical silica tetrahedral lattice structure.

All clay minerals are part of the phyllosilicate mineral family. The various stackings of the different crystalline structures above, the amount of isomorphic substitution (to be discussed later), and the bonds between each successive layer determines the type of clay mineral (Mitchell & Soga, 2005).

Although there are a large number of different clay minerals, geotechnical engineers commonly refer to just three: kaolinite, illite, and smectite (montmorillonite). Despite having different behaviours and characteristics, these three clay minerals all have a platy structure with well-defined cleavage planes (Chattopadhyay, 1972). Figure 2.2 provides illustrations of these three common clay minerals.

Kaolinite differs from illite and montmorillonite as it is a 1:1 phyllosilicate. Its mineralogical linkages are stacked in groups of two: an aluminum (or Gibbsite) octahedral sheet combined with a silica tetrahedral, as shown in Figure 2.2a. The mineral's basal spacing (typical dimension location shown in Figure 2.2) is 0.72 nanometres (nm). Illite is a 2:1 phyllosilicate mineral comprised of a Gibbsite sheet – silica tetrahedral – Gibbsite sheet as shown in Figure 2.2b. The basal spacing of illite is 1 nm.

Montmorillonite is also a 2:1 phyllosilicate, with the same three building blocks as illite. The basal spacing of montmorillonite is not a fixed value as it varies from 0.9 to 2 nm, as indicated in Figure 2.2c. One of the fundamental differences between these three minerals are the interlayer bonds between mineralogical units. In kaolinite, the linkages are bound together by Van der Waals forces and strong hydrogen bonds. Illite also has strong interlayer bonds due to the cationic bonds provided by the potassium ions present between each layer. Montmorillonite features extremely weak interlayer bonds, having only Van der Waals forces present between each layer. The lack of bond strength, and montmorillonite's high level of isomorphic substitution, allows water and other interlayer cations to easily penetrate and change montmorillonite's interlayer spacing. Conversely, due to the strong interlayer bonds between successive linkages in kaolinite and illite, the interlayer spacing of these minerals remains relatively unaltered during hydration.

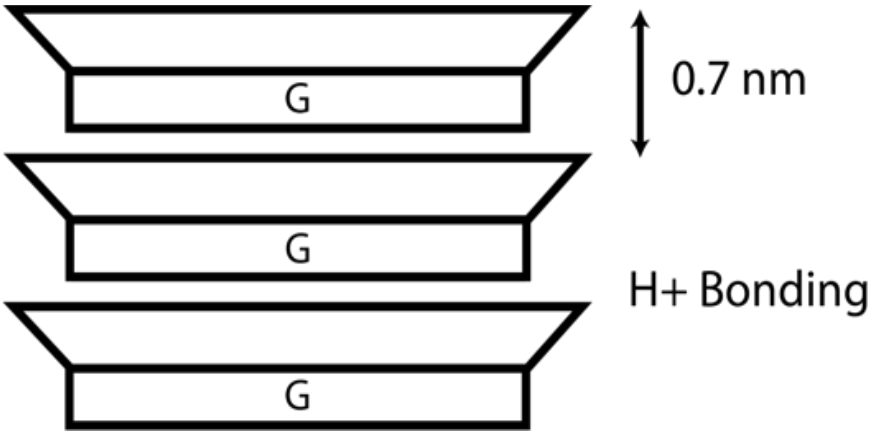

a.)

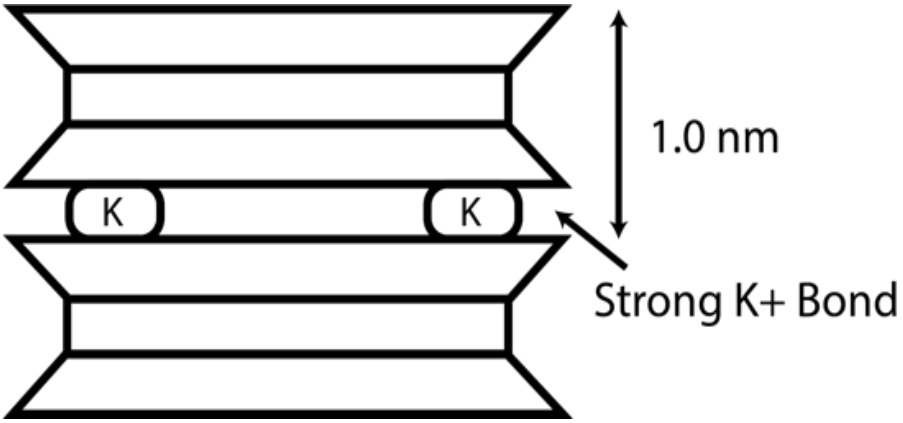

b.)

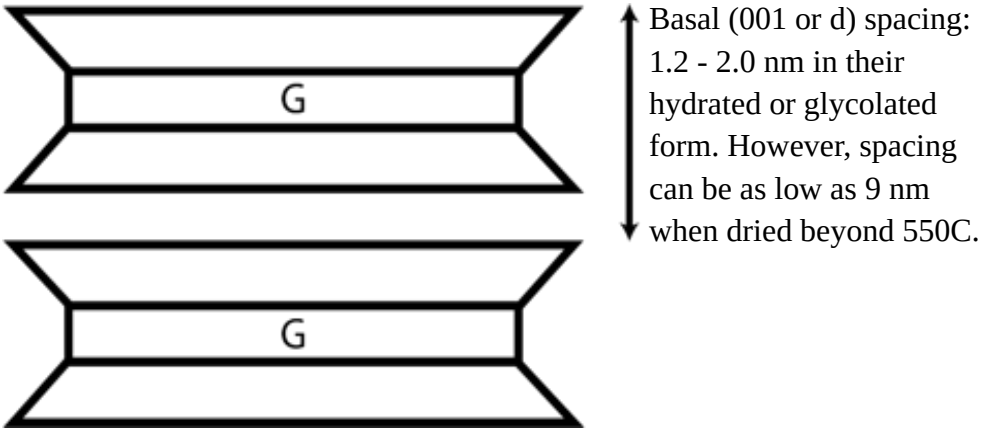

c.)

Figure 2.2: a.) The structure of a kaolinite mineral. b.) The structure of an illite mineral. c.) The structure of a montmorillonite mineral.

2.3 The Role of Isomorphic Substitution and Cation Exchange Capacity

Isomorphic substitution is a process whereby cations of a lesser valence replace cations that are present within the crystalline structure of a clay mineral (Mitchell & Soga, 2005). The amount of substitutions made as a result of isomorphic substitution varies depending on the clay mineral in question. Common examples of isomorphic substitution occur when some of the silicon (Si^{4+}) cations are substituted for trivalent cations such as aluminum (Al^{3+}) or iron III (Fe^{3+}) cations in the silica sheet of a clay mineral. In the octahedral sheets, it is common for divalent cations such as magnesium (Mg^{2+}), iron II (Fe^{2+}), or manganese (Mn^{2+}) to replace an Al^{3+} ion.

The concept of isomorphic substitution is a heavily studied phenomenon, and it is well known that these substitutions result in a net negative charge on the surface of clay particles (Brindley & Brown, 1980; Garrison, 2004; Kaufhold, 2006; Mackenzie & Mitchell, 1966; Maes & Cremers, 1977; Moore & Reynolds, 1989; Terzaghi, Peck, & Mesri, 1995). The level of isomorphic substitution in a clay mineral can be directly related to the net negative surface charge on a clay mineral.

The negative surface charge on a clay mineral is balanced by the adsorption of cations when clay particles are brought into a cationic solution. Therefore, the level of isomorphic substitution for a given clay mineral can also be used to indicate how the mineral will be influenced by electrolytes present in solution. The term used to describe the quantity of exchangeable cations is aptly termed the “Cation Exchange Capacity” (CEC) (Bolt, 1956; Mitchell & Soga, 2005; Sparks, 1999). CEC is often expressed in terms of milliequivalents per 100 grams (mEq/100g) of dry clay.

Typical values for CEC and specific surface area (SSA) for kaolinite, illite, and montmorillonite are given in Table 2.1. As shown, the SSA increases with increasing CEC. It is unknown whether kaolinite minerals experience isomorphic substitution because it has not been effectively measured (Garrison, 2004; Mitchell & Soga, 2005). Despite the uncertainty surrounding kaolinite’s participation in isomorphic substitution, it has been demonstrated that the mineral still features a small negative surface charge of 3 to 15 mEq/100g (Garrison, 2004; Mitchell & Soga, 2005). A possible mechanism of isomorphic substitution that would produce a CEC value so low could be one Al^{3+} ion being exchanged for every 400^{th} Si^{4+} ion (Mitchell & Soga, 2005). Unlike

kaolinite, illite has a definite mode of isomorphic substitution. Si^{4+} ions in the silica sheet are occasionally replaced by Al^{3+} ions. This defined mechanism of isomorphic substitution gives illite a CEC in the range of 10 to 40 mEq/100g.

Montmorillonite, and all smectitic minerals, undergo high levels of isomorphic substitution. Up to 15% of Si^{4+} ions may be replaced by aluminum. In the octahedral sheets of montmorillonite, the Al^{3+} ions may be replaced by several different divalent cations. The extent of aluminum ion replacement varies from sporadic to complete substitution (Bradley, Grim, & Clark, 1937; Brindley & Brown, 1980; 1938; Mackenzie & Mitchell, 1966; Maes & Cremers, 1977; Marshall, 1949; Mitchell & Soga, 2005; Ross, 1945; Stul & Cremers, 1979; Terzaghi et al., 1995). This significant amount of isomorphic substitution causes a large negative charge on the surface of the montmorillonite minerals, which leads to high CEC values in the range of 80 to 150 mEq/100g (Mitchell & Soga, 2005).

Table 2.1: Summary of common clay mineral characteristics

Clay Mineral	**Specific Surface Area (m^2/g)**	**D Spacing (nm)**	**Bond Type**	**CEC (mEq /100g)**
Kaolinite	10-20[1]	0.72[1]	Secondary Valence + Hydrogen Bonds[2]	3-15[1]
Illite	65-100[1]	1.0[1]	Secondary Valence + Potassium Linkages[2]	10-40[1]
Montmorillonite	50-120[1]	Minimum of 0.96[2,3]	Secondary Valence + Exchangeable Ion Linkages[2]	80-150[1]

Mitchell & Soga, 2005[1], Chattopadhyay, 1972[2], Norrish, 1954[3]

2.4 Clay-Water-Electrolyte Interaction

The previous sections have briefly described the structure, bond mechanisms, and fundamental properties of kaolinite, illite, and montmorillonite. It is these fundamental principles of each clay mineral that govern their behaviour in the presence of water. Extensive research has aimed to identify the mechanisms of clay mineral hydration, and cation selectivity (Kaufhold, 2006; Laird, 2006; Laird & Shang, 1997; Laird, 1987; Mitchell & Soga, 2005; Norrish, 1954; Shainberg, 2006). The following section provides an examination of the existing literature pertaining to the processes involved with the hydration of a clay mineral.

The discussion above has focused on the mineral structure of the three main clay minerals. However, by comparing the structure, interlayer bonds, levels of isomorphic substitutions, and resulting values of CEC, it is apparent that montmorillonite will be most greatly affected by its surrounding porewater and in particular the dissolved electrolytes. Accordingly, Sections 2.4.1 and 2.4.2 address in turn the two separate mechanisms that contribute to the swelling of montmorillonite: interlayer swelling and diffused double layer (DDL) swelling.

2.4.1 Interlayer Swelling

Interlayer swelling within montmorillonite can be generalized as the uptake of water between the silicate sheets of the clay mineral (Laird, 1987). During this process, the water content in montmorillonite is increased to a maximum of approximately 0.5 grams of water per gram of clay (Mitchell & Soga, 2005). Norrish (1954a; 1954b) and Norrish & Quirk (1954) found that during interlayer hydration, the interlayer spacing of montmorillonite varied in a step wise fashion from 0.96 nm to 2.0 nm. Within this range of swelling, there are four discrete layers of hydration, with each layer having a thickness of approximately 0.25 nm (Norrish 1954; Bradley et al., 1937, Laird, 1987; 2006, Laird & Shang, 1997). The valence and hydrated radius of the cations present in the hydrating fluid were found to be significant factors effecting the interlayer spacing. Norrish (1954b) found that polyvalent ions typically develop larger interlayer spacings than monovalent ions, as did ions of a larger hydrated radius.

Norrish & Quirk (1954) observed that following this initial “hydration” phase, an “osmotic” phase would take place, but only in the presence of monovalent cations. In the osmotic phase, Norrish and Quirk observed interlayer spacings in excess of 4.0 nm. They derived a relationship

between bulk solution normality and the interlayer spacing; this relationship is given in Equation 2.4.1, where *N* is the normality of the bulk solution and *d* is the interlayer spacing in angstroms.

$$\frac{1}{\sqrt{N}} = d \tag{2.4.1}$$

The effects of layer charge play a major role in interlayer swelling and cation selectivity (Laird, 1987, 1996, 2006; Maes & Cremers, 1977). Layer charge is defined as the resulting charge on a clay's surface following isomorphic substitution (Laird, 1996). Since each degree of swelling in the initial hydration phase of montmorillonite can be considered discrete, the level of interlayer swelling within each of the four layers described by Norrish (1954) may be thought of as a separate "stage" of swelling. Each stage of swelling will therefore determine the ion selectivity, which will create a dominant ionic composition within the interlayer. Alterations to a soil's interlayer composition will impact the clay's layer charge. Following this logic leads to a circular pattern, and thus a feedback loop (Figure 2.3) is formed.

Figure 2.3 represents a model proposed by Laird (1996) that has been used to explain the discrepancy in experimental results obtained from Maes & Cremers (1977) and Sawhney (1969). Maes & Cremers found that for a montmorillonite exchanging calcium (Ca^{2+}) cations for sodium (Na^{+}) cations, an increase in layer charge resulted in a greater affinity for Ca^{2+}. The results were interpreted to mean that increasing layer charge made polyvalent ions more favourable. A contradicting study done by Sawhney (1969) showed that the affinity for Ca^{2+} when exchanging K^{+} cations for Ca^{2+} cations decreased as layer charge increased. These two studies present contradicting arguments pertaining to ion selectivity and valence.

The model proposed by Laird (1996) predicts that for the exchange of cations with similar hydrated radii, such as a Na^{+}- Ca^{2+} exchange, the interlayer will show selectivity for the ion of higher valence. Laird's model is founded on the principle of potential energies and assumes that each phase has its own energy requirements. Therefore, for ions with similar hydrated radii, the net energy balance of sorbing an ion of greater valence is lower than sorbing an ion of like valence but smaller hydrated radii.

In an alternate scenario (i.e., the study presented by Sawhney (1969), when an ion with a weakly hydrated radius is present, an increase in layer charge will cause the clay to exhibit a greater affinity for the small, weakly hydrated cation. Sorbing an ion of greater hydrated radius would require more energy; therefore, the ion of smaller hydrated radius is preferred.

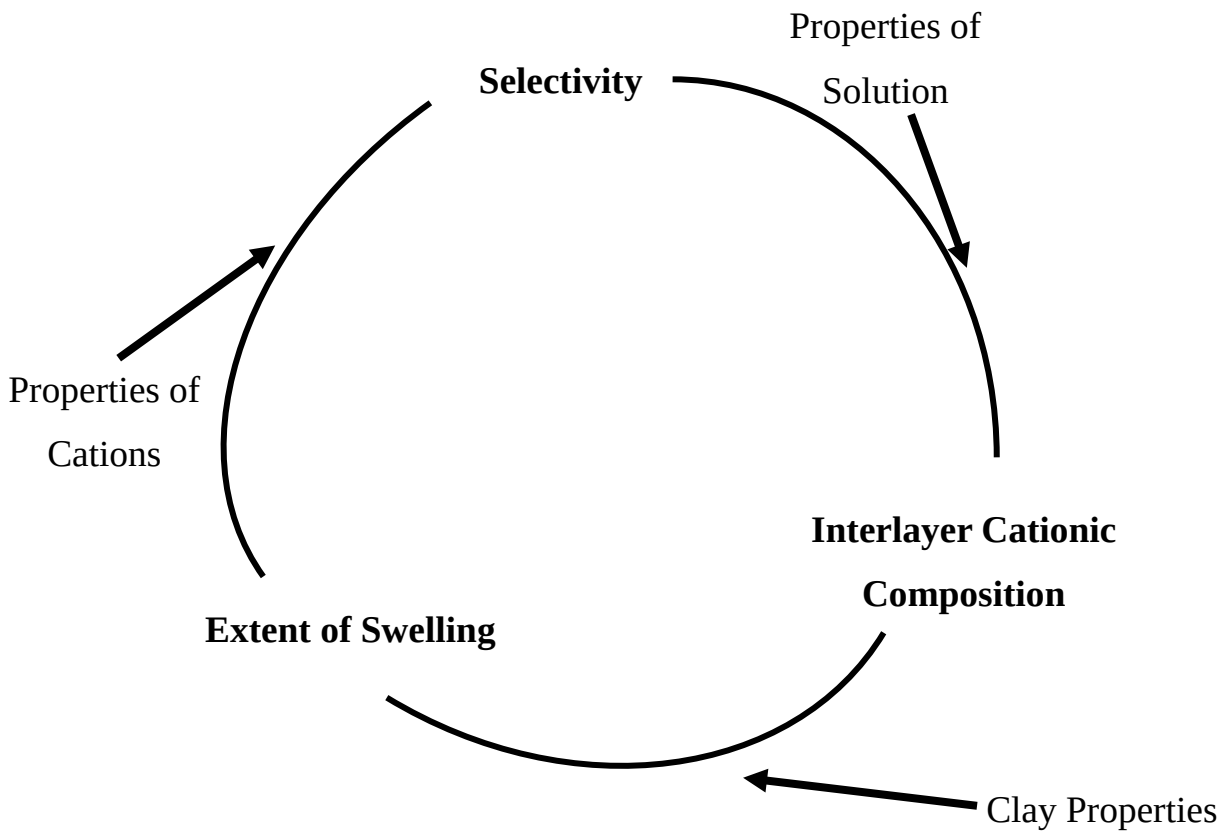

Figure 2.3: Interlayer selectivity feedback loop (Laird, 1996; Laird & Shang, 1997)

The relationship between bound water (water held within the interlayer) and free water has been shown to dominate the permeability and swelling characteristics of montmorillonite (Benson & Meer, 2009; Jo, et al., 2004; Jo, et al., 2001; Kolstad, et al., 2004. Jo et al. (2001) demonstrated the effects that different species of cations have on the swell potential and hydraulic conductivity of bentonites. These studies all concluded that ion species played a larger role for monovalent ions as opposed to polyvalent ions. Benson and Meer (2009) defined a ratio of monovalent to divalent molar concentrations and used this variable to predict the long-term behaviour of geosynthetic clay liners (GCLs). The results of their study demonstrated that with

increasing bulk solution concentration (and therefore decreasing layer charge), an affinity for Ca^{2+} ions was shown.

The works listed above, in conjunction with the model proposed by Laird (1996), are consistent in suggesting that ion concentration, valence, and hydrated radius size are all factors that affect the interlayer swelling of the montmorillonite mineral. Furthermore, via the work by Benson & Meer (2009), Jo, et al. (2001; 2004), and Kolstad, et al., 2004, it was shown that the interlayer composition dominates several aspects of montmorillonite's macroscopically observable behaviour, such as swell potential and permeability.

2.4.2 Diffused Double Layer Swelling

Unlike interlayer swelling, DDL swelling is common to all clay minerals. The thickness of a clay mineral's DDL is directly related to the mineral's negative charge and SSA (Mitchell & Soga, 2005; Puppala et al., 2017). Therefore, the montmorillonite mineral can form DDLs of much greater thicknesses in comparison to kaolinite and illite.

The DDL forms as a result of cations from the bulk porewater solution being attracted to the negative charge that is present on the clay's surface, while simultaneously being drawn back by the anions in the bulk solution (Bolt, 1956; Van Olphen, 1977). The Gouy-Chapman theory is the most common model used to describe DDL behavior despite several limitations of its ability to describe the role cations play regarding the behavior of smectitic clays in solution (Chapman, 1913; Gouy, 1910). Gouy-Chapman theory is founded on the following four assumptions (Mitchell & Soga, 2005):

1. Ions within the DDL are point charges, with no interaction amongst each other;
2. The charge on a clay particle's surface is uniformly distributed (Figure 2.4);
3. The size of the particle's surface is large relative to the thickness of the DDL; and,
4. The permittivity of the medium (pore fluid) is independent of the position of the particle's surface.

In accordance with the first assumption, Gouy-Chapman theory states that an infinite number of ions can exist along the surface of a clay platelet. These ions are arranged in a Maxwell Boltzmann distribution. (Mitchell & Soga, 2005; Sposito, 2004). For this reason, the theory becomes invalid for describing the clay-water interaction when the concentration of electrolytes in the bulk solution is in excess of 0.001 M (Sposito, 2004).

Several researchers have developed explicit solutions relating the concentration of ions near a clay's surface and the thickness of the DDL (1/*K*). This expanded Gouy-Chapman model is now commonly referred to as DLVO theory, named after its creators Boris Derjaguin and Lev Landau, Evert Verwey and Theodoor Overbeek, (Mitchell & Soga, 2005). The equation describing the thickness of the DDL is shown below in Equation 2.4.2 (Bolt, 1955, 1956; Mitchell & Soga, 2005; Van Olphen, 1977; Verwey & Overbeek, 1948):

$$\frac{1}{K} = \left(\frac{\epsilon k T}{8\pi e_c^2 v^2 n}\right)^{1/2} \qquad (2.4.2)$$

Where

$1/K$ = the thickness of the DDL

ϵ = dielectric constant of the pore fluid (80.4)

k = Boltzmann constant (1.38×10^{-16} J°K^{-1})

T = temperature (°K)

n = molarity of bulk solution x (6.02×10^{23} mol^{-1}) x 10^{-3}

e_c = charge given by an electron charge (4.803×10^{-10} esu)

v = cation valence

Stern theory (1924) adequately mediated the issues with Gouy-Chapman theory by allowing for the consideration of a cation's hydrated radius. He postulated that there is a rigid-like layer of ions that arrange themselves along the negatively charged surfaces of clay particles, as shown in Figure 2.4. The thickness of this rigid-like layer is roughly equivalent to the thickness of the hydrated radius of the cation along the clay platelet's surface. Despite thermal motion causing the cations along a clay platelet's surface to be constantly interchanging, the term "rigid-like" has been used to describe the cations within this layer because the thickness of this layer remains

constant. This layer of closely held cations is aptly named the “Stern layer”. Equations based on Stern theory were adopted by Van Olphen (1977).

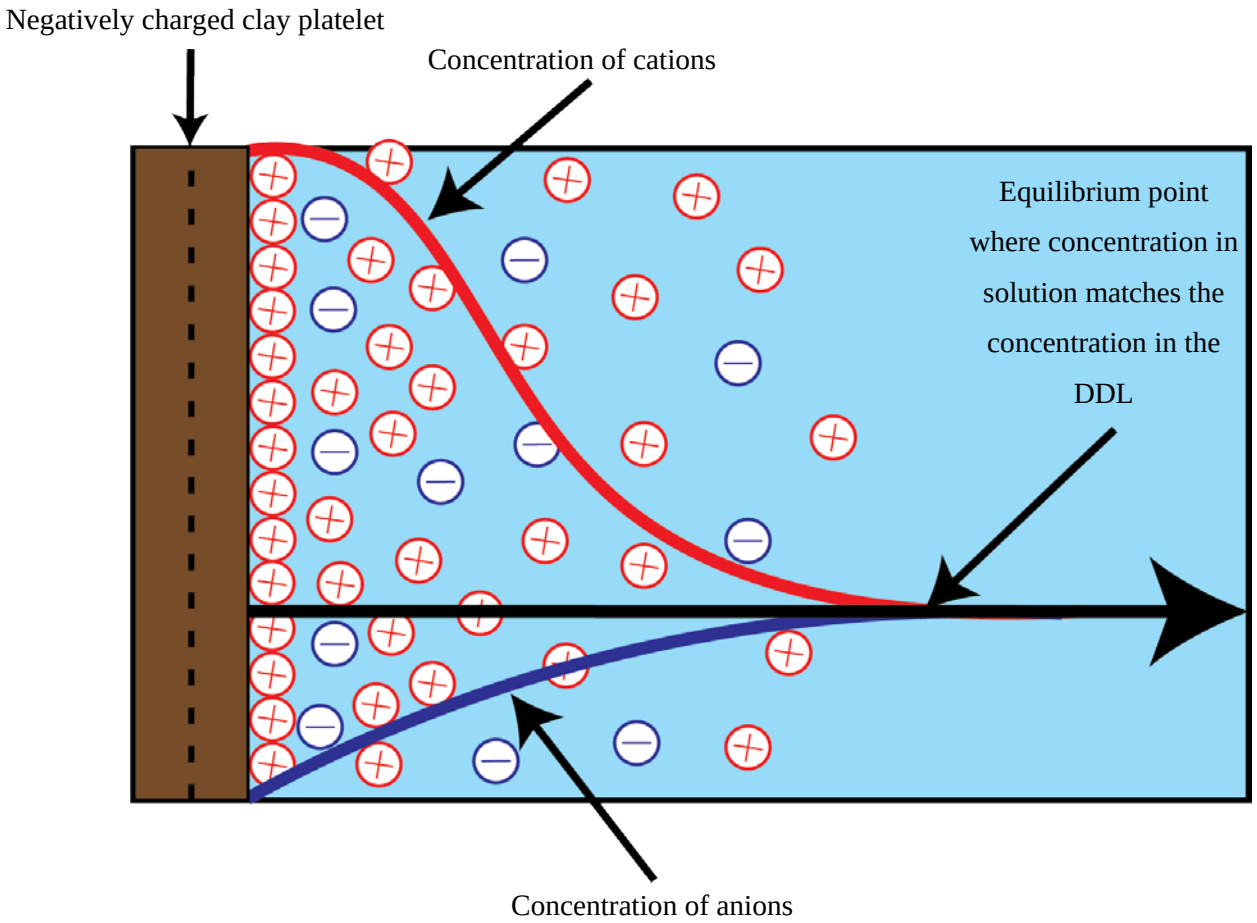

Figure 2.4: The distribution of cations and anions within the DDL as proposed by Gouy-Chapman-Stern theory. Adapted from Mitchell & Soga (2005).

Numerous researchers have investigated a method for quantifying the repulsive pressures that form between interacting DDLs of clay particles under Gouy-Chapman theory (Bolt, 1956; Sridharan & Jayadeva, 1983; Van Olphen, 1977). The first reported assessment of repulsive pressures between clay particles using Gouy-Chapman theory was given by Bolt (1956). Bolt used Gouy-Chapman theory to develop what is commonly referred to as “Osmotic Pressure theory”. In osmotic pressure theory, the DDL surrounding a clay particle acts as a semi-permeable membrane. When applying a load to a soil, a certain amount of fluid must leave the system so that the pressure difference in the central planes between clay platelets and the bulk pore solution match that of the applied load. The difference in osmotic pressure between the

system and the bulk pore solution is considered equal to the DDL repulsive forces between clay particles (Bolt, 1956; Schanz & Tripathy, 2009a; Sridharan & Jayadeva, 1983). One of the key assumptions from Bolt's theory is that clay particles are arranged as parallel plates. This assumption often leads to deviations between experimentally measured and theoretically determined values for repulsive pressures.

The formulas presented by Sridharan & Jayadeva are largely similar to those implemented by Balasubramonian (1972), Barbour (1987), Bolt (1956), and Chatterji & Morgenstern (1990), despite using different notation. The proposed equation for determining the repulsive pressures between clay particles is given in Equations 2.4.3 to 2.4.6. The notation used in consistent with that of Balasubramonian.

$$R = 2C_o rT(\cosh y_c - 1) \quad (2.4.3)$$

For $y_c < 1$:

$$y_c = 2\ln(\cosh\Delta + 1)/(\cosh\Delta - 1) \quad (2.4.4)$$

For $y_c > 1$:

$$y_c = 2\ln(\frac{\pi}{\Delta}) \quad (2.4.5)$$

$$\Delta = K(x_o + d) \quad (2.4.6)$$

And K = Eq. 2.4.2.

Where:

R = repulsive pressure between particles

C_0 = ion concentration of bulk solution (molar concentration x 10^{-3})

r = universal gas constant (85 kg-cm/mol/°K)

x_o = the distance from the surface of infinite charge density to a surface at which the charge density is equal to that of the soil of interest (equivalent to 4/*v*, where *v* is the valence of the cation, as given by Balasubramonian, 1972)

d = interparticle half space ($\frac{e}{SSA} x\ G$), where e is void ratio and G is the specific gravity of the soil

Successful applications for predicting the behaviour of pure Na^+ treated Na-montmorillonites have been recognized by Sridharan & Choudhury (2002); however, the theoretical solutions have not had as much success for predicting the repulsive forces of natural montmorillonite soils that have been hydrated in a solution with other species of cations. Aside from the previously stated issues with Gouy-Chapman theory, the following realizations and issues arise when considering the theoretical assumptions with reality:

- The assumption that clay plates are of uniform size and arranged parallel with a uniform separation distance is often invalid
- The void ratio/separation distance between clay plates is not a unique function of stress, and therefore, fabric and structure are important.
- As the particle proximity increases due to applied stresses, the swelling pressure obtained will be greater than that predicted by diffuse double layer theory due to hydration forces

2.5 Concept of True Effective Stress

The previous section described the fundamental information pertaining to the hydration of a clay mineral. Section 2.4.2 placed an emphasis on the repulsive forces that form between DDLs. The first mechanistic model that accounted for these attractive and repulsive forces as they pertained to the macroscopic behaviour of fine grained soils was developed by Lambe (1958; 1960). Lambe reconsidered the traditional effective stress equation given by Terzaghi (1923) for fine grained soils. Effective stress only considers forces that are transferred at intergranular contact points, but Lambe (1958) hypothesized that the repulsive and attractive forces between adjacent particles may also contribute to the overall stress state of the soil system. These additional physico-chemical forces proposed by Lambe are shown in Figure 2.5.

Sridharan (1968) furthered Lambe's theory by analyzing the variations in attractive forces between clay particles at varying levels of hydration. Subsequent works by Balasubramonian (1972), Chattopadhyay (1972), Sridharan & Rao (1973), and Sridharan & Venkatappa Rao (1979) all built upon the osmotic pressure theory developed by Bolt (1956) and the mechanistic

model created by Lambe (1958,1960). These works established the basis for considering the repulsive forces resulting from interacting DDLs and attractive forces that arise from Van der Waals' forces, Coulombic attraction, and cationic bonding. A new variable dubbed "True Effective Stress" ($\sigma^{"}$) was formed to describe the stress on clay particles under such physico-chemical forces. The True Effective Stress theory implemented the repulsive and attractive forces as a difference and expressed them as a stress state variable, like porewater pressure. The true effective stress equation is given in Equation 2.5.1.

$$\sigma^{"} = \sigma' - (R - A) \qquad [2.5.1]$$

Where:

$\sigma^{"}$ = true effective stress

σ' = effective stress

R = repulsive pressure between particles

A = attractive pressure between particles

Unlike repulsive forces, there is a lack of certainty regarding what the primary contributor to attractive forces is (Maio et al., 2002). A common assumption is that Van der Waals forces play a major role in these attractive forces, and that the strength of these attractive forces vary as the seventh power of the distance between each cation. Therefore, much like interlayer phenomena, the size of an ion's hydrated radius plays a significant role in DDL behaviour. For ions of larger size, the distance between each particle increases, which reduces the Van der Waals forces between clay particles. With decreasing ion size, the attractive forces between clay particles increase. This principle has been demonstrated by several researchers, notably Sridharan & Rao (1973) and Sridharan & Venkatappa Rao (1979). In addition to ion size being a contributing factor to the attractive force, it is also widely accepted that attractive forces increase with decreasing dielectric permittivity, and increasing in cation concentration and valence (Maio et al., 2002). The factors above are all synonymous with a suppression of DDL thickness.

There are two different mechanisms governing the macroscopically observable behavior of clays Sridharan & Rao (1973). Sridharan & Rao analyzed the behaviour of kaolinite rich and

montmorillonite rich soils. They found that decreasing the dielectric permittivity and/or increasing the electrolyte concentration of a kaolinitic soil's porewater lead to an increase in sedimentation volume. The increase in volume is attributed to an increase in attractive stresses (A) between clay particles, and therefore, higher shear resistances at particle contact points.

For a soil with a high montmorillonite content, decreasing dielectric permittivity decreases the thickness of the DDL. Reduction in the DDL thickness causes an increase in attractive stresses between particles. The increased attractive forces promote face-to-face aggregation of the clay particles and ultimately decreases the volume of the soil. These two situations result in opposite behaviors as a result of the same interaction with the soil's porewater. The difference in macroscopically observable behaviour between these two clay minerals demonstrates the dominance of interparticle contact stresses over DDL phenomena for kaolinitic soils, and the inverse for soils with a high montmorillonite content.

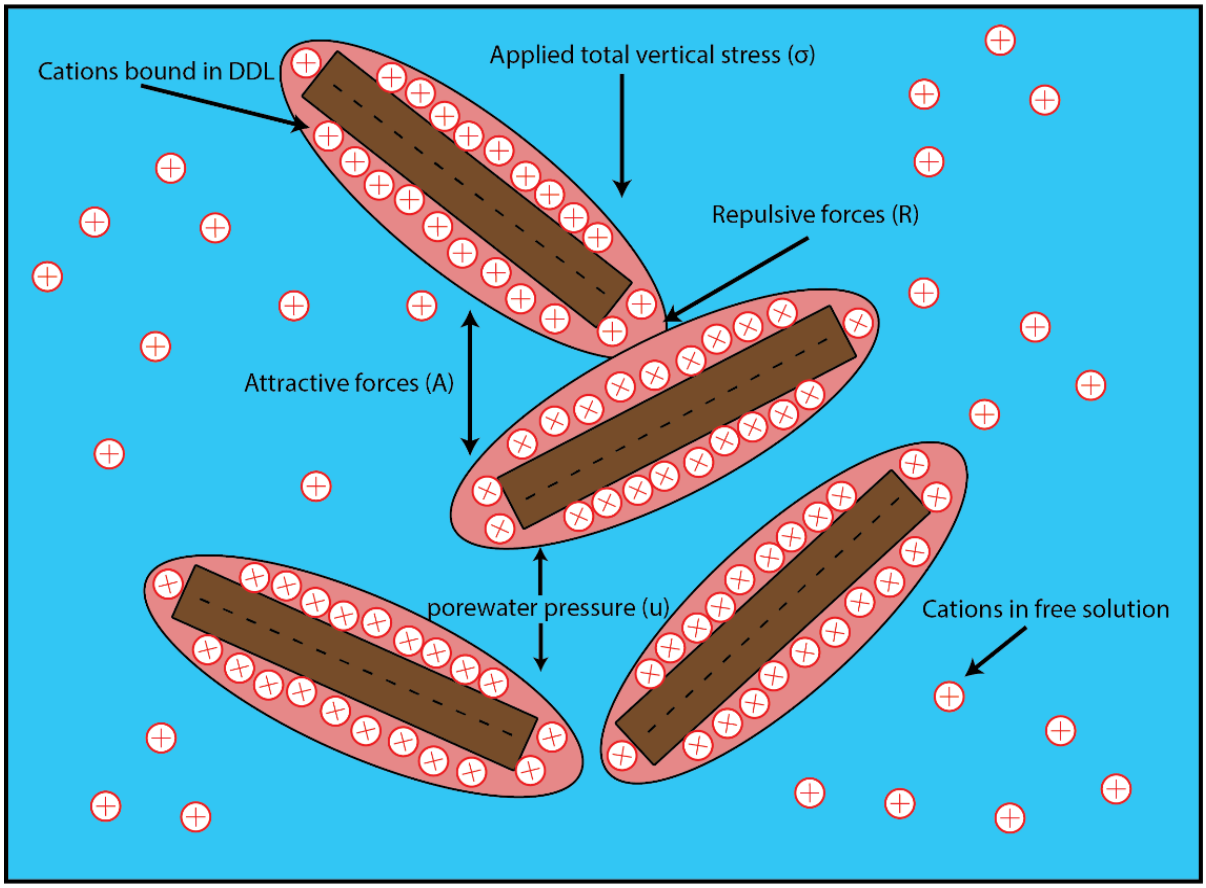

Figure 2.5: Conceptual image of the different forces present within a fine-grained soil.

2.5.1 Measuring Repulsive and Attractive Stresses

It is difficult to measure the repulsive and attractive stresses in a clayey soil because these physico-chemical stresses cannot be isolated and can only be exemplified in ideal conditions. To resolve this issue, Barbour (1987) proposed an indirect method of evaluating R-A by assuming the attractive forces between particles are negligible and only measuring apparent changes in repulsive forces. The resulting constitutive model is similar to that of the one provided by Fredlund & Morgenstern (1976) for evaluating increases in effective stress due to matric suction.

Barbour's method measures the changes in osmotic pressure that develop within the DDL upon changing the porewater electrolyte concentration. As described earlier, if DDLs are thought of as a semi-permeable membrane, then a pressure is required to force the solvent through the membrane in response to a mechanically applied load. The difference in pressure between the midplane of the DDL and the bulk solution is termed the osmotic pressure. This osmotic pressure is assumed to be equivalent to the repulsive forces between clay particles. An explanation of how to use Barbour's method is described more fully in Section 4.3.3.2 of this thesis in the context of analyzing some one-dimensional consolidation testing. Alternatively, more details on the method used by Barbour are provided in his thesis (1987).

Figure 2.6 presents a three-dimensional plot depicting the constitutive model described by Barbour (1987). As shown, changes in osmotic pressure, in response to increasing porewater salinity, may induce volume changes for the same mechanically applied stresses. Barbour found success using this constitutive model when comparing his indirectly measured values with those theoretically determined for an artificial soil comprised of sodium montmorillonite and Ottawa Sand. For a natural soil, Regina Clay, he found that his experimental values deviated substantially from those predicted from osmotic pressure theory (Barbour & Fredlund, 1989; Barbour, 1987).

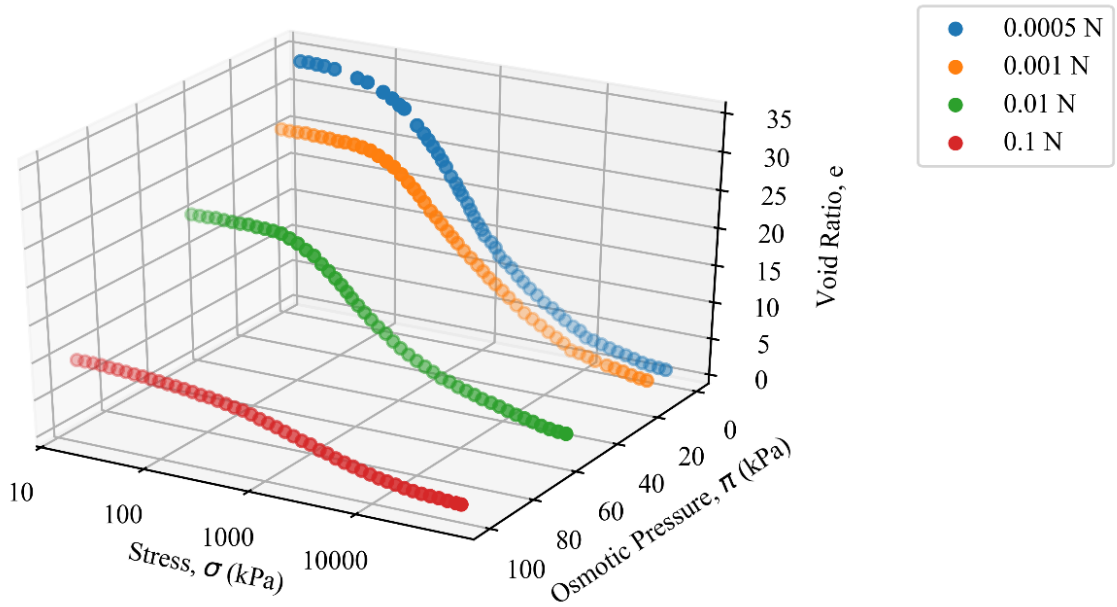

Figure 2.6: Three-dimensional constitutive surface for montmorillonite as proposed by Barbour (1987), data taken from Mesri & Olson (1971).

Chatterji & Morgenstern (1990) presented a complex, time consuming method to measure R-A stresses in a Na-montmorillonite. They leached homo-ionized Na-montmorillonites with distilled deionized (DDI) water while shearing them in a direct shear box. They found a strong agreement between their theoretically predicted repulsive stresses and their measured changes in R-A stresses. However, the strong correlation between their measured and theoretical data may be attributed to their sample preparation. The soil tested, a Na-montmorillonite, was completely homo-ionized via repeated sedimentations in 35g/L NaCl solutions over a period of nine months.

The lack of agreement for Regina Clay that was observed by Barbour (1987) and the excellent agreement found by Chatterji & Morgenstern (1990) between theoretical and experimental values can be explained by the same phenomena. In Barbour's case where he tested Regina Clay, the most likely reason for the lack of agreement stems from the assumption that clay platelets are arranged in a perfectly parallel orientation. Montmorillonite that is hydrated in the presence of ions such as Ca^{2+} is known to form domains of particle packets (Aylmore & Quirk, 1959; Mesri & Olson, 1971). Natural soils often exist in a mixed cation system, therefore the formation of these packets, and a lack of perfectly parallel platelets is likely. Additionally, under increasing

mechanical load, the number and size of packets has also been shown to increase. The increased number and size of these packets would further contribute to the lack of uniformity among clay platelets (Mesri & Olson, 1971).

In the case of Chatterji & Morgenstern (1990), meticulous sample preparation ensured that the soil was completely homo-ionized with sodium ions. It is known that sodium ions are not held as tightly along a clay's surface in comparison to divalent cations or other monovalent cations, such as potassium (Di Maio, 1996). Therefore, if the sodium ions exist along the outer portion of the DDL, and all clay minerals have alike DDL compositions, a consistent, parallel-arranged fabric is more likely to develop. This increased sense of uniformity would allow for better predictions of repulsive stresses from the osmotic pressure theory.

2.6 Residual Shear Strength

The previous sections have largely been focused on establishing the basis for how clay particles interact with one another in electrolyte rich solutions. Section 2.5 introduced the concept of True Effective Stress and described its relevance to fine grained soils. Equation 2.5.1 proposed that the inclusion of the physico-chemical stresses between clay particles may result in a different effective stress than that of what is being mechanically applied. This theory becomes extremely important when analyzing the insitu shear strength of a clay mineral. The following paragraphs will introduce an important slope stability soil property called residual shear strength. Subsequently, a discussion of some key pieces of work investigating how alterations to a soil's porewater can influence residual shear strength will be presented.

Skempton (1964) first presented the concept of residual shear strength when he recognized a post peak strength in highly plastic clays. He noted that, for clayey soils, these residual shearing resistances were similar to those measured by Horn & Deere (1962) for various crystal lattice type minerals. In a review paper published in 1985, Skempton defined residual shear strength as "the minimum constant value attained (at slow rates of shearing) at large displacements".

Following the initial work of Skempton, several researchers began investigating factors that impact residual shear strength. Kenney (1967) subjected several soils to a variety of saline porewater solutions and subsequently sheared them to their residual state in a direct shear box.

From this work, he concluded that altering a soil's porewater in the following ways increased a soil's residual shear strength:

1. Adding cations of a higher valence ($Ca^{2+} > K^{+}$);
2. Adding cations of greater polarizability ($K^{+} > Na^{+}$); and
3. Increasing the concentration of ions within the porewater.

Chattopadhyay (1972) related residual strength to the mode of cleavage of constituent minerals of soils, and hence to particle shape. He found that low residual friction angles were associated with platy particles and that subangular and/or needle-shaped particles gave high residual friction angles. He stated that at large strains the resistance offered between basal planes of two clay particles is equal to the residual shear strength of a mineral. His findings were in good agreement with the statements made by Skempton (1964).

Lupini, et al. (1981) defined three modes of residual shearing: turbulent, sliding, and transitional. Turbulent shearing occurs when a high degree of friction exists between particles. This mechanism is common for soils that have a high proportion of rotund particles (i.e., sand and silt). The sliding residual shear mechanism stems from platy clay particles with low friction shear surfaces and is associated with high degrees of particle orientation. Transitional shearing consists of a combination of turbulent and sliding shearing. After identifying the three modes of residual shearing, Lupini et al. presented evidence towards the governing factors for the turbulent and sliding mechanisms. For turbulent shearing, they suggested that the packing and shape of rotund particles govern the mechanism, not the coefficient of interparticle friction. In the case of sliding friction, the residual friction angle depends primarily on mineralogy, porewater chemistry and on the coefficient of interparticle friction.

Like Chattopadhyay (1972), Moore (1991) suggested that in soils with a high clay fraction, the residual shear strength is influenced by the nature of the clay minerals (i.e., particle size, shape and surface area) and the type, valency, and concentration of cations in the porewater. In a discussion of his paper, Moore (1992) proposed that increases in residual shear strength and decreases in plasticity with increased salt concentration and cation valence are due to an increase in the strength of the interparticle bonding. He recommended that more representative residual

shear strengths would be obtained if naturally occurring groundwater from sampling sites was used during testing.

Anson & Hawkins (1998) performed liquid limit and ring shear testing on pure kaolinite and Wyoming bentonite (Na-montmorillonite). Their testing procedure involved subjecting these soils to various concentrations of calcium chloride ($CaCl_2$) that were representative of some insitu groundwater samples taken from a calcareous mudrock. They found that the liquid limit of montmorillonite declined rapidly with an increase in concentration of porewater salinity. Conversely, they found that the liquid limit of kaolinite increased by 8% when low concentrations of Ca^{2+} were added to the soil's porewater. Both of these findings were in line with the mechanisms identified by Sridharan & Rao (1973). The ring shear testing was performed at five different normal stresses. There was no significant increase in the residual shear strength of kaolinite samples, but the montmorillonite soil demonstrated an increase in residual shearing angle of approximately 5° at all increments of normal stress tested.

With the exception of Chattopadhyay (1972), all other works attributed the increase in residual shearing resistance to a collapse of the soil's interlayer spacing and reduction of DDL thickness, without ever discussing True Effective Stress theory. Anson & Hawkins (1998) went so far as to suggest that when the DDL is collapsed, the attractive forces between clay particles increase due to an increase in proximity, therefore increasing the residual shear strength.

With reference to True Effective Stress theory, the findings of Kenney (1967) are of particular interest. His results can be directly correlated to factors affecting DDL thickness, and therefore repulsive stresses between clay minerals. Cations of a higher valence are known to result in smaller DDLs. Therefore, polyvalent cations will produce lower repulsive stresses, which will result in an increase in true effective stress. Kenney also states that ions of greater polarizability produce higher residual shear strengths; reconsidering this statement from the perspective of hydrated ionic radius once again frames the conclusion in reference to DDL thickness. Ions of a smaller hydrated radius are known to create smaller DDLs (Maio, 1996; Sridharan, Rao, & Murthy, 1986). The third conclusion from Kenney's work directly correlates with the effect that concentration has on DDL thickness, as given in Equation 2.4.2.

2.7 Effect of Ion Species

Maio (1996) investigated the reversibility of the effects that different electrolyte solutions had on a Na-montmorillonite. She subjected a Na-montmorillonite to saturated solutions of sodium chloride (NaCl), potassium chloride (KCl), and calcium chloride ($CaCl_2$) while performing direct shear and one dimensional oedometer tests.

Her direct shear tests showed an increase in residual shear strength and reduction of volume upon introducing saturated electrolyte solutions. The magnitude of osmotic volume change decreased with increasing mechanical loads. After reaching equilibrium within the new porewater regime, the porewater surrounding each sample was reverted to distilled deionized (DDI) water. NaCl samples demonstrated a complete reversibility in engineering behaviour while the effects of the latter two saline modifiers appeared to be permanent.

Maio also performed XRD and Scanning Electron Microscopy (SEM) analysis of all samples tested to observe any possible mineralogical alterations. XRD testing revealed that NaCl treated samples that had been washed with DDI shared the same montmorillonite basal spacing as those that had not been treated. KCl and $CaCl_2$ treated samples showed a shift in the montmorillonite peak. The results of the SEM testing were inconsistent and appeared to be subjective to testing conditions. In some cases, salt treated samples represented clay particles that were thicker than the particles imaged in untreated samples.

The hydrated radius of the K^+ ion provides a possible explanation for the seemingly permanent alterations to a potassium treated montmorillonite's engineering behaviour (Maio, 1996; Sridharan et al., 1986). It is believed that the hydrated radius of K^+ ions is sufficiently sized to become fixed within the hexagonal oxygen holes in the surface of the silicate layer (Sridharan, 1991). The permanence of this fixation remains unclear to researchers, but it is likely a function of the clay's long-term porewater environment post treatment (Maio, 1996).

Most researchers agree with the claims made by Sridharan & Rao (1973) that the effects of DDL thickness govern the volume and shearing behaviour of montmorillonite. However, when considering that the interlayer ionic composition of montmorillonite plays a vital role in the development of DDLs, the statement above must be reassessed. As discussed previously, in cases

where insufficient DDL development occurs, particles begin to form in domains (Mesri & Olson, 1971). In such cases, Gouy-Chapman theory has been shown to be insufficient in describing the behaviour montmorillonite (Barbour, 1987, Schanz & Tripathy, 2009a). Therefore, a more holistic approach to qualitatively assessing the macroscopically observable behaviour of montmorillonite may state that the interlayer governs DDL development; and as a result, indirectly controls the behaviour of the soil.

2.8 Previous Research with the Guanidinium Ion in Geotechnics

Considering the importance of a cation's valency and hydrated radii, the present research investigates the feasibility of using a monovalent saline porewater modifier called guanidinium chloride (GuCl). GuCl biodegrades naturally in surface water (Mitchell, 1987), has been shown to cause a collapse of the smectitic interlayer (Plötze & Kahr, 2008), and has yielded desirable engineering traits when mixed with idealized plastic soils (Minder, 2016).

As shown in Figure 2.7, the guanidinium ion is planar trigonal, which means that when approximating its radius one should consider it to be more oval-like than round (Marcus, 2012). Despite the mean radius of the guanidinium ion being 0.21 nm, the ion's flat shape allows it to behave as though it has a radius ranging from 0.17 to 0.28 nm, depending on its orientation (Marcus, 2012). It is likely that the unique shape and versatility in size allow it to fix itself in the holes of the octahedral sheets of clays, much like potassium ions. Plötze & Kahr (2008) first cited mineralogical changes due to the guanidinium ion when they used it as a tool for analyzing XRD patterns. Their research found that the cation proved capable of collapsing the smectite interlayer for periods long enough to perform additional XRD work without having to re-treat samples with the guanidinium ion.

Minder (2016) used a commercially available calcium bentonite to show that adding guanidinium chloride to a soil's porewater regime resulted in larger pore sizes, an increase in hydraulic conductivity, peak, and residual shear strength, reduced swelling hysteresis, and no major reductions in soil stiffness.

The work of Minder demonstrated the potential applications of guanidinium salts but did not fully explain the mechanism or speak to the uniqueness of the guanidinium ion. Furthermore, there are several concerns pertaining to the real-world applications of guanidinium salts that had remained to be answered. The work presented in this thesis is intended to address these gaps in the knowledge, while further quantifying the effects of guanidinium salts on a natural, non-idealized soil.

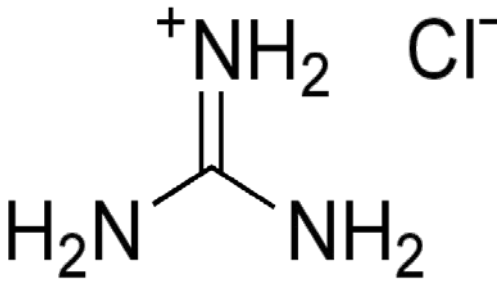

a.) Guanidinium ion with a chloride (GuCl).

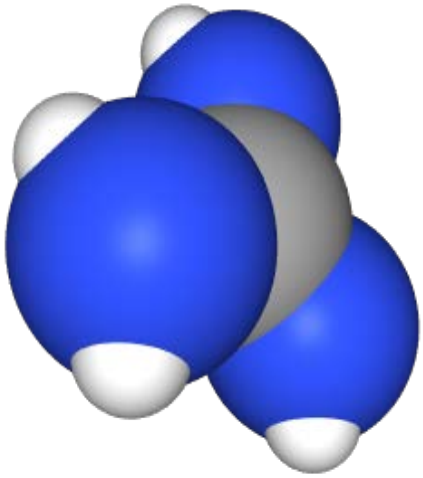

b.) A 3D rendering of the planar trigonal structure of the guanidinium ion

Figure 2.7: a.) Chemical formula for guanidinium chloride; b.) the structure of a single guanidinium ion.

Chapter 3 Methodology

3.1 Introduction

Chapter 3 outlines the methodologies and laboratory procedures that were undertaken to complete two primary objectives: 1.) clearly identify the mechanism, at a mineralogical scale, by which guanidinium salts can alter the properties of expansive clay soils; and,
2.) assess and quantify potential implications associated with the full-scale use of this insitu soil strengthening technique.

The first task of the laboratory program was to generally characterize four natural soils. This procedure is described in Section 3.1. Section 3.2 describes the methodologies employed to investigate the mineralogical alterations associated with GuCl treatment. Section 3.3 will explain the methodology of various tests that were used to assess potential impacts of full-scale implementation, such as the permanence of the treatment, required solution concentrations, and the potential for osmotic volume change.

3.1.1 General Soil Characterization

The laboratory analysis was limited to four local prairie soils: Regina Clay, Whitecourt Clay (a clayey soil from northern Alberta), Floral Till, and Battleford Till. Regina Clay, Floral Till, and Battleford Till have been well documented through the works of Christiansen (1971) and Fredlund (1975). These three common soils vary greatly in their mineralogical composition and macroscopically observable behaviour. Grain-size analysis and clay fraction testing were both completed following ASTM D6913 and ASTM D7928–17, respectively.

3.1.1 Quantitative X-ray Diffraction (XRD)

A semi-oriented quantitative XRD analysis was performed by the Saskatchewan Research Council (SRC). Their methodology consisted of sampling a random 0.5 g aliquot of each pre-ground specimen that was provided. Each sample was glycolated overnight in a sealed chamber set at 60°C. Sample powders were rotationally backpacked into a stainless-steel holder to create a preferred orientation of the clay minerals. The minimum sample thickness was 1 mm – sufficient breadth to be considered infinitely thick for XRD using a Cu source.

Samples were irradiated with Cu Kα radiation in a Bruker D4 Endeavor X-ray diffractometer. Samples were measured from 3.0 to 70° 2θ with a 0.02° step size and 0.35 seconds dwell time. The Jade software suite was used for data analysis.

3.1.2 Cation Exchange Capacity (CEC)

The CEC of each soil was measured using the methylene blue spot test. The methylene blue test was used due to its simplicity and reputation for providing the most representative results for calcareous, clayey soils, as suggested by Holden et al. (2012). The procedure was a slightly modified version of that outlined by Santamarina et al. (2002) and Cokca & Birand (1993).

One gram of soil passing the #200 sieve was dispersed in a beaker filled with 50 mL of DDI water and set on a magnetic stirrer. While under constant agitation, a 0.01 N solution of methylene blue was titrated in 0.5 mL increments. Following each addition of methylene blue, the solution was permitted to mix for one minute. After mixing for one minute, a drop of the mixture was deposited onto a piece of filter paper. This process was repeated until the sample became saturated, which was indicated by a light blue “halo” that formed around the drop of solution. The point at which a halo forms around the droplet is considered the end point. Five more samples, taken at one-minute intervals, were deposited onto a filter paper to verify this end point; if the blue halo remained, the end point was considered verified. Alternatively, additional methylene blue was required. The experimental setup and an example of the blue halo that forms around the droplets are shown in Figures 3.1 and 3.2, respectively.

To calculate the CEC, the following Equation is used:

$$CEC = \frac{100}{M_s} * V_{MB} * N_{MB} \quad [3.1.1]$$

Where:

M_s = the mass of soil in grams (g)

V_{MB} = the volume of the methylene blue solution added (mL)

N_{MB} = the normality of the solution used (mEq/L)

Therefore, when using these proportions, the CEC = volume of methylene blue added (mL).

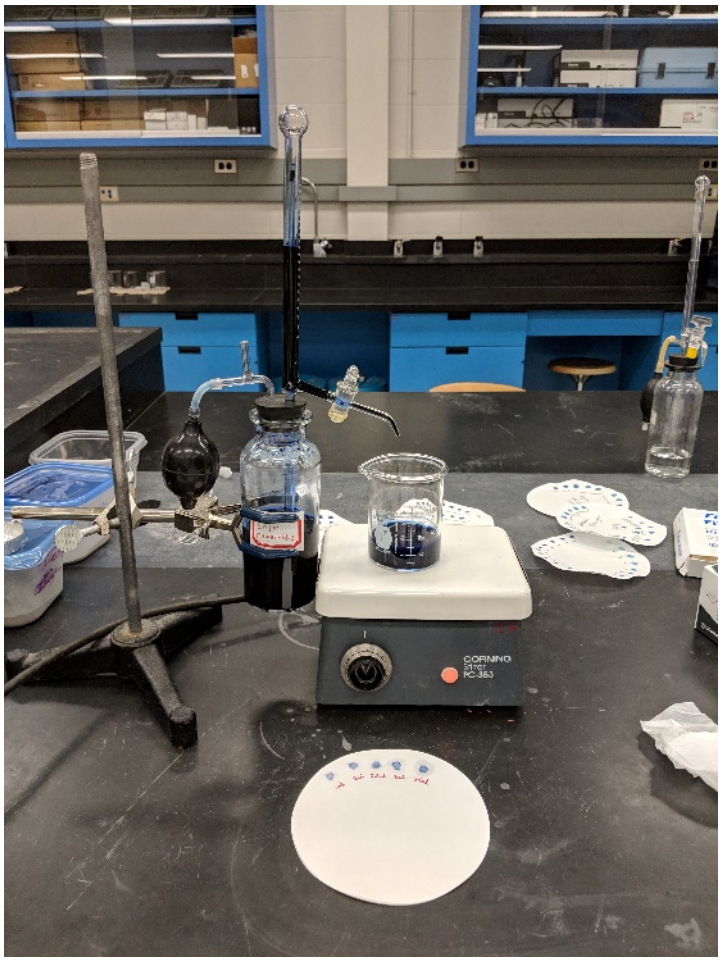

Figure 3.1: The experimental setup used for CEC testing**.**

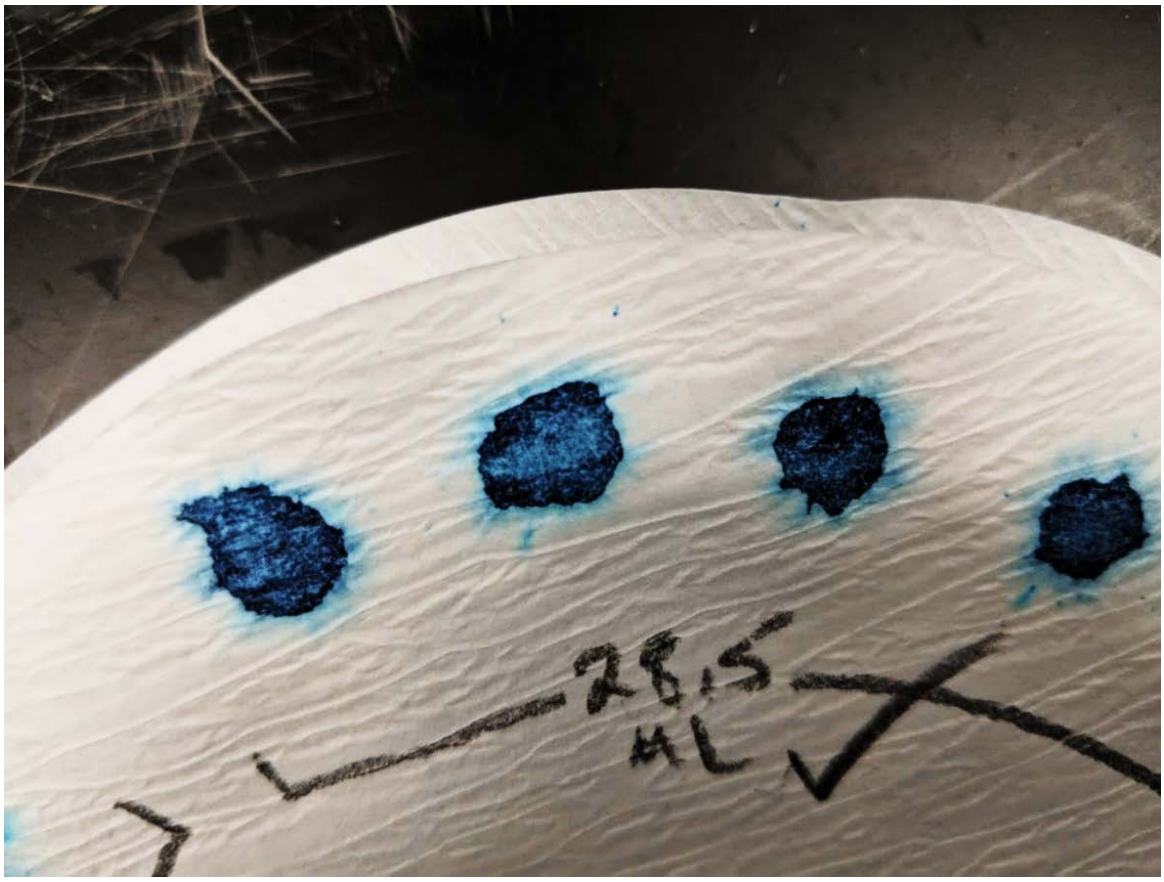

Figure 3.2: An example of the blue halo that forms at the end point of a methylene blue spot test.

3.1.3 Porewater Analysis

In attempt to best represent insitu conditions during testing, reverse engineered synthetic porewaters were created for each of the four soils. The use of a synthetic porewater solution to measure soil properties, such as residual shear strength, has been shown to yield more representative insitu values that those obtained using DDI water (Moore, 1991).

To create a synthetic porewater solution, small samples of a soil's actual porewater were obtained by consolidating reconstituted samples at their insitu moisture content. Clean tubing was attached to ports at the base of each consolidation apparatus, so that the expelled porewater could be collected. No water was added during the reconstitution of these samples, as they had been stored in a humidity-controlled room which permitted them to have a sufficiently high insitu moisture content. The apparatus used to squeeze the porewater from each soil sample is shown in Figure 3.3.

Samples were analyzed via inductively coupled plasma mass spectrometry (ICPMS) to determine their cationic compositions. Ion chromatography (IC) testing was performed to determine the anionic concentrations in each solution. Following IC analysis, the pH, electrical conductivity (EC), Total Dissolved Solids (TDS), and alkalinity of each sample were determined. The pH, EC, TDS, and alkalinity measurements were used for quality assurance and control during the creation of synthetic solutions.

Figure 3.3: The apparatus used to collect porewater samples. Each tube connects to a sample of the same soil. The porewater collected from each tube was combined in a single beaker to create a single porewater sample.

3.2 Investigating the Mechanism

3.2.1 Qualitative XRD

Qualitative XRD analysis was performed on untreated and treated samples for each of the four natural soils. The purpose of the qualitative XRD analysis was to determine the extent of interlayer collapse induced by guanidinium salts. The samples were prepared using the Millipore transfer method outlined by Drever (1973). The Millipore transfer method was chosen because of its robust ability to saturate samples with a cationic solution (Moore & Reynolds, 1989). Soil samples were dispersed by a mechanical mixing apparatus into 300 mL DDI water. In the case of Regina Clay, the soil was first dispersed in 100 mL of a 5 g/mL sodium hexametaphosphate solution. After dispersing the Regina Clay in the sodium hexametaphosphate solution, an additional 200 mL of DDI water were added.

It was found through trial and error that without the use of the dispersant, the Regina Clay would create large flocculated particles incapable of being successfully deposited onto filter papers. Conventionally backpacked samples of Regina Clay were scanned in the XRD with and without dispersant. It was found that there was no difference in outcome from the guanidinium salt treatment. Therefore, the dispersant was permitted for use during the Millipore transfer method.

Following dispersion, each slurry was placed in an ultrasonic bath for 15 minutes. After 15 minutes, the slurries were decanted and centrifuged for 3 three minutes at 1000 RPM. Using equations provided by Moore and Reynolds (1989), it was determined that these specifications would separate out all particles larger than 2 µm. After centrifuging, the supernatant (process yield) was decanted.

For untreated slurry samples, the supernatant collected after centrifuging was deposited onto a 0.45 µm filter using the Millipore apparatus (process shown in Figure 3.4). Care was given to ensure that the time of deposition and level of suction during deposition was consistent. Diligence regarding these two aspects of sample preparation was paramount to ensure uniform thicknesses among all samples. Sample thickness were maintained at approximately 1 mm to create an infinitely thick sample for XRD purposes.

Supernatants intended for treated samples were spiked with 0.1 M or 1.0 M GuCl solutions during deposition onto the filter paper using the Millipore apparatus. These solutions were then drawn through the filter cake that formed on top of the filter paper. In an effort to remove any excess salts, DDI water was then drawn through the filter cake. For a few samples, the DDI washing was followed by washing with a synthetic porewater solution to verify whether the peak collapse was reversible upon re-exposure to insitu conditions. In cases where synthetic porewater was used, samples were rinsed with DDI a final time to remove any excess salts during exposure to the synthetic porewater solution.

To verify that complete saturation of the sample was achieved in the process above, supernatants collected after centrifuging were directly mixed with saline solutions. The resulting slurry was subjected to constant agitation for 24 hours. These slurries were then deposited onto a filter paper in the same manner described above. The results from XRD analysis revealed that there was no difference between sample preparation methodologies. Therefore, the former was employed due to its efficiency.

After transferring the samples from their filter papers to a glass slide, as shown in Figure 3.4, samples were dried in an oven at 60°C for approximately five minutes. Following this drying period, samples were analyzed immediately. Samples were fixed in sample holders and mounted in an Empyrean XRD machine from PANalytical. The apparatus was equipped with a 1° fixed slit on the incident ray. Samples were analyzed from 3° to 50° using Cu Kα radiation. A step size of 0.16 2θ was used. All samples were analyzed in both their air dried and glycolated states.

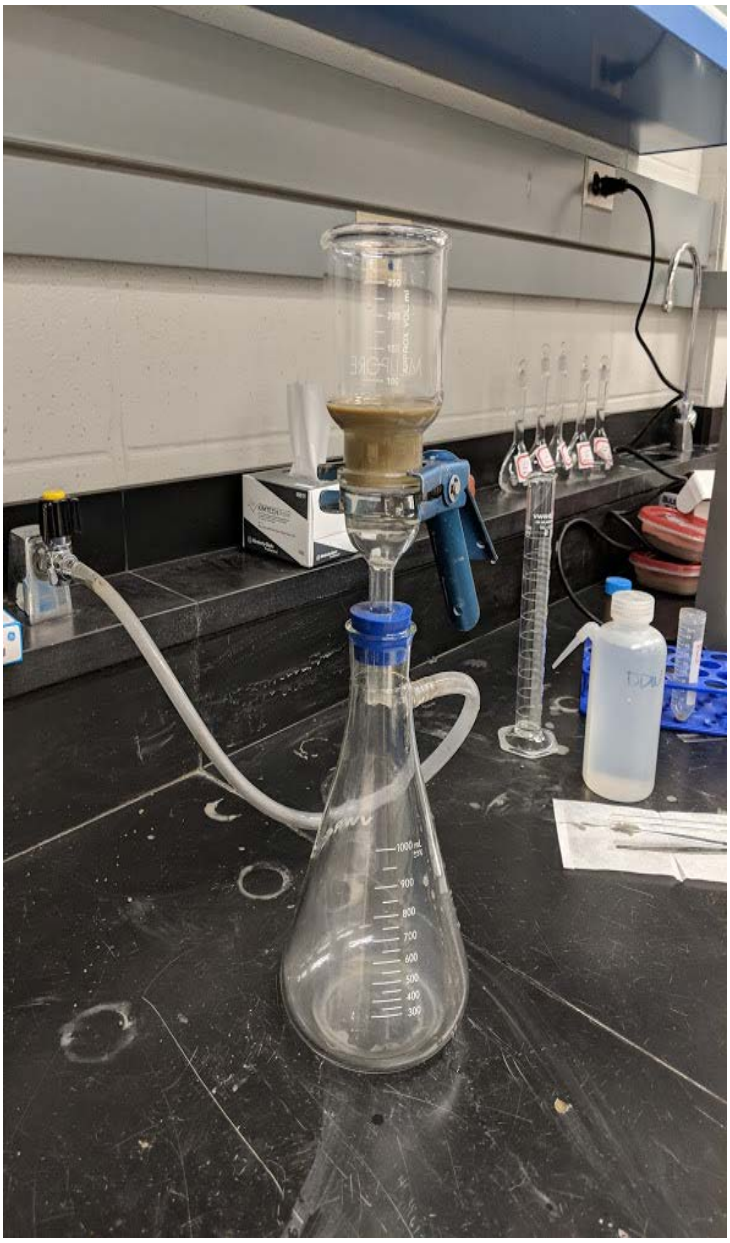

a.)

b.)

c.)

Figure 3.4: a.) Depositing a sample onto a 0.45 µm filter via a Millipore apparatus; b.) a sample deposited onto a glass slide; c.) a sample mounted in the XRD sample holder.

3.2.2 Batch Ion Exchange Testing

A batch-style series of tests were conducted to analyze the changes in cation composition within the bound water of Regina Clay after adding guanidinium salt. Regina Clay was dried, ball-milled, and sieved so that only the fine-grained fraction was retained. The soil was partitioned into 10 g amounts in individual centrifuge tubes. Solutions of NaCl, KCl, GuCl, and $CaCl_2$ at respective concentrations of 0.05, 0.1, and 0.5 normality (N) were added to the 10 g mass of dried Regina Clay. These twelve samples were prepared at a 2:1 liquid to solid ratio. All slurries were subjected to agitation for 7 days. After the 7-day period, the samples were centrifuged multiple times, with their supernatant being the yield each time. Following centrifuging, the samples were filtered to 0.45 μm to ensure a complete removal of fines. Finally, samples were preserved using nitric acid and their cationic compositions were analyzed via ICPMS.

3.2.3 Scanning Electron Microscopy and Environmental Scanning Electron Microscopy

High magnification Scanning Electron Microscopy (SEM) was performed on Regina Clay and two commercially available soils. The two commercially available soils were a calcium bentonite and pottery clay (kaolinite). The two manufactured clay products were used as controls to compare the images obtained from the Regina Clay.

The purpose of the imaging was to investigate possible changes in clay fabric induced by guanidinium salts. Samples were homo-ionized by repeated washings of NaCl, KCl, GuCl, and $CaCl_2$ solutions at strengths of 0.05, 0.1, and 0.5 N, respectively. After homo-ionization, the samples were washed with DDI water to remove any excess salts. EC measurements were taken after each washing until a residual conductivity was obtained. In total, 12 treated samples were prepared. Samples were sputter coated with gold prior to mounting. Imaging was performed using a Hitachi SU8010. Mounted samples and SEM device are shown in Figure 3.5.

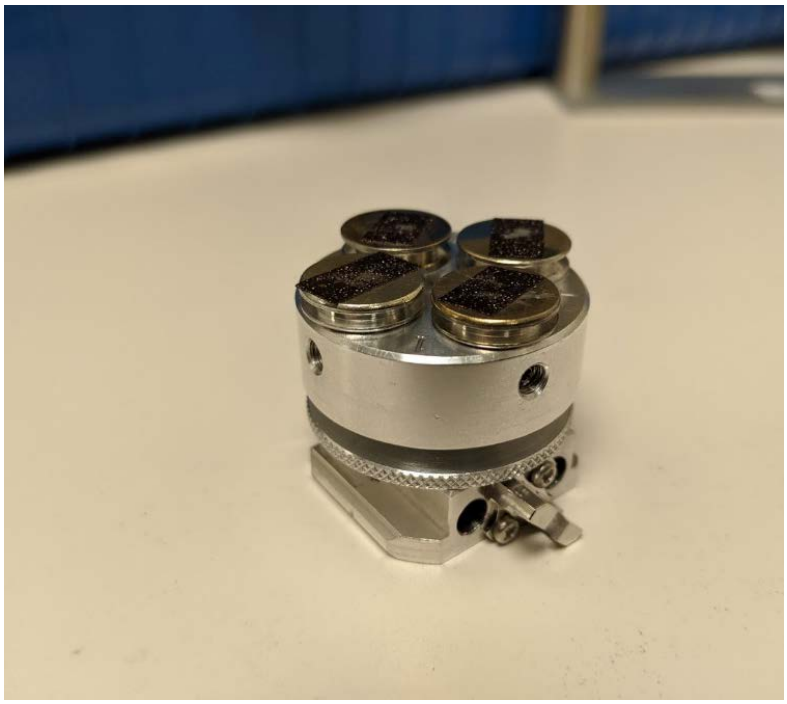

a.)

b.)

Figure 3.5: a.) Sputter coated and mounted SEM samples; b.) Hitachi SU8000 SEM device.

Environmental scanning electron microscopy (eSEM) was performed along the sheared surfaces of untreated and 0.1 M GuCl treated Regina Clay samples. The samples were sheared in a Bromhead ring shear apparatus, as described in Section 3.3.1. Post-shearing, samples were unloaded and carefully removed from the apparatus. Each piece was comprised of a “top” and “bottom”, as shown in Figure 3.6. Before imaging, each sample was separated along the shear plane. Several samples were damaged during this process; however, some samples contained clearly defined shear planes and were separated with ease. An example of an easily separated sample is shown in Figure 3.6.

Figure 3.6: A sample used for eSEM. Note the clearly defined shear plane between the two pieces of clay.

After exposing the shear plane, samples were placed in a Zeiss EVO LS15 EP-SEM instrument, located at the University of Alberta, for imaging. The chamber conditions during imaging were 4°C with a relative humidity of 50%. These settings were chosen based upon the conditions that samples were sheared in (see Section 3.3.1 for more details). The relative humidity of the chamber was lower than that of the humidity during the shearing of each sample, however, a relative humidity in excess of 50% did not allow for clear images. Despite this less than ideal condition, samples were still relatively hydrated upon removal from the apparatus.

3.3 Quantifying the Effects and Assessing Potential Implications of GuCl Treatment

3.3.1 Liquid Limit Testing

Liquid limit testing was conducted using a fall cone apparatus, rather than a Casagrande cup, as the fall cone has been shown to yield more consistent values for clayey soils (Koumoto & Houlsby, 2001). Synthetic porewater solutions were made for all four natural soils, and then combined with guanidinium salts at concentrations of 0.05 M, 0.1 M, 0.25 M, 0.5 M, 1 M, 2 M, and 4 M. Soil samples were allowed to equilibrate with the wetting fluid for a minimum of 16 hours prior to testing. The liquid limits obtained using guanidinium salts were compared with those obtained with DDI water and the synthetic porewater solution. For Regina Clay, the same experiment was conducted on fresh samples using potassium chloride (KCl) with the intent of comparing the effects of guanidinium treated to potassium treated samples.

3.3.2 Ring Shear Testing

The residual shear strength of Regina Clay was determined in a variety of conditions using a Bromhead ring shear apparatus (Figure 3.8). The objectives of the ring shear testing were to 1.) quantify the increase in residual shear strength that can be attributed to altering the soil's porewater with guanidinium salts; and, 2.) determine the permanence of this treatment technique.

Samples were prepared by mixing either DDI water or synthetic porewater with the finer <0.075 mm fraction of Regina Clay at the liquid limit. Samples were placed within the ring shear mould, surrounded by a bath of the wetting fluid, and confined by a 5 kPa load for 24 hours to ensure no air was trapped within the sample. Following this 24 hour period, the sample was consolidated in a stepwise fashion to a desired normal stress. The normal stresses tested were 100, 200, and 400

kPa. The ring shear apparatus was located in a climate-controlled room which ensured a temperature of 3°C and relative humidity >50% was maintained.

After consolidation was completed, the sample was sheared at a rate of 0.003 mm/min in an attempt to minimize any excess porewater pressure that may have developed during shearing. This rate of movement would be categorized as a very slow to slow moving landslide as per Cruden and Varnes (1996). Additionally, the nature of landslides that are intended to be remediated by GuCl intervention are very slow moving (Christiansen, 1983; Sauer, 1984). Therefore, this shearing rate also aimed to replicate field conditions while maintaining reasonable testing times. After approximately 25 mm of displacement occurred, the samples appeared to reach their residual shearing resistance. After reaching a residual state, shearing was halted while the normal stress was increased. In some instances, once the sample reached its residual shearing resistance, the bath surrounding the sample was exchanged for a 0.1 M GuCl solution without stopping the shearing process or changing the applied normal stress. In cases where a saline bath was implemented, the bath was refreshed every 24-48 hours to ensure close to steady-state conditions were maintained.

The EC of the bath solution was used as a surrogate measurement of the salt content. Measuring EC during geotechnical testing as an estimate of salt content has been done by several past researchers (Kenney, 1967; Tiwari, et al., 2005). EC was monitored using an Atlas Scientific EC meter. A datalogging code written in Python was incorporated with the EC meter to automate and regulate the timing at which measurements were being taken. The EC meter was placed in a vial with two holes drilled in it. Tubes were connected to each hole; each tube corresponded to the inlet and outlet of a peristaltic pump, respectively. The pump ensured a constant agitation of sample's bath, and a transient sample of liquid to be drawing EC measurements from. A photo of this set-up is shown in Figure 3.9.

The "treated" residual shearing resistance was taken after samples achieved a new residual shearing resistance and the EC became steady-state. On two separate occasions, while continuing to shear the sample, the GuCl solution surrounding the sample was removed from the bath container after the treated residual shearing resistance had been established. After removing the GuCl solution, the bath container was rinsed with DDI to remove any excess salts. Next, the bath

was reverted to a fresh DDI water or synthetic porewater solution. The DDI water bath or synthetic porewater solution was refreshed every 24-48 hours with regular EC measurements until the bath reached a steady-state EC. The residual shearing resistance of the sample was monitored for changes to address the permanence of GuCl treatment for smectitic clays. A flow chart describing the complete process of the ring shear testing program is shown in Figure 3.7.

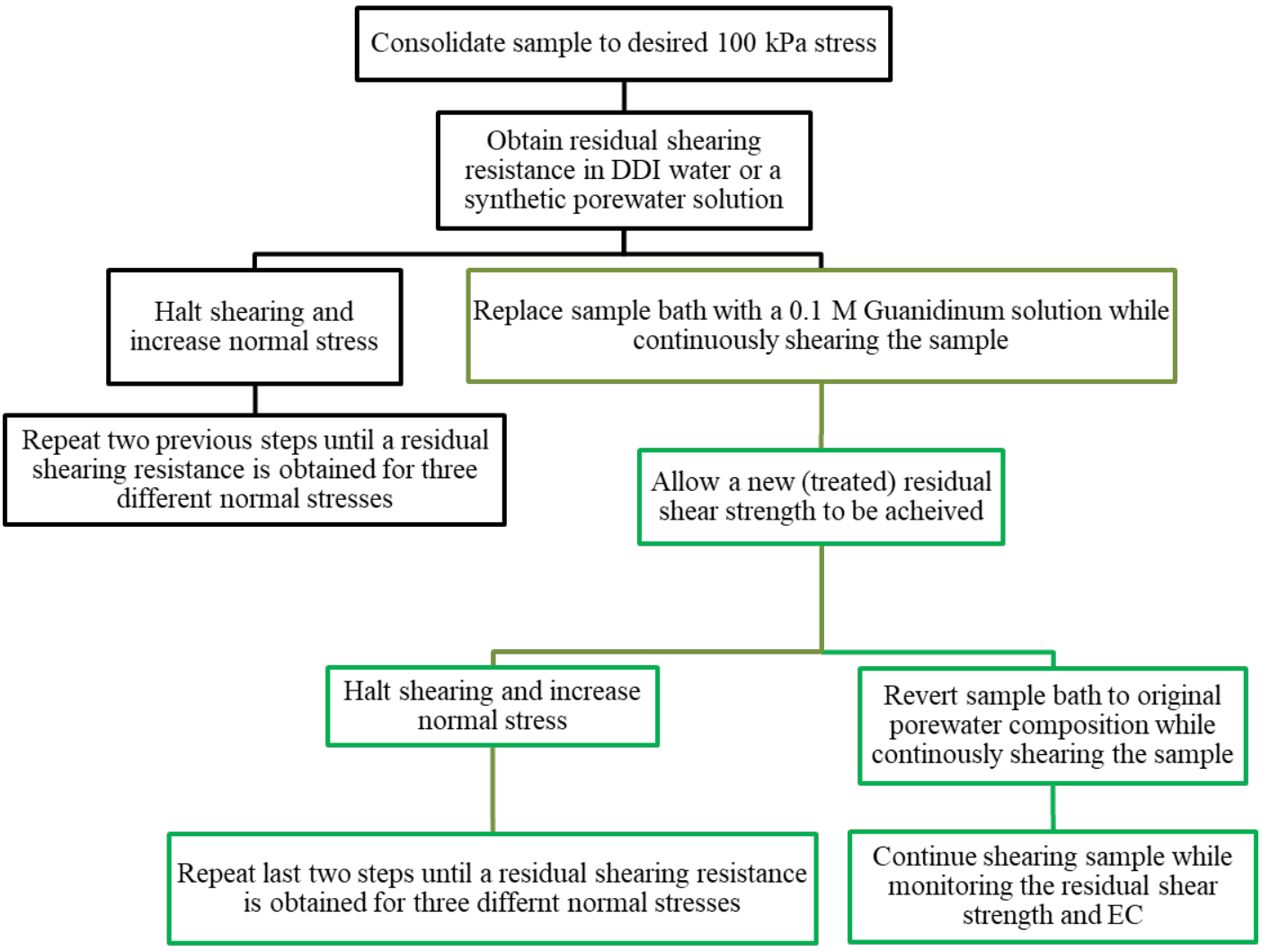

Figure 3.7: Work-flow for the different types of ring shear testing.

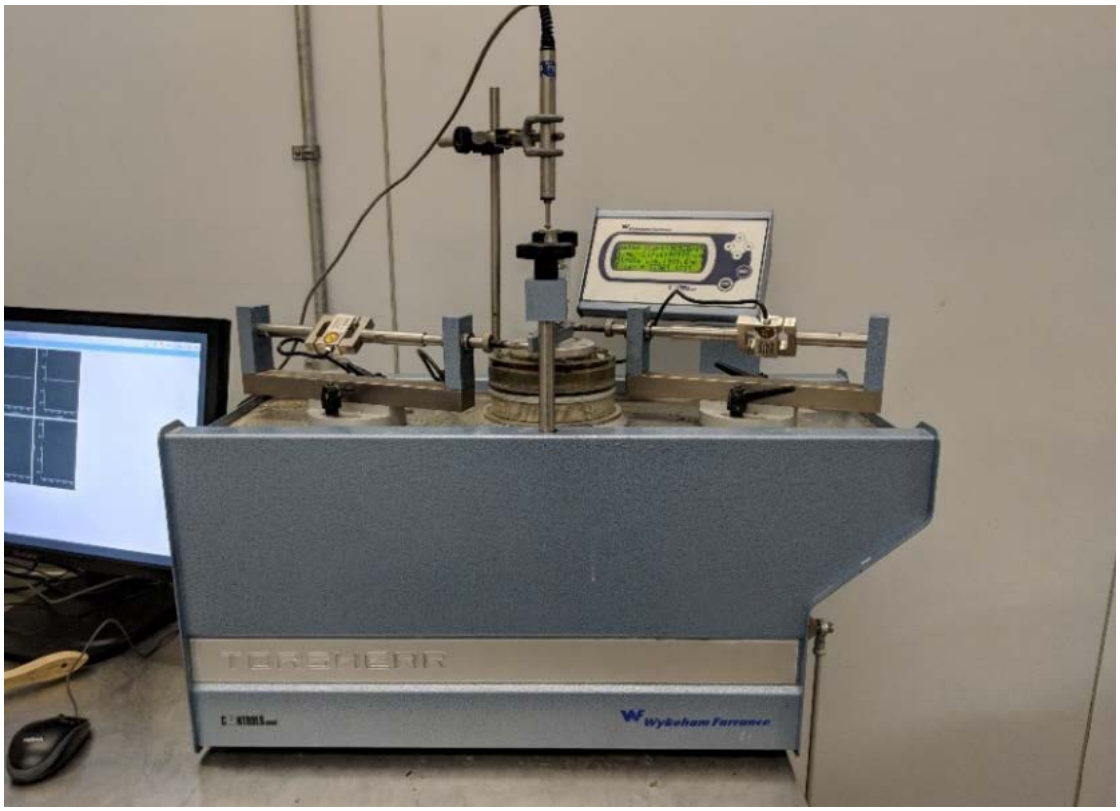

Figure 3.9: The Bromhead Ring Shear Apparatus used for testing.

a.)

b.)

Figure 3.8: a.) The EC probe; and, b.) the peristaltic pump set-up for ring shear testing.

3.3.3 Free Swell Testing

The free swell index of Regina Clay was assessed in a variety of saline solutions. The procedure followed was a slightly modified form of the methodology outlined in ASTM D5890. $CaCl_2$, NaCl, KCl, and GuCl were all used as wetting fluids. The purpose of this testing was to determine relative reducrtions in volume for a given soil under a variety of different daline solutions. The saline solutions had concentrations of 0.05, 0.1, and 0.5 N, respectively. Ten grams of dry soil were used as opposed to the ASTM recommended two grams. ASTM D5890 is typically employed to test the free swell index of Na-bentonite. Since Regina Clay would have a lower swell index than Na-bentonite prior to treatment, the differences between swell indicies obtained using different saline solutions would be harder to differentiate. Therefore, by using more soil, the differences between each saline solution were expected to be amplified.

Despite the increased amount of soil, a 100 mL graudated cylinder was still used. Soil was added in 0.2 gram increments as opposed to 0.1 grams. The experimental set-up is shown in Figure 3.10.

Figure 3.10: Experimental setup of all free swell index tests.

3.3.4 Oedometer Testing of Regina Clay

3.3.4.1 Assessment of Permeability and Stiffness

Samples of Regina Clay were prepared at a liquidity index of 1 to evaluate changes in the hydraulic conductivity and stiffness, due to modifying the soil's porewater with GuCl. Approximately 20 mm thick samples were prepared at their liquid limits using a synthetic porewater solution. Samples were placed in the testing apparatus (typical oedometer apparatus, shown in Figure 3.11) and confined with a seating load equivalent to the load platen for 8 hours. Following this 8-hour period, a 7 kPa load was applied. The previous two steps were taken to ensure to that no air bubbles were present in the sample. In total, five samples were prepared.

After the seating load, consolidation took place in a stepwise fashion up to 800 kPa before being unloaded. The bath surrounding each sample was refreshed every 24-48 hours to ensure a constant salt content was preserved throughout testing. Periodically, the sample bath would be rinsed with DDI water to remove excess salts from the bath container. EC measurements of each sample's bath were taken daily to ensure steady-state conditions were preserved throughout testing.

The permeabiltiy was assessed using the coefficient of consolidation as per Terzaghi's consolidation theory. The stiffness was assessed by comparing the slopes of the normal and recompression curves (i.e., the lambda and kappa values in a critical state soil mechanics framework).

3.3.4.2 Osmotic Consolidation

One dimensional osmotic consolidation testing was performed to quantify the volume changes that may be induced by adding GuCl to a smectitic soil's porewater regime. This testing was only performed on Regina Clay because the general soil characterisation showed that Regina Clay had the highest montmorillonite content.

20 mm samples were prepared in the same manner described in Section 3.3.4.1, albeit synthetic porewater was the only wetting fluid used. The subsequent workflow for any given sample is presented in Figure 3.13.

Samples were consolidated in a stepwise fashion, having the applied weight approximately doubled with each increment. One sample was used as a control (i.e., synthetic porewater was used throughout the entire consolidation process), while the other four halted consolidation at normal stresses of 45 kPa, 100 kPa, 200 kPa, and 400 kPa. When each sample reached its intended normal stress, the bath surrounding the sample was exchanged from a synthetic porewater solution to a 0.1 M GuCl solution. After the exchange, samples were monitored for changes in volume while having their bath refreshed every 24 to 48 hours. EC measurements were taken to ensure the salt content of the bath remained steady-state.

Figure 3.11: Typical Oedometer used for testing.

After completing the osmotic consolidation phase, all samples were loaded to 800 kPa, and subsequently unloaded to 45 kPa. At this point, the sample bath was reverted to a synthetic porewater solution. Once again, the sample was monitored for any changes in volume. After the sample showed a steady-state rate of strain, the sample was unloaded to 7 kPa.

In cases where volume change did occur, this data was used to assess changes in the R-A stress state. These changes were compared to theoretically determined values for a 0.1 M GuCl solution and results obtained from the ring shear testing.

Osmotic volume change has been known to occur on the same time scale as secondary compression (Barbour 1987). To distinguish the difference between secondary compression and osmotic consolidation, the slope of the secondary compression line was clearly established prior to introducing the saline porewater modifier. Any substantial deviations from a projection based upon the slope of the secondary compression line was attributed to osmotic consolidation. Osmotic volume change was complete when the slope of the compression curve matched the slope of the sample's initial secondary compression curve. Figure 3.12

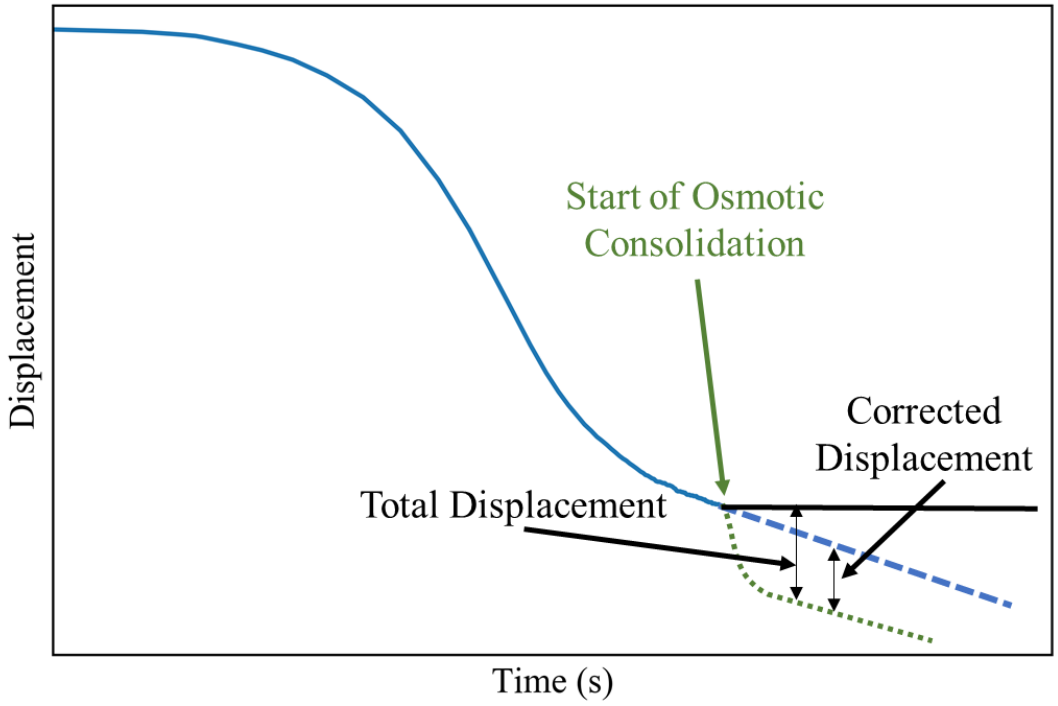

Figure 3.12: Typical image assessing the volume change due to osmotic consolidation. Adapted from Barbour (1987).

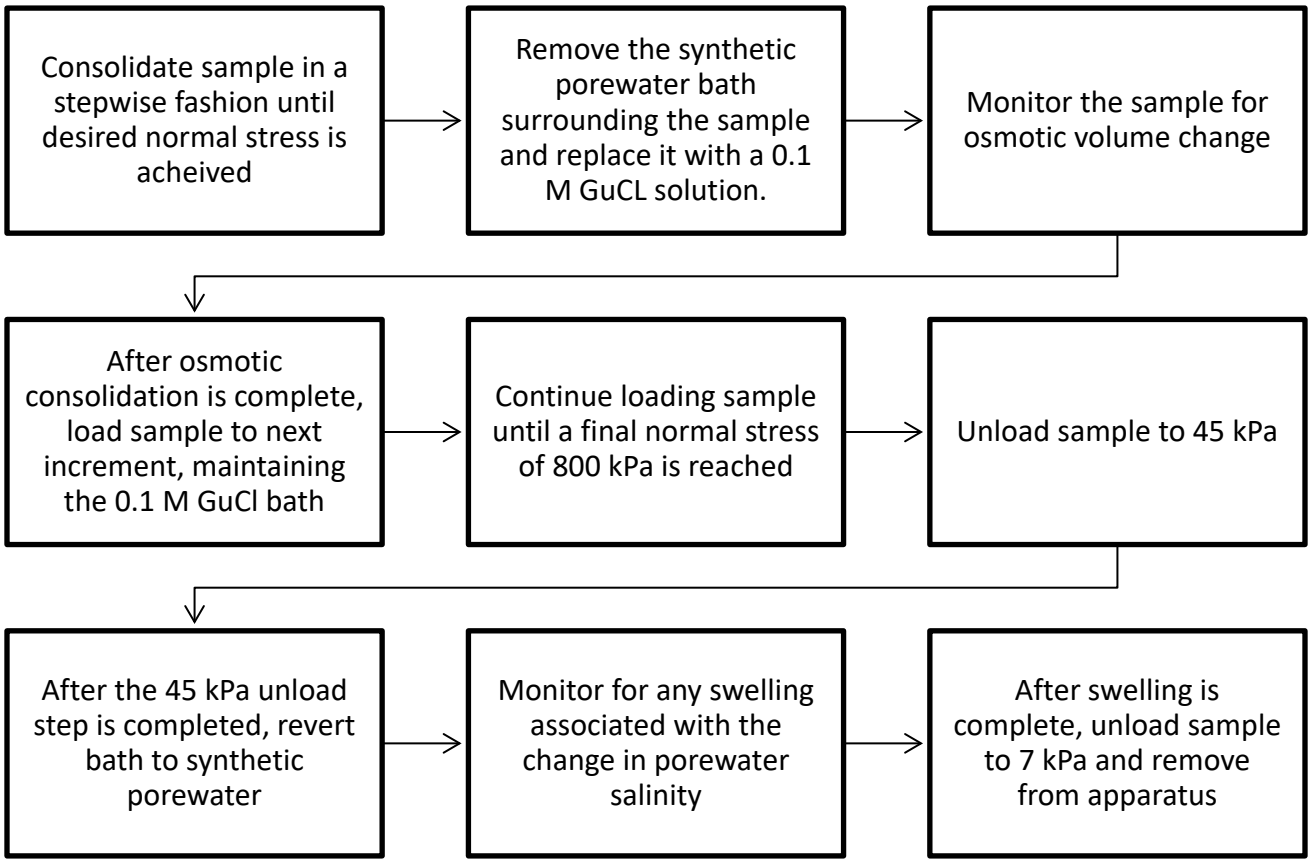

Figure 3.13: Workflow for osmotic consolidation testing.

Chapter 4 Results and Discussion

4.1 Introduction

4.1.1 General Soil Characterization

The grain-size analysis of the four natural soils is shown in Figure 4.1 It is evident that Regina Clay and Whitecourt Clay are fine grained soils, with 79% and 82% of the soils passing the #200 sieve, respectively. Hydrometer analysis of the four soils showed that Regina Clay, Whitecourt Clay, Floral Till, and Battleford Till have clay sized particle contents of 58%, 59%, 25%, and 15% respectively. The data obtained during the general soil characterisation is summarized in Table 4.1.

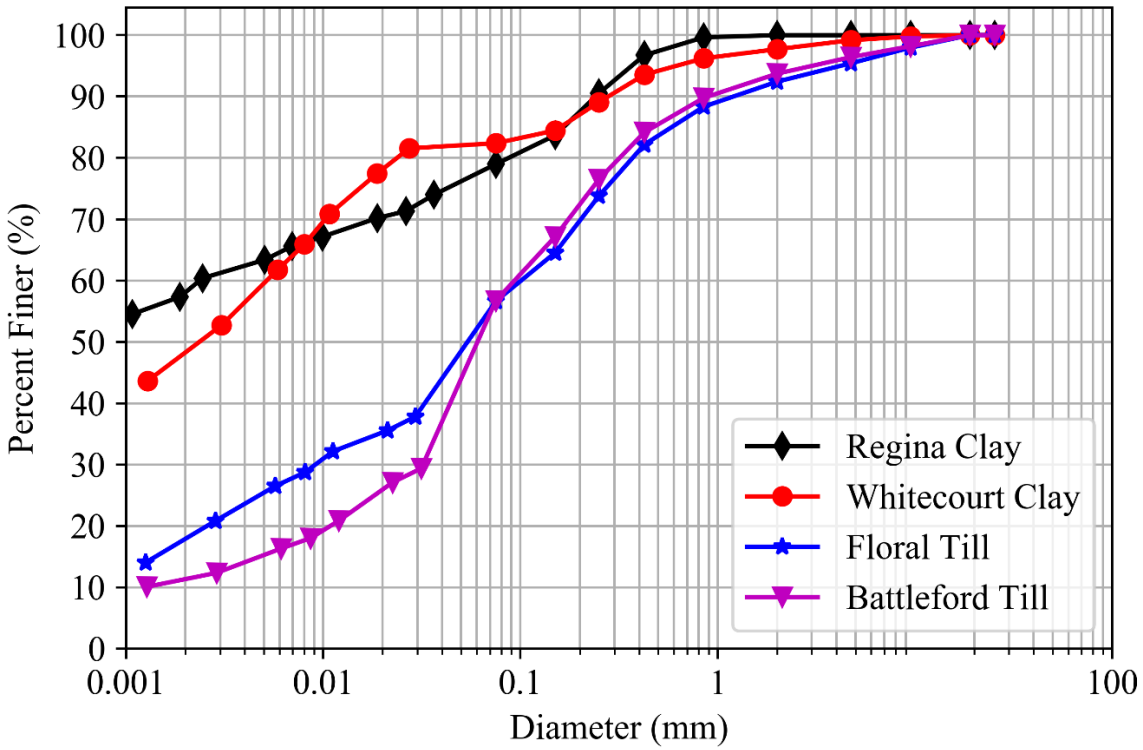

Figure 4.1: Grainsize analysis for the four natural soils.

Results from quantitative XRD and CEC testing are given in Table 4.1. The compositions listed have been normalized against the total clay content of each sample. Regina Clay has the highest montmorillonite content at 53%, while Whitecourt Clay, Floral Till, and Battleford Till have respective montmorillonite contents of 27%, 24%, and 40%. The two soils with the highest clay

contents yielded the highest CEC values. However, despite Regina Clay and Whitecourt Clay having a nearly identical amount of clay sized particles, Regina Clay's CEC value is nearly 70% higher. This finding is substantiated when considering the montmorillonite content of Regina Clay is double that of Whitecourt Clay.

The exchangeable sodium percentages (ESPs) of the four natural soils are given in Table 4.1. ESP can be used to assess the stability of a soil's fabric when in water. Regina Clay has a high montmorillonite content, high CEC value, and an ESP well above 2%, which are strong indicators of a dispersive soil (Mitchell & Soga, 2005). These three factors make the glacial lacustrine clay a good candidate for GuCl treatment; therefore, the majority of macroscopically observable geotechnical tests were performed on Regina Clay only.

4.1.2 Porewater Analysis

The piper (trilinear) plot given in Figure 4.2 and Table 4.2 show the porewater compositions of the four natural soils in mEq. All of the porewaters appear to have a somewhat mixed cationic composition, while sulphate dominates the anionic composition. The raw data given by the ICMPS results indicated that, for all four soils, the amount of potassium present was insignificant in comparison to the sodium content. Therefore, when regarding the lower left triangle of Figure 4.2, it is important to consider that the majority of the monovalent ions present are sodium.

4.1.3 Summary of General Soil Characterisation

Prior to the general soil characterisation, it was expected that both Regina Clay and Whitecourt Clay could be used to assess and quantify the changes induced by GuCl salts in natural soils. However, the results summarized in Table 4.1 show that Whitecourt Clay would not make an ideal candidate for GuCl treatment, given its low montmorillonite content. For this reason, the majority of the following test procedures were performed solely on Regina Clay.

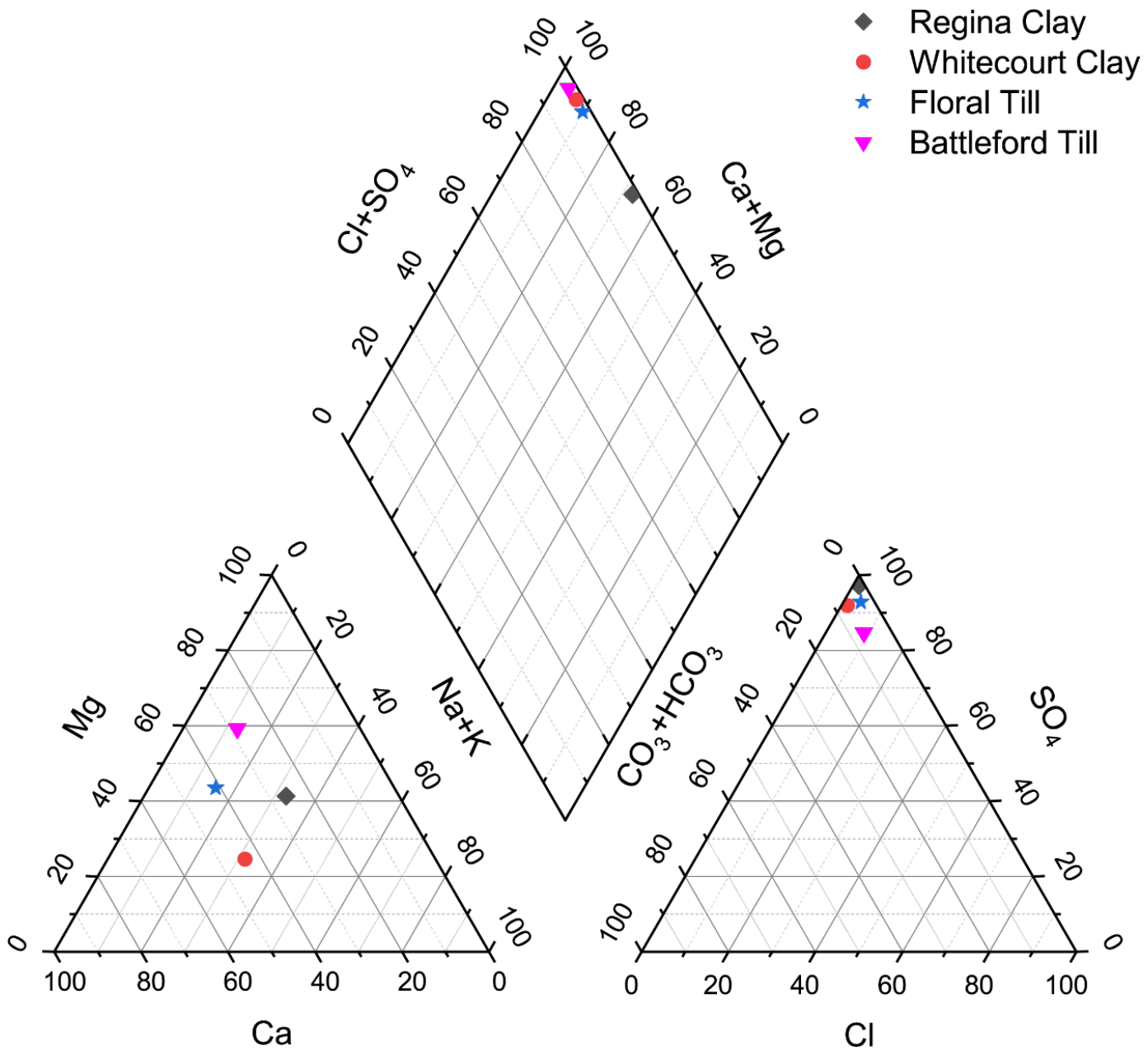

Figure 4.2: Piper (trilinear) plot of the insitu porewater ionic compositions.

Table 4.1: Clay Fraction, Quantitative XRD, CEC, and Exchangeable Sodium Percentage

Soil	Clay Fraction (%)	Montorillonite (%)	Illite (%)	Kaolinite (%)	Chlorite (%)	Activity	CEC (mEq/L)	Exchangeable Sodium Percentage (%)
Regina Clay	58	53, 55[1]	23, 30[1]	14, 15[1]	10, 0[1]	0.95	29, 31[1]	3
Whitecourt Clay	59	27	43	18	12	0.46	20	11
Floral Till	30	24	35	28	13	0.52	9	14
Battleford Till	15	40	20	31	8	0.64	6	4

[1]Fredlund (1975)

Table 4.2: Insitu Porewater Major Ion Compositions

Soil	Ca^{2+} (mg/L)	Mg^{2+} (mg/L)	Na^{+} (mg/L)	K^{+} (mg/L)	SO_4^{-2} (mg/L)	HCO_3^{-} (mg/L)	Cl^{-} (mg/L)
Regina Clay	515	497	715	10	4908	89	51
Whitecourt Clay	191	65	144	16	1233	114	12
Floral Till	533	342	205	32	2761	117	90
Battleford Till	167	211	76	10	1294	125	100

4.2 Investigating the Mechanism Results

4.2.1 Qualitative XRD

The purpose of the qualitative XRD analysis was to verify a collapse of the interlayer peak produced by guanidinium salts. Depending on the level of hydration, the 001 smectitic peak is visible around 6° 2θ in XRD space (Moore & Reynolds, 1989; Norrish, 1954a). A selection of the qualitative XRD scans from Regina Clay samples are shown in Figures 4.3 to 4.6. The results for an untreated Regina Clay sample in both the air dried and glycolated form are shown in Figure 4.3. Figure 4.3 also shows scans from 1.0 M and 0.1 M GuCl treated Regina Clay samples. The non-glycolated, untreated sample resembles a broad shoulder that begins around 5.0° 2θ, which is common for natural soils with interlayered smectites (Moore & Reynolds, 1989). Glycolation of the same sample is given in red, where evidence of smectite in the soil becomes apparent from the 1.7 nm peak at 5.2° 2θ. Additionally, glycolation revealed a small chlorite peak on the shoulder of this smectite peak.

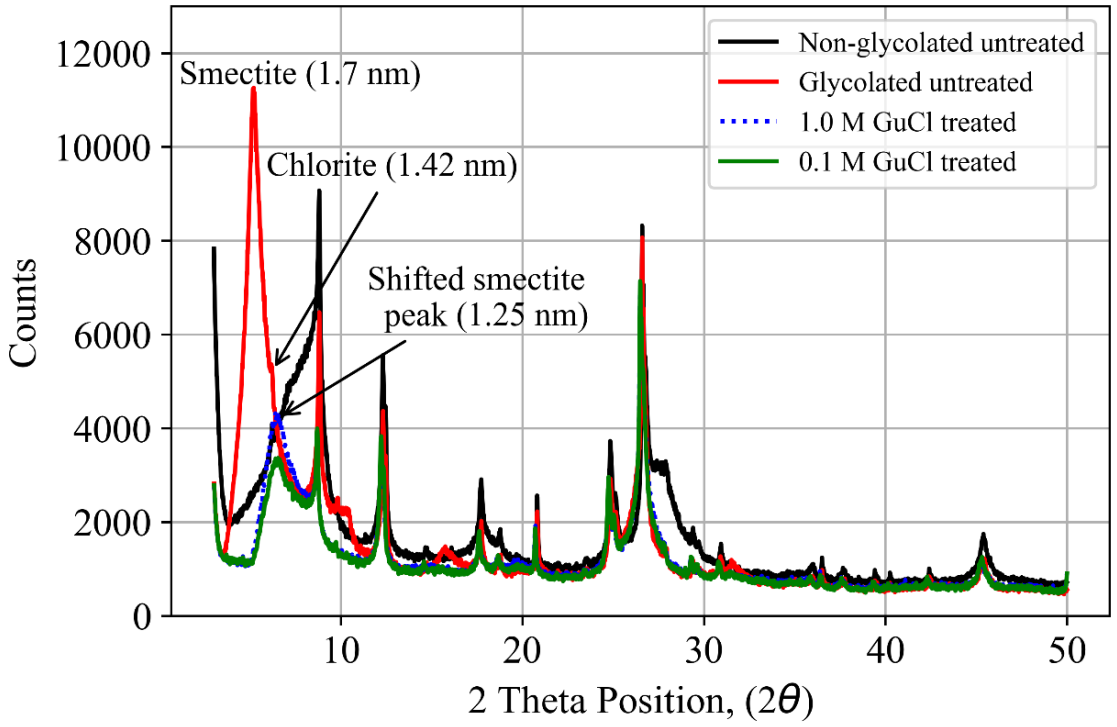

Figure 4.3: Regina Clay XRD traces.

Comparatively, the 001 smectite peak is no longer visible for the two treated XRD traces. It appears as though the smectite mineral's basal spacing collapsed to approximately 1.25 nm. However, the broad peak in this location suggests that the shift in the smectite peak is partially masked by the chlorite peak that is present at 6.5° 2θ. The 1.25 nm basal spacing is synonymous with a single layer of interlayer water as stated by Norrish (1954b), and is consistent with the peak spacings observed from Plötze & Kahr (2008).

There appears to be no difference in basal spacing between samples exposed to 0.1 M GuCl or 1.0 M GuCl. The lowest concentration tested was 0.1 M, therefore a threshold concentration for interlayer collapse was not established. However, based on this testing, treatment of smectite rich soils with a concentration of GuCl in excess of 0.1 M will cause only DDL-related changes.

Since the smectite peak was indistinguishable in the non-glycolated Regina Clay sample, confirmation of the smectite peak shift was verified in the other three natural soils. As shown in Figures 4.4, 4.5, and 4.6, there is an obvious collapse in basal spacing from approximately 1.5 nm to 1.25 nm. The range of initial basal spacings amongst samples has been attributed to variances in sample thicknesses and not a variance in the initial interlayer ion composition. The air dried basal spacing of a smectite interlayer with either Mg^{2+} or Ca^{2+} ions is 1.54 nm. Therefore, it was presumed that the interlayers of all four soils are originally populated by one of, or a combination of, these two divalent cations (Norrish, 1954b).

There are duplicate traces for the 0.1 M treated samples in Figures 4.4, 4.5, and 4.6, which represent samples that were re-exposed to a synthetic porewater solution after treatment, as described in Section 3. Based upon these traces, the interlayer effects caused by GuCl treatment will be permanent and the interlayer spacing will not revert back to its initial condition after being flushed with naturally occurring groundwater.

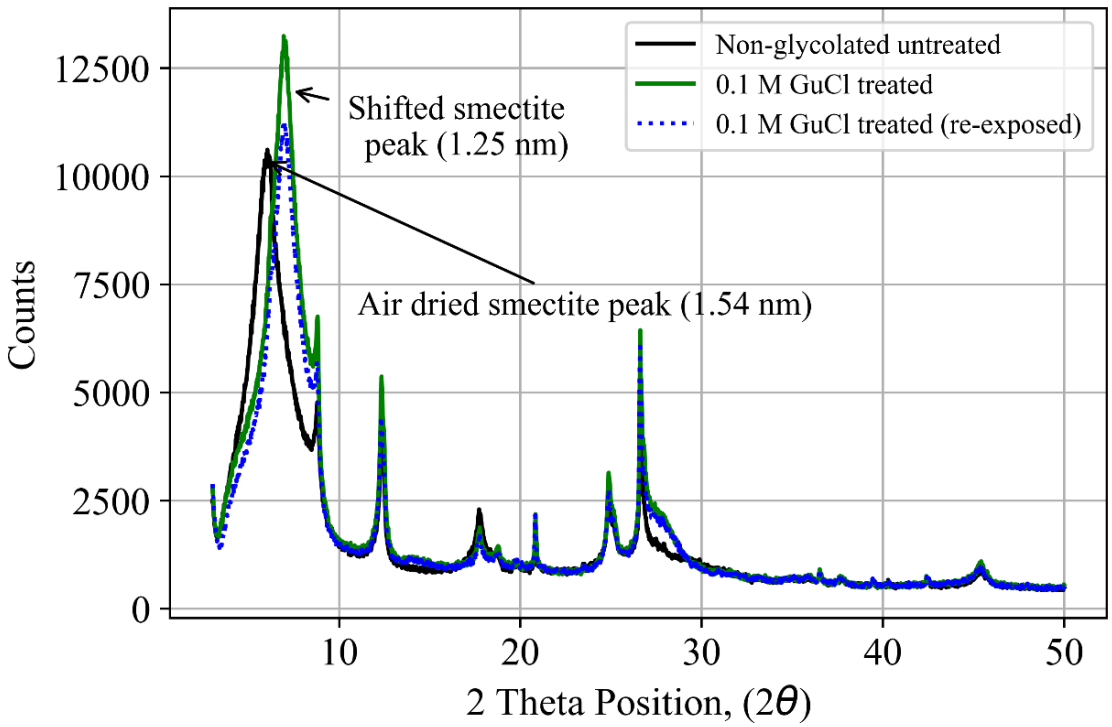

Figure 4.4: Whitecourt Clay XRD traces.

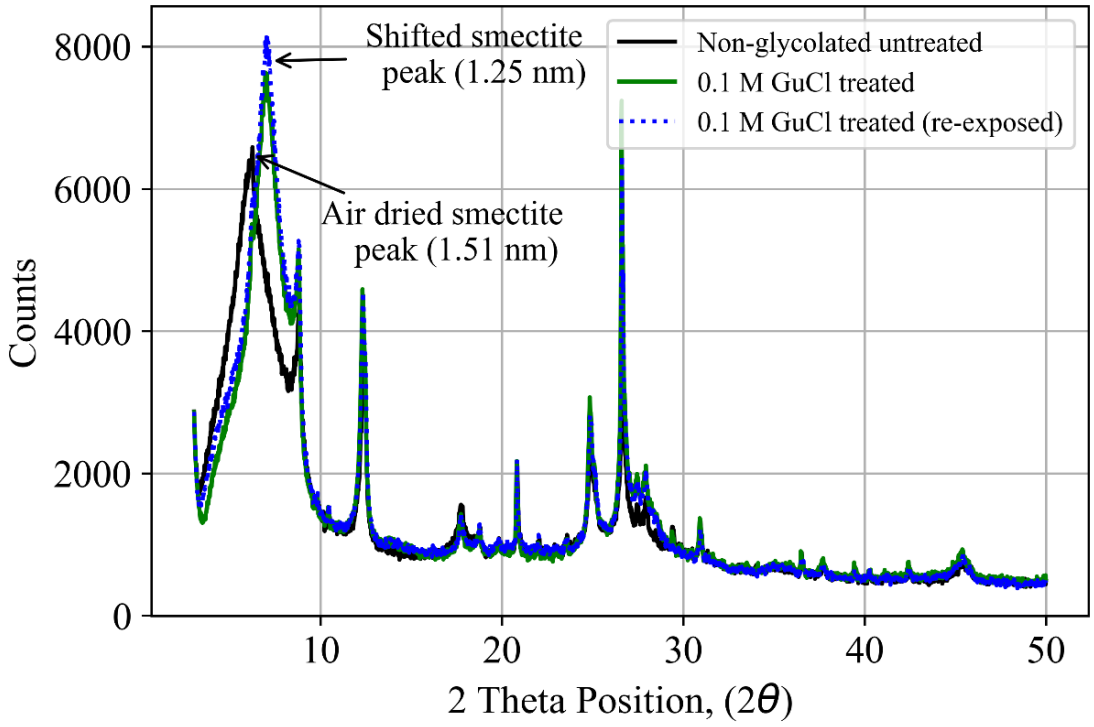

Figure 4.5: Floral Till XRD traces.

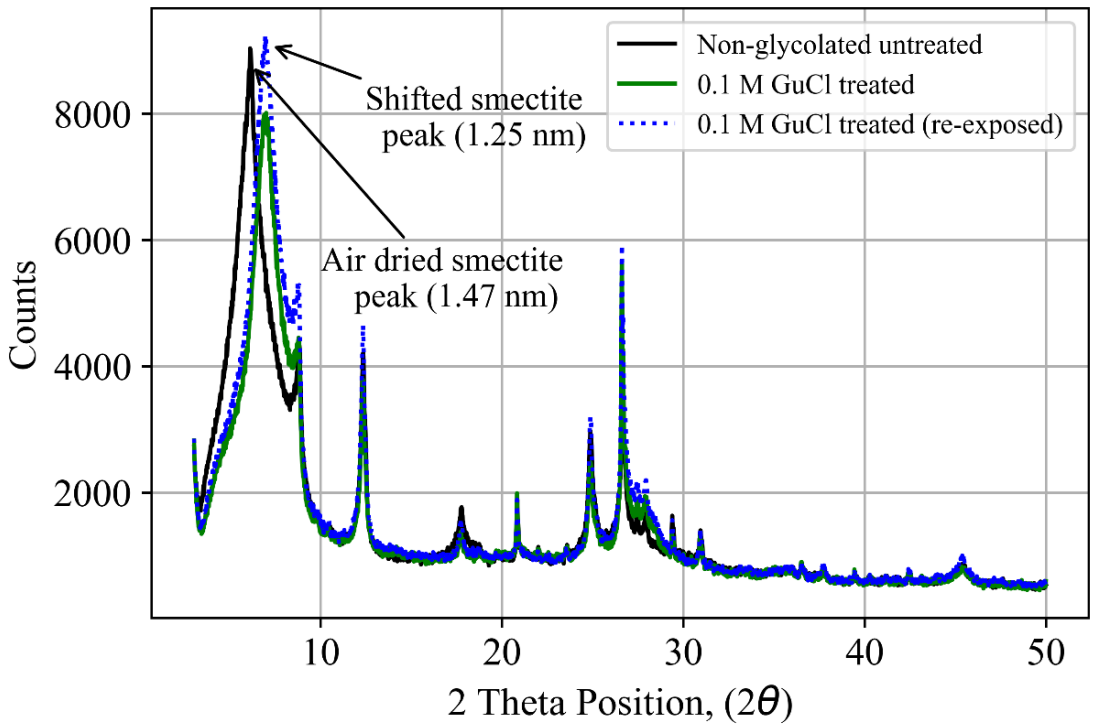

Figure 4.6: Battleford Till XRD traces.

4.2.2 Batch Ion Exchange

The batch ion exchange test was intended to: 1) verify that calcium was the dominant cation in bound positions within Regina Clay; and 2) measure the smectitic soil's sorption efficiency of the guanidinium cation relative to its CEC. Figures 4.7 to 4.10 show the results of the different batch ion experiments. The results from the ICPMS analysis have been represented in mEq on the y-axis and are plotted against the concentration of wetting fluid used. With increasing concentrations of saline solution, the concentrations of the other major cations in the free porewater increased. The increase of cations in the free porewater can be attributed to the displacement of these cations from bound water positions in the interlayer and DDL.

A ratio of the summation of the displaced cations to the CEC of the soil may be representative of the sorption efficiency for a given cation across various strengths of added saline solution. The cation of the added saline solution (i.e., Ca^{2+} for Figure 4.7) has been excluded from the results to allow for a comparison of only the displaced cations.

Based on Figure 4.7, the bound cations in Regina Clay are almost entirely divalent. Among the major cations, the concentration of Mg^{2+} in the free porewater was the only ion to increase by an appreciable amount. Analysis of Figures 4.8 to 4.10 indicate larger amounts of Ca^{2+}, relative to Mg^{2+}, being displaced into the free porewater solution. The larger concentrations of Ca^{2+} being released indicates that the bound ions are predominantly Ca^{2+}. This finding is in agreement with the claims made by Barbour & Fredlund (1989) and Fredlund (1975).

As stated earlier, comparing the summation of displaced ions yields a relative sorption efficiency. Therefore, the sorption efficiencies of the monovalent ions in increasing order are $Na^+ < K^+ < GDN^+$, at 52%, 81%, and approximately 100%, respectively. These results agree with the model proposed by Laird (1996), which states that with increasing solute concentration, montmorillonite will show an affinity for ions of smaller hydrated radii.

It is important to note that the sorption efficiency for the GDN^+ ion is greater than K^+ and, furthermore, that it is approximately 100%. The high sorption efficiency of the GDN^+ ion can likely be attributed to the ion's unique ability to vary in hydrated radii depending on its orientation. The term "approximately" is used to describe the sorption efficiency of GDN^+, as it can be seen in Figure 4.10 that the summation of the displaced cations exceeds the CEC. This finding suggests error in the measurements of cations via ICPMS or the measured CEC value. Given that the CEC values measured coincide with the work from past work with Regina Clay (Fredlund, 1975), this small discrepancy was deemed to be within the experimental error of the CEC and ICMPS method for measuring the concentration of cations in solution.

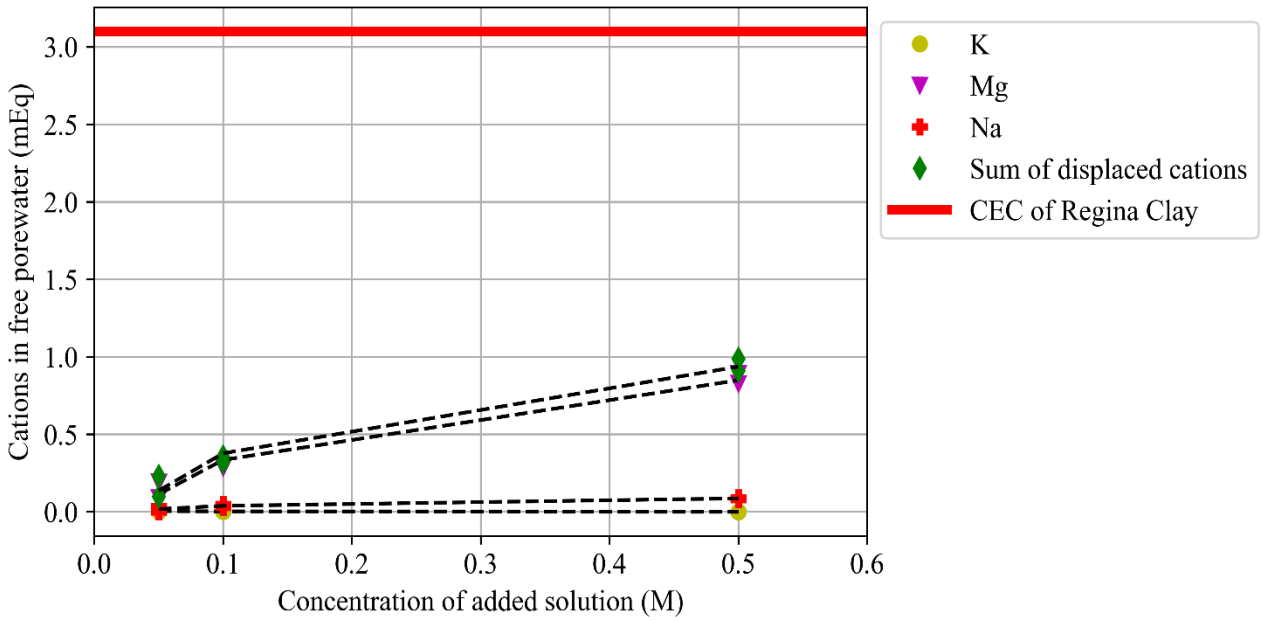

Figure 4.7: Cationic composition of Regina Clay free porewater with addition of $CaCl_2$.

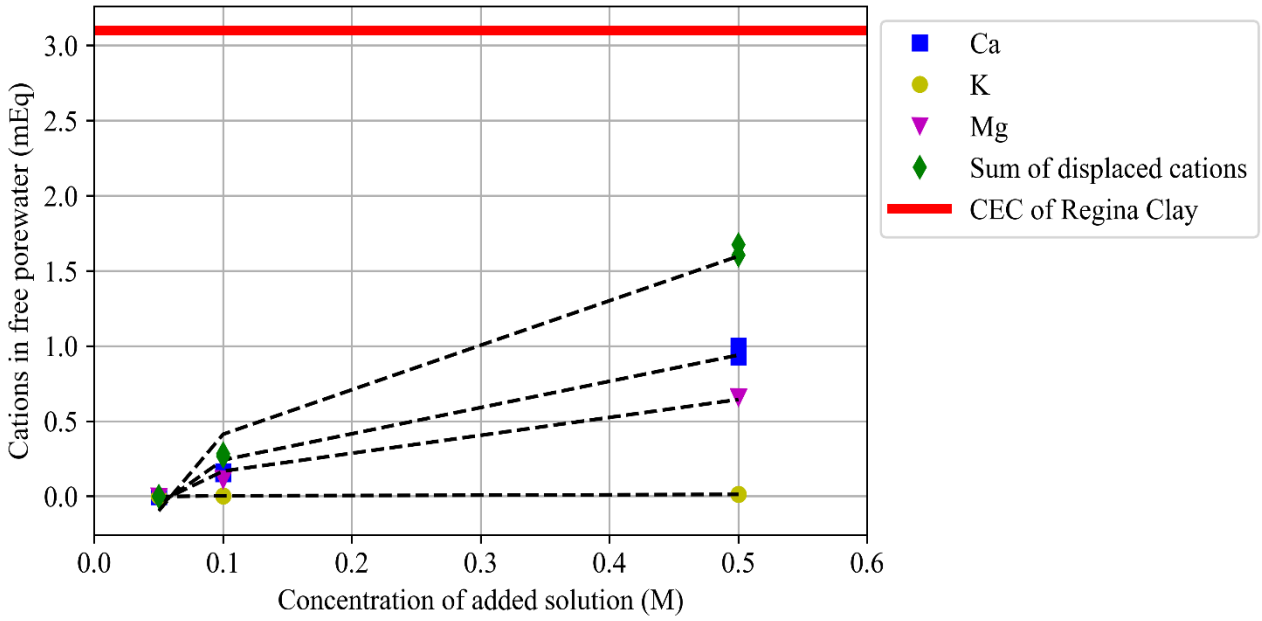

Figure 4.8: Cationic composition of Regina Clay free porewater with addition of NaCl.

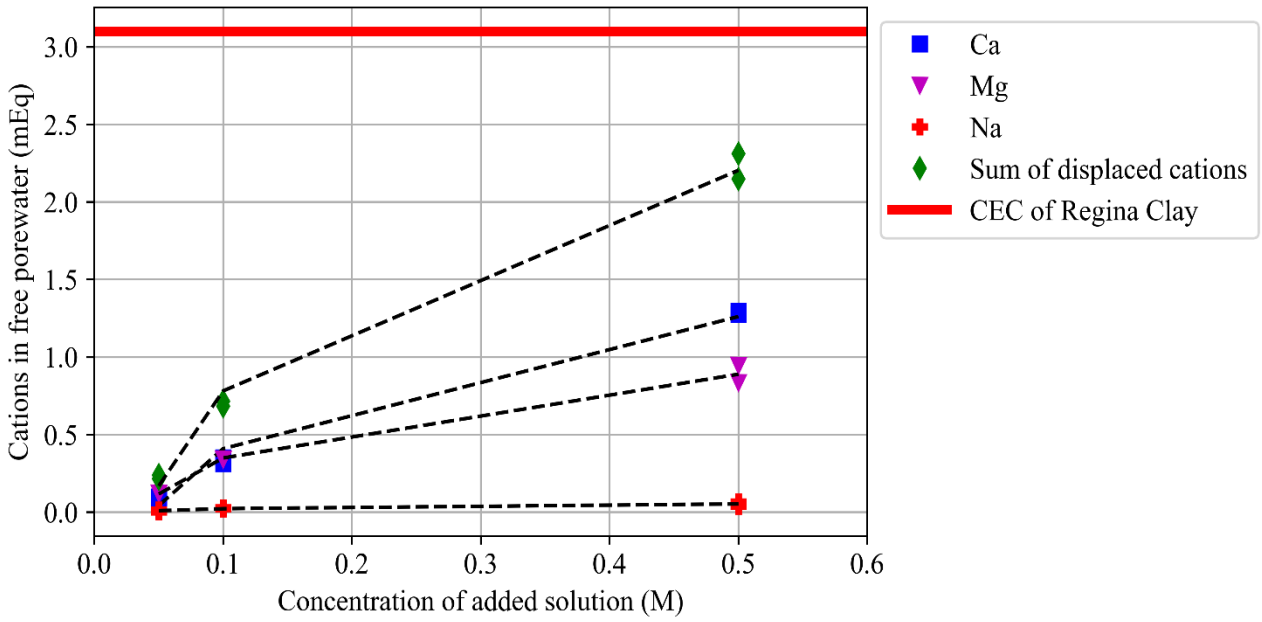

Figure 4.9: Cationic composition of Regina Clay free porewater with addition of KCl.

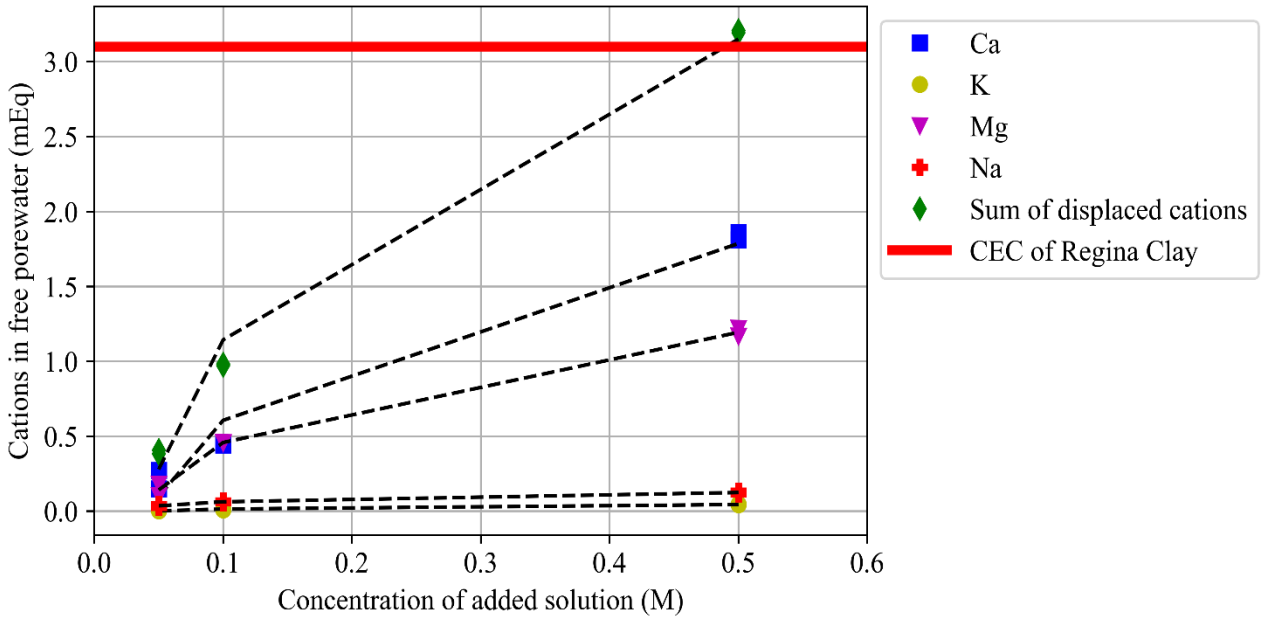

Figure 4.10: Cationic composition of Regina Clay free porewater with addition of GuCl.

4.2.3 SEM and eSEM

Images from the high magnification SEM analysis are presented in Figures 4.11 and 4.12. Figure 4.11 shows an untreated Regina Clay sample that was hydrated using DDI water, as described in Section 3.2.3. The most striking difference between the two images is the size of the clay particles. The particles in Figure 4.11 are, on average, significantly smaller than those shown in Figure 4.12. Since the larger particles shown in Figure 4.12 are domains of aggregated smaller clay particles, the term “effective” particle size has been adopted to describe the difference in sizes displayed in each figure.

The second major difference between the two images is the arrangement of the particles. In Figure 4.11, the clay particles are dispersed with minimal face to face aggregation. This structure allows for a larger area of the sample to be held in focus when being imaged. In comparison, the area of focus in Figure 4.12 is limited to a small section in the centre of the image, indicative of more face-to-face particle aggregation (i.e., the particles are stacking).

Maio (1996) made similar observations for a saline treated commercial bentonite when investigating increases in residual shear strength attributed to a saline porewater modifier. However, Maio was unable to conclude that there was any structural alteration in the shear surfaces of specimens. The images in Figures 4.11 and 4.12 oppose this opinion, as the increase in effective particle size and decreased uniformity is quite apparent and consistent among several images.

As discussed in Section 2.6, the mechanism of shear for platy clay particles, such as montmorillonite, is sliding (Lupini et al., 1981). Based upon these SEM images, it is expected that the increase in residual shear strength following GuCl treatment is at least partially associated with an alteration of the clay’s fabric. The larger effective particle size of the treated samples likely forces particles to override one another when a load is applied. Therefore, this increase in effective particle size may impair the sliding shear mechanism, allowing more force to be exerted when clay particles come in contact.

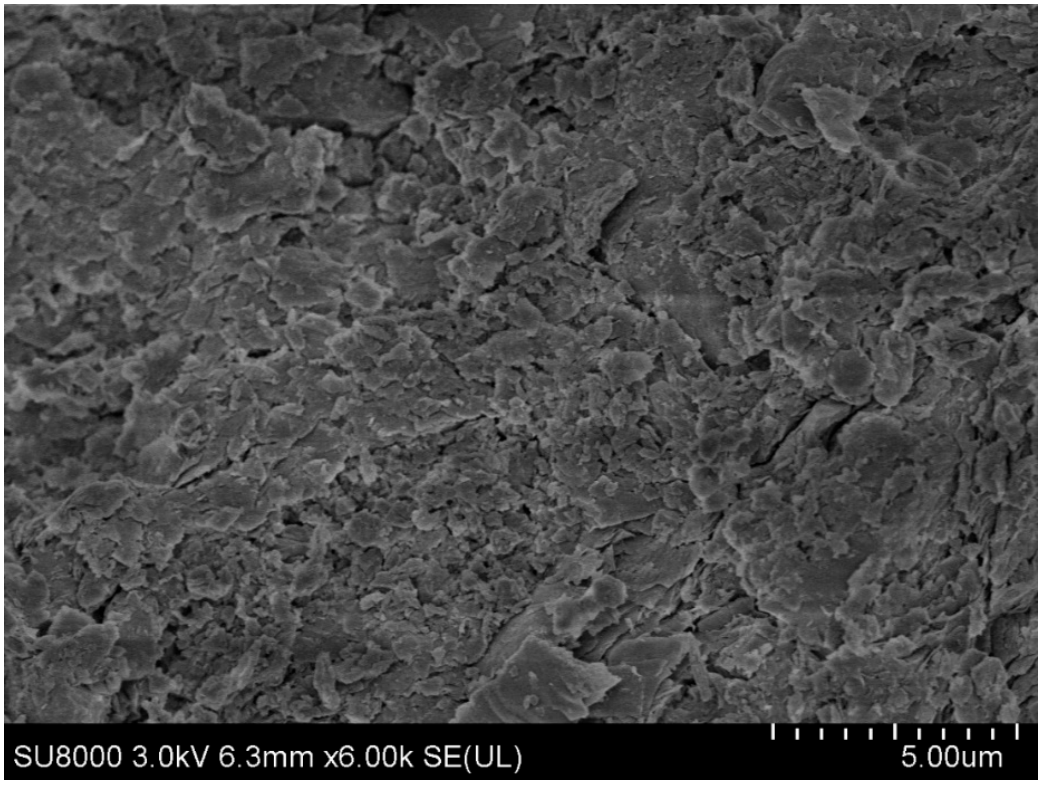

Figure 4.11: SEM image of an untreated Regina Clay sample at 6000x magnification.

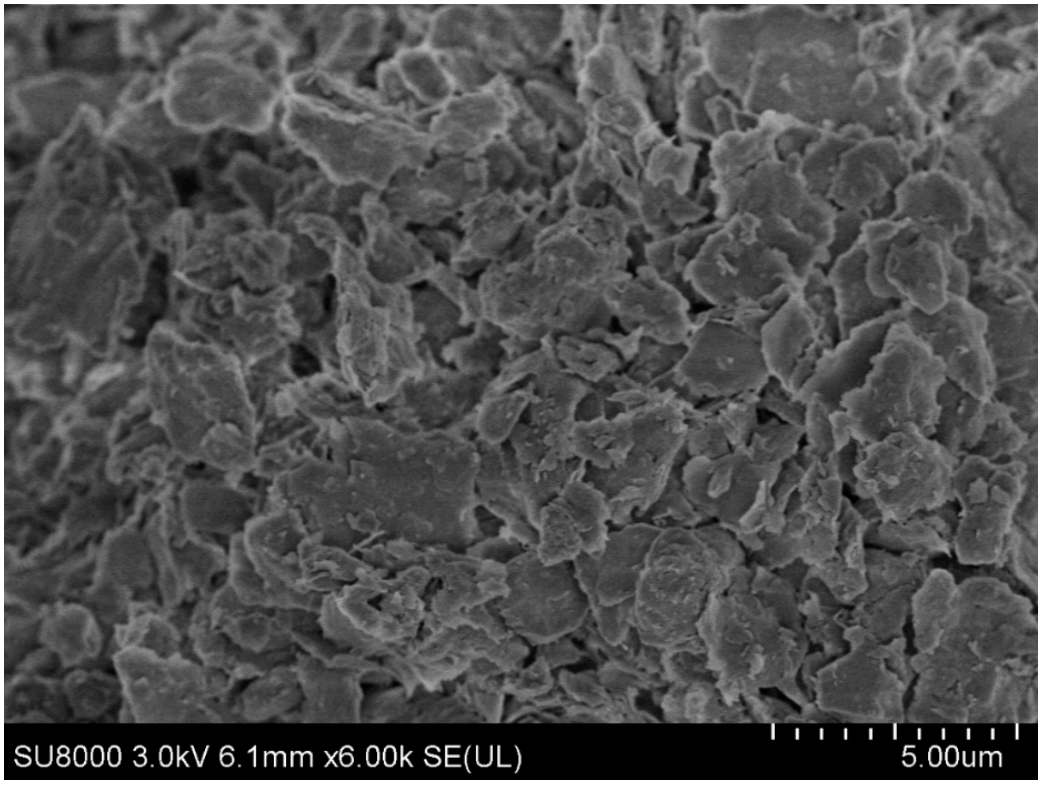

Figure 4.12: SEM image of an 0.1 M treated Regina Clay sample at 6000x magnification.

To examine this hypothesis, the shear planes of untreated and treated Regina Clay samples were imaged in an eSEM, as described in Section 3.2.3. The untreated and 0.1 M treated samples are shown at 100x magnification in Figures 4.13 and 4.14, respectively. In the untreated sample, attention is drawn to the vertical lineaments (micro striations), the texture of the shear surface, and the size of the desiccation cracks.

The micro striations are symptomatic of a slickenside surface forming at the shear plane. These characteristics are consistent with observations of several shear planes by Lupini et al. (1981) for a different low shear strength clay. Lupini et al. observed several shear planes with varying mixtures of coarse aggregate and high plasticity clay. They found that with decreasing clay content, the slickensides faded. Much like the samples with low clay fractions tested by Lupini et al., there appears to be no preferred orientation or slickensides in the 0.1 M treated sample. Instead, the surface of the shear plane in Figure 4.14 appears to be grainy, with several rotund looking particles.

The desiccation cracks in the untreated sample are much larger than those in the treated sample. Therefore, for an equivalent loss of moisture, less volume change has occurred in the treated sample. This finding suggests that the shrinkage limit of the soil has been reduced, which may be an additional benefit of GuCl treatment for soils that are exposed to climates that can cause large alterations of the moisture content of an expansive soil.

Considering the results from the XRD, SEM, and eSEM, there is a firm foundation of evidence that suggest the addition of GuCl to a soil's porewater regime causes mineralogical alterations that change the soil's fabric. It is likely that this change in fabric contributes to the increase in residual shear strength following GuCl treatment. Therefore, the increase in residual shear resistance is partially due to a mechanical phenomenon and cannot be entirely accounted for by True Effective Stress theory.

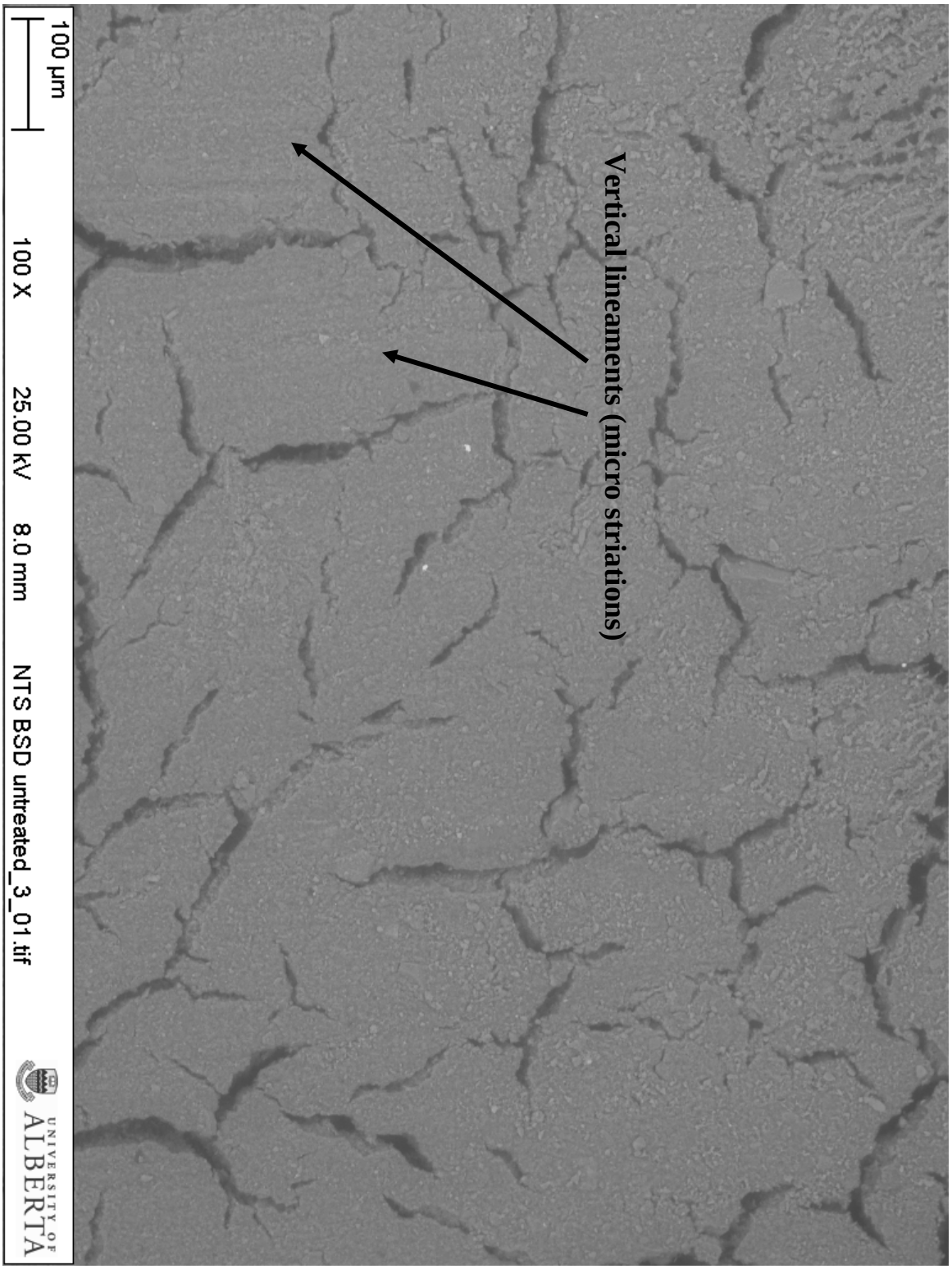

Figure 4.13: eSEM image of the shear plane of an untreated Regina Clay sample at 100x magnification. Note the vertical lineaments (micro striations) in the sample, and the “smooth” surface.

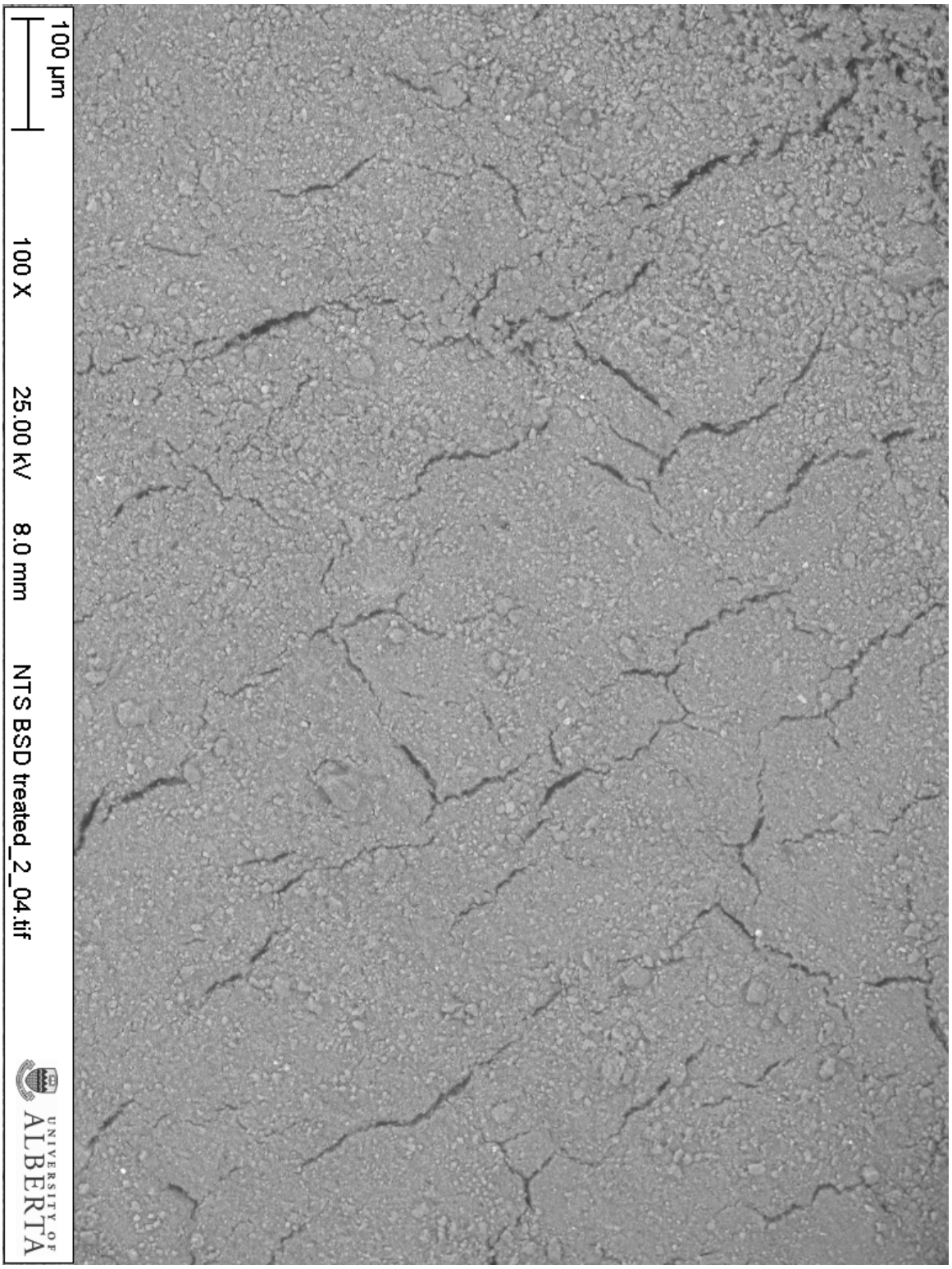

Figure 4.14: eSEM image of the shear plane of a 0.1 M treated Regina Clay sample at 100x magnification. Note the “rough” surface with rotund looking particles.

4.3 Quantifying the Effects and Assessing Potential Implications of GuCl Treatment

4.3.1 Liquid Limit Testing and Free Swell Testing

Figure 4.15 shows the results of the liquid limit testing of the four natural soils when hydrated with GuCl. An additional test using KCl was performed on Regina Clay to compare the effects of the two salts. The baseline of all the soils was established using a synthetic porewater solution. The liquid limits shown below have been corrected for dried salt content within the samples as per the methodology discussed in Helle et al. (2016).

The initial 7% increase of the liquid limit of Regina Clay when tested with low concentrations of GuCl was unexpected. Typically, soils with a high montmorillonite content undergo rapid decrease in their liquid limit with increasing electrolyte concentration (Anson & Hawkins, 1998; Maio, et al., 2004; Maio, 1996; Moore, 1991). The initial increase in the liquid limit may be a result of alterations to the clay fabric. It is possible that domain formation occurred and large intragranular pore spaces inside of these domains trapped more water (Van Olphen, 1977). While this hypothesis is admittedly conjectural, it is consistent with the differing clay fabrics observed in Figures 4.11 and 4.12. A similar finding was made by Helle, et al. (2017) when treating quick clays with KCl.

Similar to GuCl, there was also an initial increase in the liquid limit for the Regina Clay when using KCl as the wetting fluid. This initial increase was much smaller for the KCl solution. It is hypothesized that there are less changes to the soil's fabric upon KCl treatment due to the lower exchange affinity for K^+ ions. Regardless of the wetting fluid used for Regina Clay, an exponential decrease in the liquid limit occurred at concentrations above 0.1 M. This decrease is attributed to rapid coagulation of the clay particles as the DDL collapses (Van Olphen, 1977).

The other three natural soils showed more predictable behaviours when hydrated with GuCl solutions. Consistent with its low montmorillonite content, Whitecourt Clay showed a small decrease in liquid limit with increasing concentration. Both tills (Battleford and Floral tills) showed an initial increase in liquid limit with increasing concentration, which was consistent with their low clay contents and relatively high kaolinite contents (Sridharan & Prakash, 1999). Sridharan & Prakash showed that the sediment volume of kaolinite increases with increasing salt

content due to an increase in shearing resistance at interparticle contact points. This increase in sediment volume promotes the formation of a structure similar to that hypothesized for Regina Clay when wetted with dilute GuCl solutions. The larger intergranular pore spaces facilitate both tills' ability to hold more water.

The slopes of the liquid limit vs concentration curves reached a constant slope for all four soils at high concentrations. This consistent slope is consistent with other researchers' liquid limit tests that investigated the effects of porewater salinity (Anson & Hawkins, 1998; Maio, et al., 2004; Maio, 1996; Moore, 1991). At high concentrations, the clay fabric is dominated by face-to-face aggregation of particles. In this state, the only reduction in liquid limit is due to further suppression of the DDL.

The results from the free swell testing are presented in Table 4.3. There were negligible differences in the swell indices across a one order of magnitude increase in solution molarity. However, the GuCl solution did produce the smallest swell index at each concentration tested.

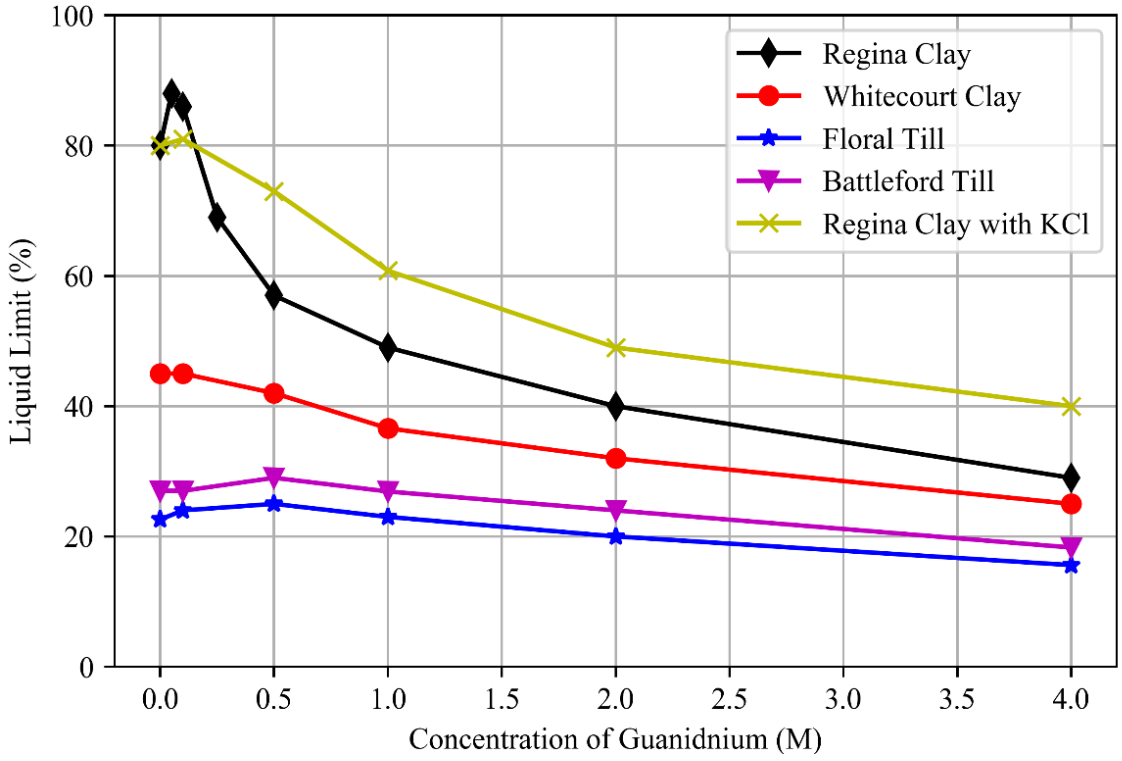

Figure 4.15: Liquid limit test results for the four natural soils when GuCl solutions were used as the wetting fluid. Regina Clay was also tested using a KCl solution to compare the effects of KCl to GuCl.

Table 4.3: Insitu Porewater Major Ion Compositions

	Free Swell (mL / 10 g)			
Concentration of Solution (M)	**$CaCl_2$**	**NaCl**	**KCl**	**GuCl**
0.05	18.5	20	19	18.5
0.1	18.5	19.5	18	17
0.5	19	19.5	17	15

4.3.2 Ring Shear Testing

The residual failure envelopes of Regina Clay tested with DDI water, synthetic porewater, and a 0.1 M GuCl solution are shown in Figure 4.16. Previous research has discussed whether the use of a cohesion intercept for representing the residual shear strength of a montmorillic soil is appropriate (Anson & Hawkins, 1998; Chandler & Skempton, 1974; Mesri & Abdel-Ghaffar 1995; Sridharan, Anson, & Hawkins, 2002). In a discussion of the 1998 paper by Anson & Hawkins, Sridharan cautioned the use of a residual cohesion intercept for soils with high montmorillonite contents. The shear and volume change behaviours of montmorillonite are believed to be entirely controlled by repulsive forces in the DDL, rendering interparticle friction and attractive forces negligible (Sridharan & Venkatappa Rao, 1979). Therefore, cohesion is not believed to exist between montmorillonite particles. The opposite is true for kaolinite, where interparticle friction and attractive forces dominate the soil's macroscopic behaviour.

However, the eSEM images in Section 4.2.3 showed a change in soil fabric along the sheared surface of Regina Clay samples, post-treatment. The evidence from the SEM images suggested domain formation among clay particles. These two findings and the assumption that the DDLs surrounding Regina Clay particles are insufficiently established (due to particle domain development) likely supports a situation where interparticle friction and attractive forces affect the shear and volume change behaviours of the clayey soil (Barbour 1987; Kjellander et al., 1990; Mesri & Olson 1971; Schanz & Tripathy, 2009; Tripathy et al., 2004). In light of these considerations, the residual failure envelopes in Figure 4.16 have been fit with cohesion

intercepts. Regardless of the suitability of using a cohesion intercept on a plot displaying residual shear strengths, Figure 4.16 is intended to demonstrate the increases in shear strength as a result of different porewater compositions.

The residual shearing resistance (ϕ_r, c') increased from 4.3°, 2.5 kPa for samples tested with DDI to 8.5°, c' = 8.2 kPa for 0.1 M GuCl treated samples that were flushed with synthetic porewater. Samples tested in a bath of synthetic porewater had marginally higher shear strengths (ϕ_r = 5.0°, 2.5 kPa) than those tested in DDI water.

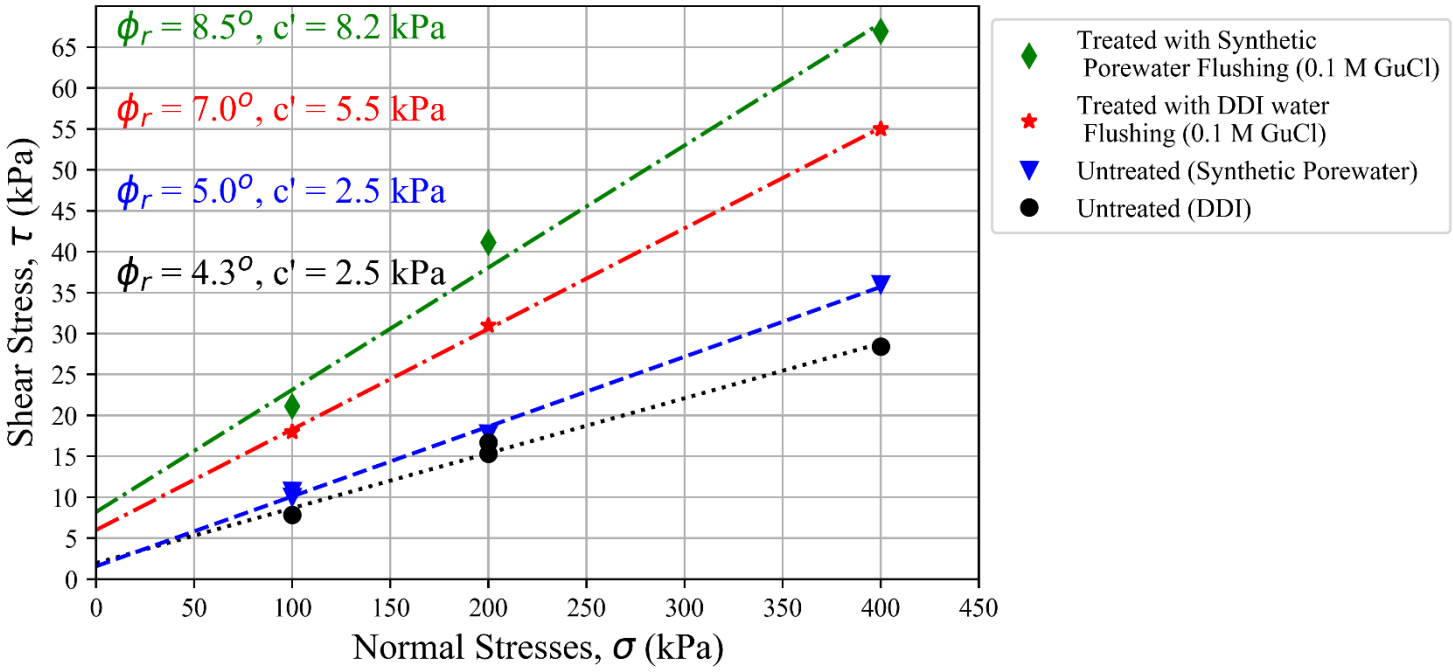

Figure 4.16 Residual failure envelopes of Regina Clay determined using DDI water, a synthetic porewater solution, and a 0.1 M GuCl solution.

The residual shear strength (τ) for the sample initially hydrated (and flushed) with synthetic porewater was consistently higher than the initially hydrated with DDI water. The divalent cations in the synthetic porewater solution likely produced a more domain-oriented structure than samples tested in DDI water. Upon GuCl treatment, the displacement of these pre-existing cations further suppressed the DDL, causing a higher final (treated) shear strength. Despite the higher net shear strength, the relative increase in shear strength following guanidinium treatment remained the same.

The permanence of guanidinium treatments is a fundamental question in assessing the feasibility of this insitu soil strengthening technique. Strong evidence of the durability of the GDN^+ ion was shown in the XRD analysis. However, the need to investigate the treatment's permanence using a more conventional geotechnical test remained. Thus, two ring shear experiments were conducted with the methodology outlined in Section 3.3.1.

Figures 4.17 and 4.18 show the increase in ϕr for samples initially hydrated with DDI water and a synthetic porewater solution, respectively. Both GuCl treatments were applied at the 100 kPa load step. The green highlighting in each figure indicates when the GuCl solution was introduced to the sample, and the portion of the test at which a 0.1 M GuCl bath was maintained.

The test conducted using DDI water as the initial wetting fluid was run longer than the test using the synthetic porewater solution, because the re-exposure of non-saline water (after 150 mm of displacement) was done in 30 mL increments with a peristaltic pump. The intention of slowly adding the synthetic porewater solution was to simulate groundwater flushing, as opposed to invoking an instant change in diffusion gradients between the DDL and the free porewater solution. The synthetic porewater solution was added over the course of one month.

As discussed in Section 3.3.1, the EC of the system was monitored in real-time. The ring shear test was continued until the steady-state EC of the bath was approximately equal to the EC of DDI water. The 300 mm of displacement shown in Figure 4.17 is equivalent to 70 days. The bath surrounding the sample reached steady-state (near zero EC) conditions after approximately 50 mm of displacement post treatment. It is clear from Figure 4.17 that, after an additional 100 mm of displacement, the residual shear strength of the sample remains unaltered, indicating that the effects of GuCl treatment are permanent.

Similar results under comparable testing conditions were observed by Maio (1996) for $CaCl_2$ and KCl treatments. In a discussion of her paper, Maio proposed that the "permanence" of the effects of these saline solutions were not "permanent", but rather that the irreversibility of $CaCl_2$ and KCl treatments are subjective to testing conditions. Maio confirmed her hypothesis by subjecting KCl and $CaCl_2$ treated samples to a saturated NaCl solution, followed by DDI water. Re-

exposure of the sample to DDI water invoked swelling that was consistent with untreated samples. These results were interpreted to mean that the exchange sites were replaced by Na^+ ions due to the high concentration gradient induced by the saturated NaCl solution. A Na^+ concentration of this magnitude would never naturally occur in groundwater, so it was assumed that – under naturally occurring circumstances – $CaCl_2$ and K^+ fixation was indeed permanent.

The aforementioned discussion necessitated verification that the insitu porewater composition of Regina Clay was indeed unable to reverse the effects of GuCl treatment. The results from Figure 4.18 indicate that the effects of the GDN^+ ion are permanent for natural conditions, as the residual shear strength does not change upon re-exposure to the synthetic porewater solution. Re-exposure of the synthetic porewater solution was done by instantaneous, complete removal of the GuCl bath. The bath was continually refreshed with the synthetic porewater solution until the EC of the bath reached state-state conditions. Re-exposure by this method significantly shortened the testing period in comparison to the slow leaching performed with the DDI water and didn't appear to affect the permanence of the treatment.

The increase in shear strength for both the DDI water and synthetic porewater cases was approximately 100%. Based on these two tests, there are no indications that GuCl treatment is not a permanent insitu strengthening technique for natural soils under natural conditions.

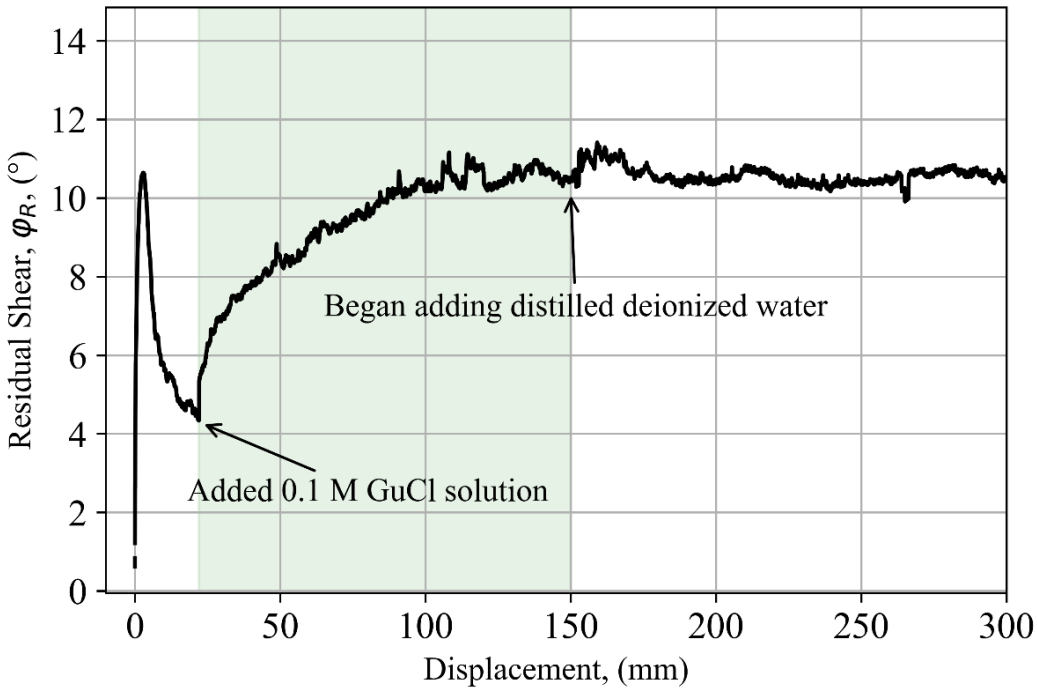

Figure 4.17: Evaluating the permanence of GuCl treatment for Regina Clay with DDI water as the initial wetting fluid.

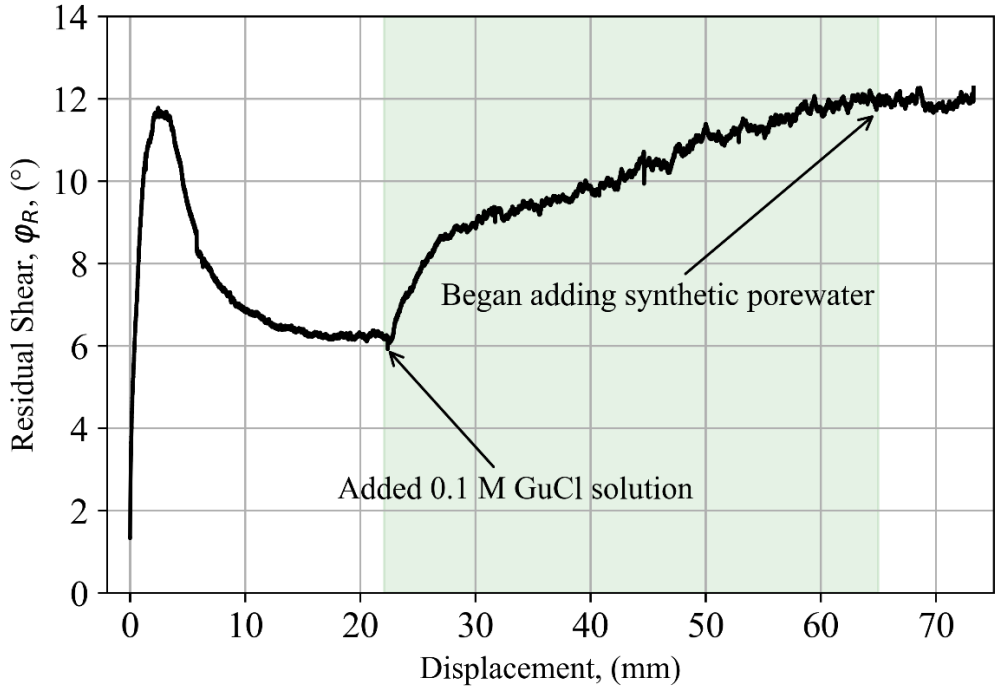

Figure 4.18: Evaluating the permanence of GuCl treatment for Regina Clay with a synthetic porewater solution as the initial wetting fluid.

4.3.3 Oedometer Testing

4.3.3.1 Permeability

The results of the oedometric testing that evaluated changes in permeability and stiffness are shown in Figures 4.19, 4.20, 4.21, and 4.22. Permeability testing was limited to comparisons between untreated (tested in synthetic porewater) and 0.1 M GuCl treated samples. Due to the decrease in liquid limit induced by higher concentrations of GuCl salts, oedometer samples could not be prepared at the same initial water contents as a sample prepared with a synthetic porewater solution. Furthermore, it has been well established that the permeability of montmorillic soils will increase with increasing porewater salinity (Jo et al., 2004; Jo, et al., 2005; Osicki, et al., 2008; Petrov & Rowe, 1997). The permeability of Regina Clay increased by approximately half an order of magnitude upon GuCl treatment. The increase in permeability was maintained at stresses that approached 1 MPa. These results were consistent with the findings of (Minder et al., 2016).

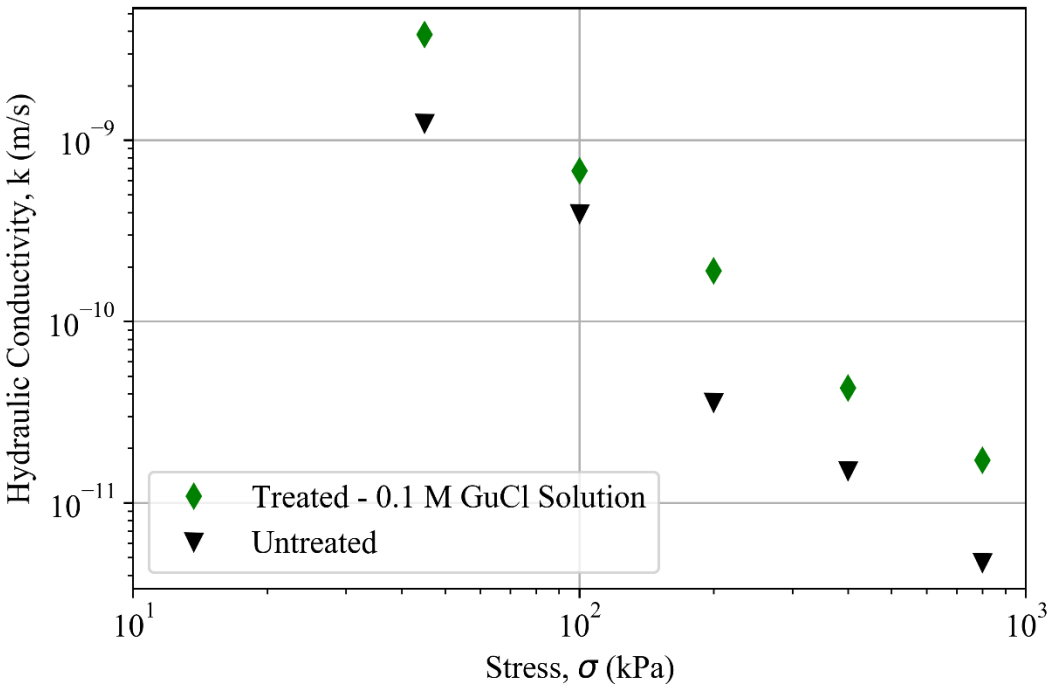

Figure 4.19: The hydraulic conductivity of 0.1 M GuCl treated Regina Clay remains approximately half an order of magnitude larger across load steps to 800 kPa.

4.3.3.2 Stiffness

Figure 4.20 plots the normal stress against volumetric strain for three different Regina Clay samples, each prepared with different wetting fluids. The normal consolidation lines (NCL) of the untreated and treated samples plot nearly on top of each other. The similarity in the NCLs among samples coincides with a negligible change in stiffness.

It was expected that there would be some change in the slope of the NCL between untreated and GuCl treated samples, due to the changes in soil fabric that are evident in the SEM images in Section 4.2.3. However, there was no change in the NCL, but rather there was a slight reduction in the recompression index and hysteresis associated with unload and reload steps. Table 4.4 shows the Lambda and Kappa values for each respective sample. These results are in agreement with consolidation testing performed on a Ca^{2+} montmorillonite by Mesri & Olson (1971). Mesri & Olson also found that the stiffness of Na^{+} montmorillonites was more dependent on porewater salinity than Ca^{2+} montmorillonite. They attributed the differences between the two types of montmorillonites to be a symptom of the clay fabric. They proposed that the clay particles in Ca^{2+} treated montmorillonites form domains, minimizing DDL effects. Based on the oedometric similarities and SEM images, it would appear that GDN^{+} treated montmorillonites undergo the same domain formation process.

Table 4.4: Stiffness Parameters Obtained from Oedometric Testing

Concentration of Solution (M)	λ	κ
0.00	0.017	0.0025
0.05	0.016	0.0017
0.25	0.016	0.0009

Samples that were subjected to osmotic consolidation were also evaluated for changes in stiffness. Figures 4.21 and 4.22 show semi log plots of void ratio (e) versus effective stress (σ) for samples that had their pore fluid switched to a GuCl bath at 45 kPa and 100 kPa, respectively.

As shown by the curves, the slope of the of the NCL changes following the change in pore fluid, suggesting a change in fabric. Subsequent loading shows that the slope of the NCL, post

treatment, attempts to resume its slope from pre-treatment. However, close inspection of these two slopes revealed that the NCL post treatment remains approximately 17% lower than the slope of the NCL prior to GuCl exposure. This minor increase in stiffness was deemed negligible, but the reduction in compressibility due to a change in soil fabric for a constant normal stress following treatment appears to be indicative of artificial aging.

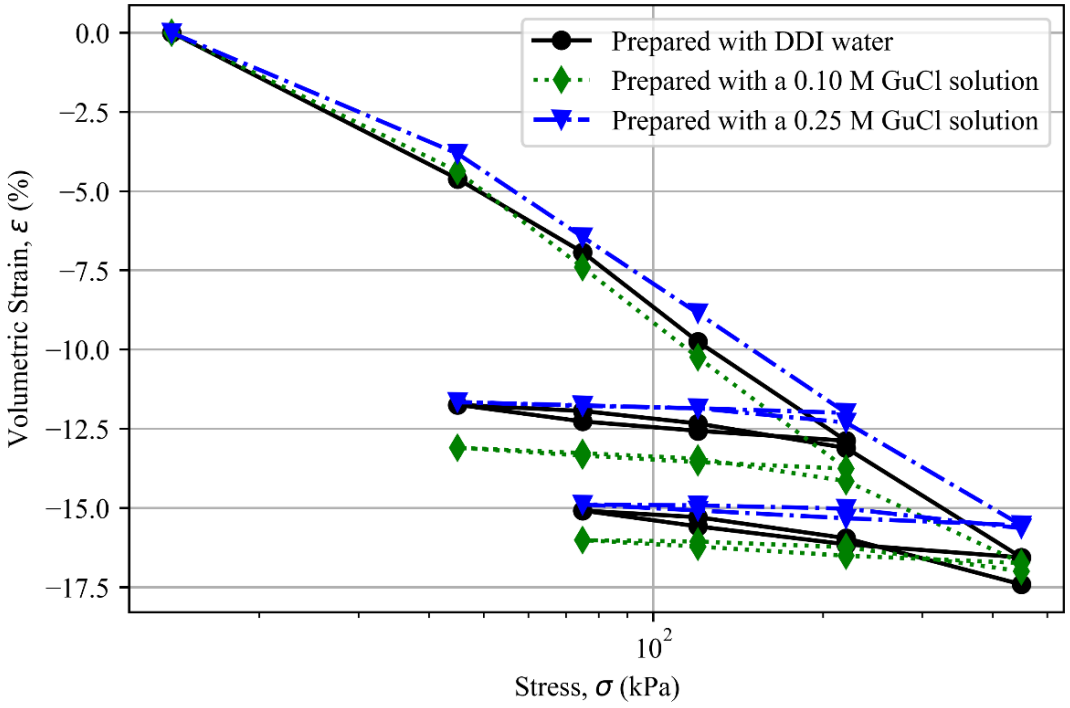

Figure 4.20: A comparison of oedometric stiffness between untreated and treated Regina Clay samples.

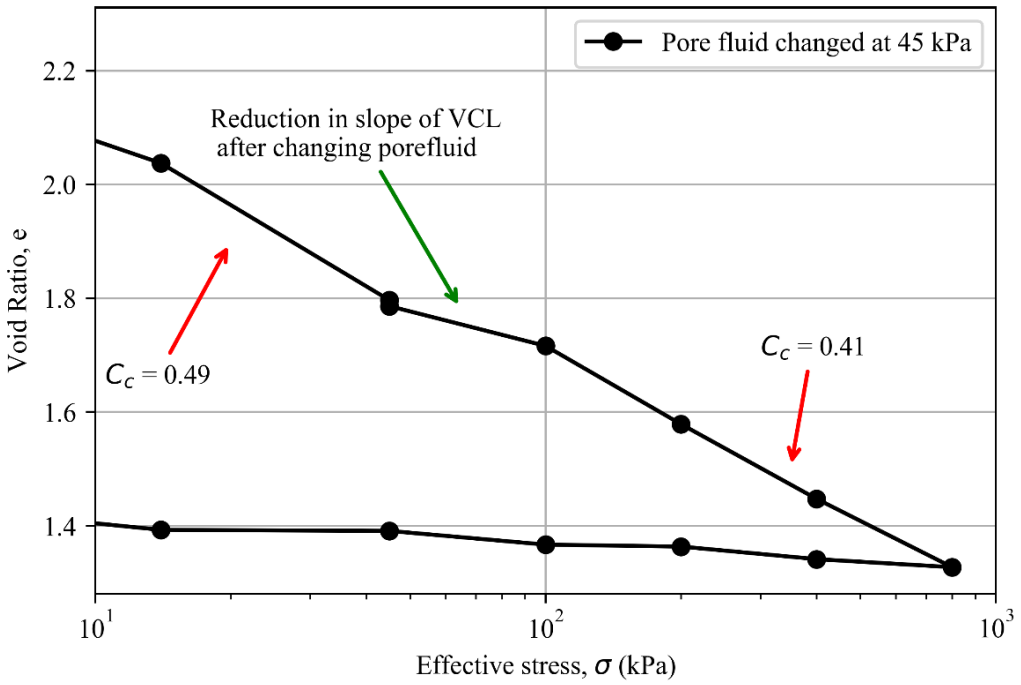

Figure 4.21: Semi-log plot of void ratio versus effective stress for RC1 (GuCl introduced at 45 kPa).

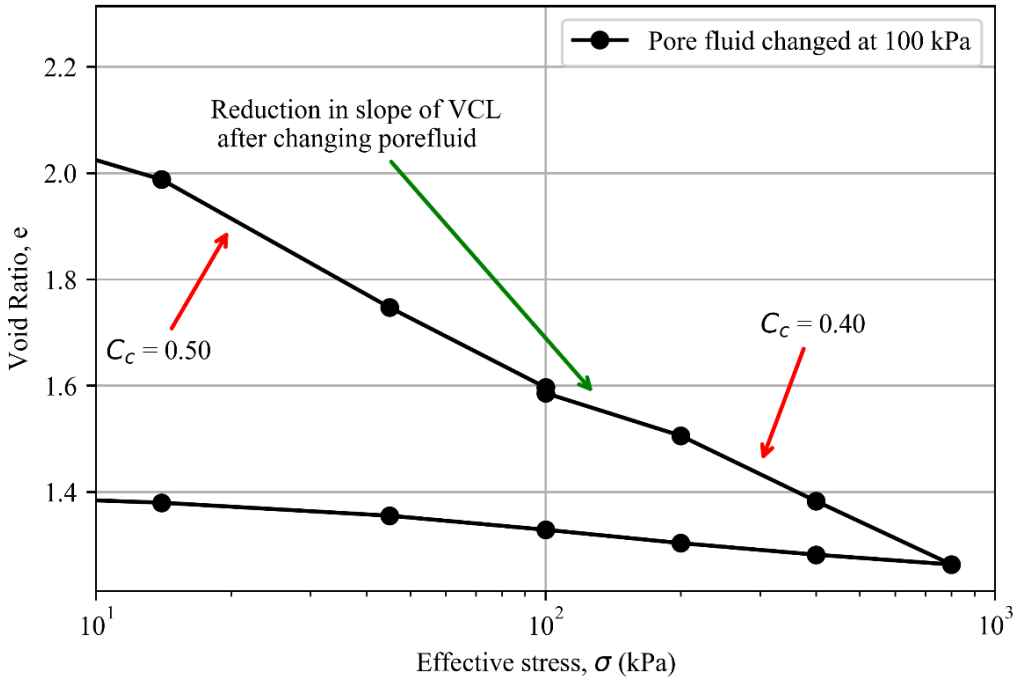

Figure 4.22**:** Semi-log plot of void ratio versus effective stress for RC2 (GuCl introduced at 100 kPa).

4.3.3.3 Osmotic Consolidation

Osmotic consolidation testing, as proposed by Barbour (1987), was performed on multiple Regina Clay samples. The intent of this thesis was to investigate an insitu strengthening technique for smectitic soils, with an emphasis on residual shear strength. Since prior testing had shown significant increases in the residual shear strength of Regina Clay after exposure to concentrations of GuCl solutions as low as 0.1 M, osmotic consolidation testing was limited to this concentration. Displacement versus time plots are given in Figures 4.21 to 4.24. Each figure represents a different sample, at a different load step. As described in Section 3.3.4.2, the bath surrounding the sample was spiked with a 0.1 M GuCl solution, indicated by the green line at the tail end of each curve. For ease of reference, RC1, RC2, RC3, and RC4 will reference soils that were introduced to GuCl at load steps of 45 kPa, 100 kPa, 200 kPa, and 400 kPa, respectively. Before adding the GuCl solution, time was permitted for the rate of secondary consolidation to be clearly established.

After correcting for secondary consolidation, the 45 kPa load step was the only mechanical normal stress tested where changes in volume due to osmotic consolidation was observed. The change in volume corresponded to a strain of less than 0.5%. For stresses greater than 45 kPa, the slope of the consolidation curve remained unaltered after exposure to a GuCl solution. The continuity of the compression slope indicates that there was no change in volume due to osmotic consolidation, or that the rate of creep exceeded that of the osmotic consolidation for these load increments. At field scale, the normal effective stress on the target soil formation is likely to exceed 45 kPa. Therefore, it is unlikely for any significant amount of volume change to occur in Regina Clay due to the introduction of a 0.1 M GuCl solution. Although there were no measurable changes in volume in this testing program, the samples tested were only two centimetres thick. Thicker deposits of smectite rich clay may experience a minor reduction in volume, and full-scale testing is recommended to investigate this possibility.

Figure 4.27 shows a semi-log plot of void ratio (e) versus mechanically applied stress (σ_m) for RC1. There are two points at σ_m = 45 kPa; these points correspond to the changes in void ratio at the end of mechanical primary consolidation (in black) and osmotic consolidation (in green). The

displacement used to determine the point representative of the end of osmotic consolidation was corrected to account for secondary consolidation.

Barbour's method (1987) proposed that by generating the e versus log(σ) plot and comparing the void ratios for a constant mechanically applied stress before and after changes in a porewater regime, you may assess the change in true effective stress. This evaluation process is shown by the arrows in the zoomed inset plot on Figure 4.27. Following the change in void ratio straight down to the point where osmotic consolidation stopped and drawing an orthogonal line tangent to the NCL yields a change in stress of approximately 3.5 kPa. Since there was no change in mechanically applied stress, reduction in void ratio is attributed to a change in the R-A stress state variable.

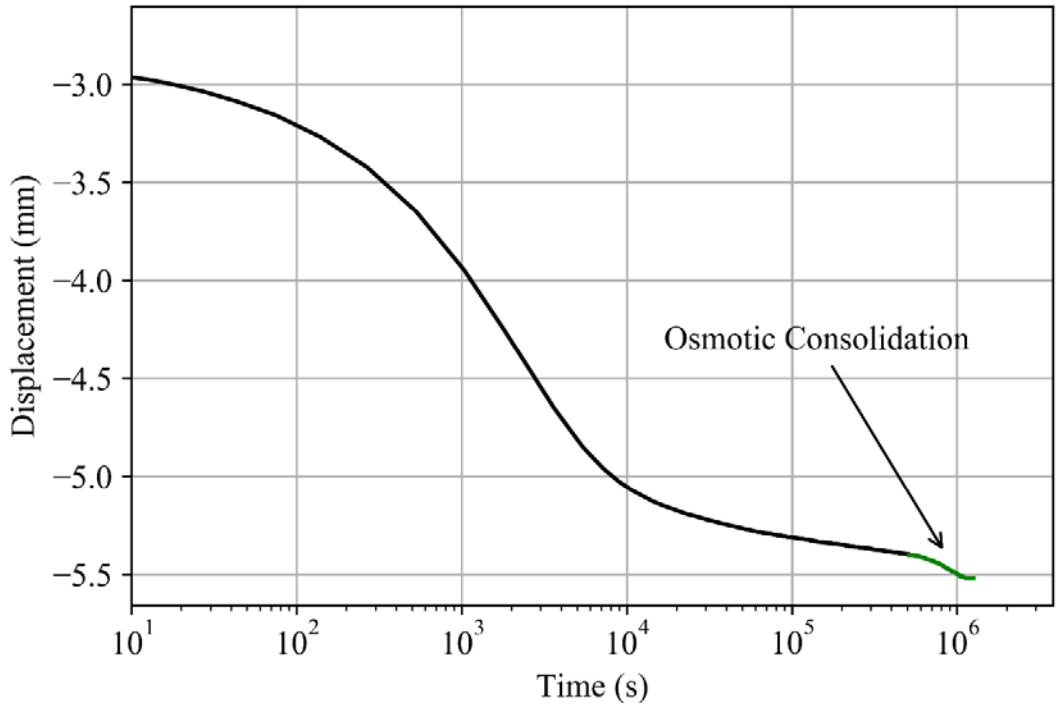

Figure 4.23: Time versus displacement for RC1: Osmotic consolidation test at 45 kPa mechanical stress.

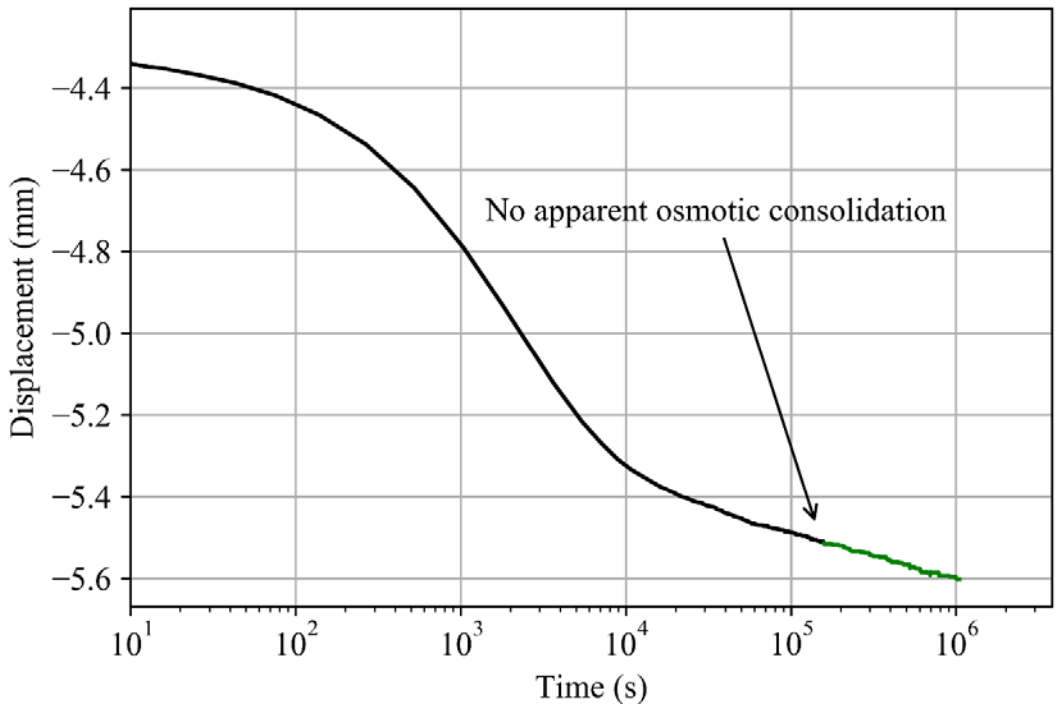

Figure 4.24: Time versus displacement for RC2: Osmotic consolidation test at 100 kPa mechanical stress.

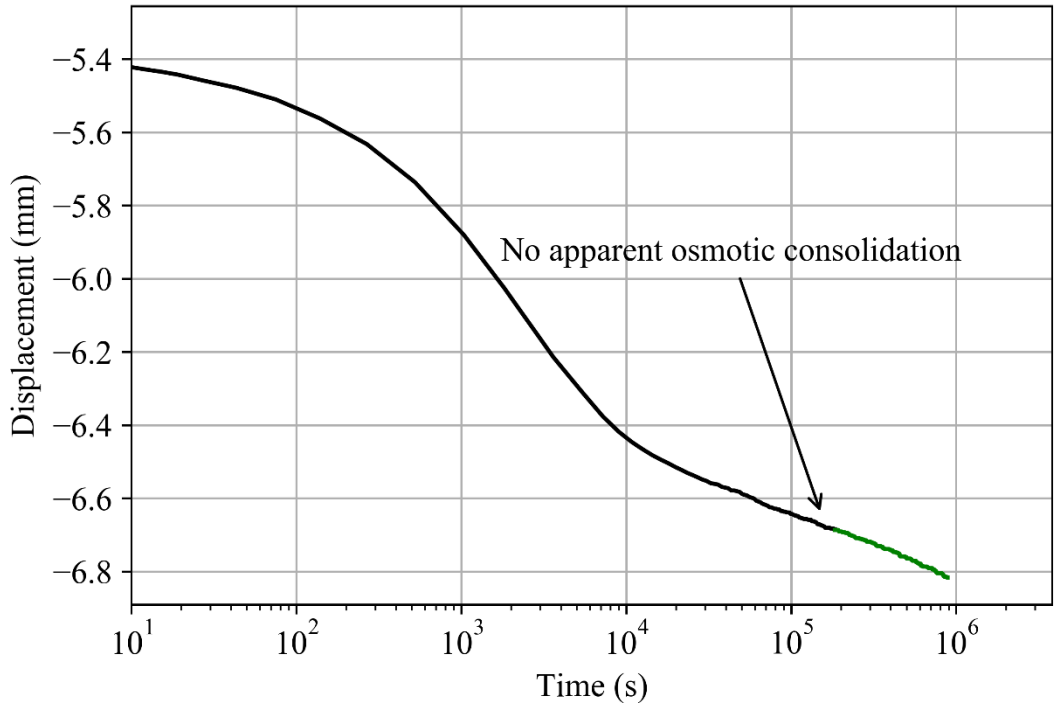

Figure 4.25: Time versus displacement for RC3: Osmotic consolidation test at 200 kPa mechanical stress.

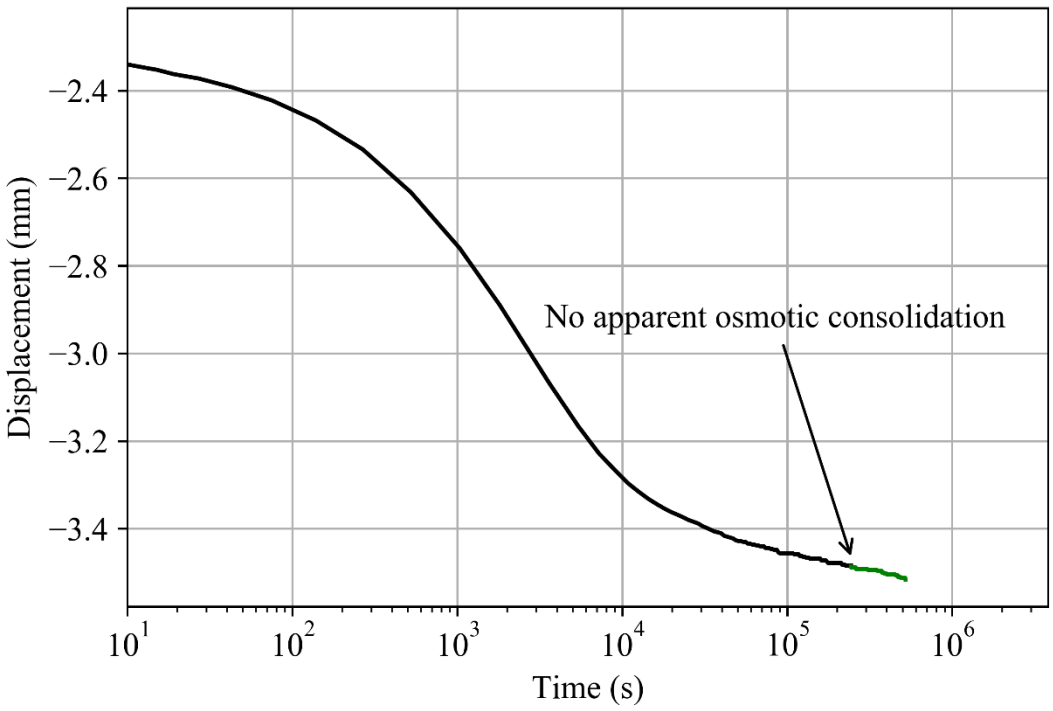

Figure 4.26: Time versus displacement for RC4: Osmotic consolidation test at 400 kPa mechanical stress.

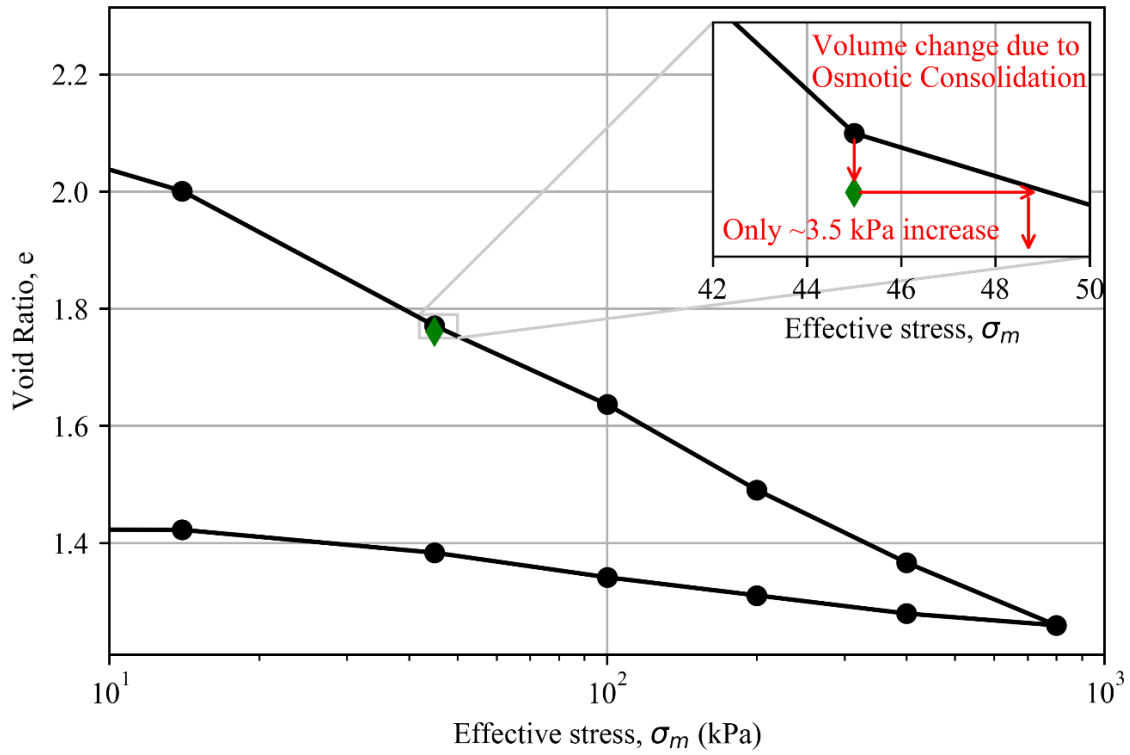

Figure 4.27: Indirect assessment of changes in the R-A stress state for a Regina Clay sample treated with a 0.1 M GuCl solution.

4.3.4 Comparing experimental and theoretical changes in R-A stresses for Regina Clay

Theoretical values of repulsive stresses for Regina Clay were determined using three different assumed specific surface areas (SSAs): 53, 100, and 150 m^2/g. The lower bound of 53 m^2/g was experimentally determined by Barbour (1987) while the other two SSAs used provide median and upper bound values These theoretical repulsive stresses are plotted against increasing normal stresses in Figure 4.28. The green line represents back-analyzed values of the R-A stress state variable (Equation 4.1) based upon the shearing resistances obtained from GuCl treated Regina Clay samples. The indirectly measured R-A values determined in Section 4.3.3.2 have been excluded from the plot because they do not show any change in repulsive forces above normal stresses of 45 kPa.

$$\frac{\tau_{unt}}{\sigma_m - R} - c' = \tan \emptyset'_{R(treated)} \qquad [4.1]$$

Where:

τ_{unt} = shear strength of untreated sample (kPa)

σ_{mech} = mechanically applied stress (kPa)

R = the change in the (R-A) stress state (kPa)

c' = the cohesion intercept of the treated sample (kPa)

$\emptyset'_{R(treated)}$ = angle of residual shearing resistance for a treated sample (°)

It is evident from a comparison of these four lines that there are large discrepancies between the theoretical and experimentally determined values. Although the theoretical repulsive stresses are highly dependent upon the assumed SSA (as shown by the blue, magenta, and red lines), no single value is capable of describing the behaviour of the back-analyzed repulsive stresses. Furthermore, the slopes of the theoretical lines are considerably flatter than that of the back-analyzed values. The difference in slopes between the lines suggests that osmotic pressure theory cannot properly account for changes in repulsive stresses for natural soil samples treated with guanidinium salts. Therefore, Figure 4.28 provides additional evidence that the increases in

residual shear strength shown by Regina Clay after GuCl treatment cannot be attributed solely to an increase in true effective stress.

Inconsistencies between the theoretical and indirectly determined *R* values were also reported by Barbour (1987). Barbour hypothesized that domain formation within Regina Clay prevented clay particles from parallel alignment, which is a requirement of Gouy-Chapman theory.

Since most natural montmorillonites are likely to exhibit some domain formation, the osmotic pressure theory is not relevant for determining their true effective stresses. As stated previously, domain formation has been shown to lead to incomplete DDL development, which limits the effect that the DDL has on the macroscopically observable behaviour of a montmorillonite (Kjellander, et al., 1990; Schanz & Tripathy, 2009; Tripathy, et al., 2004). Until a method for accurately assessing the R-A stress states of natural soils is founded, changes in volume and shear strength for these soils cannot solely be attributed to DDL behavior.

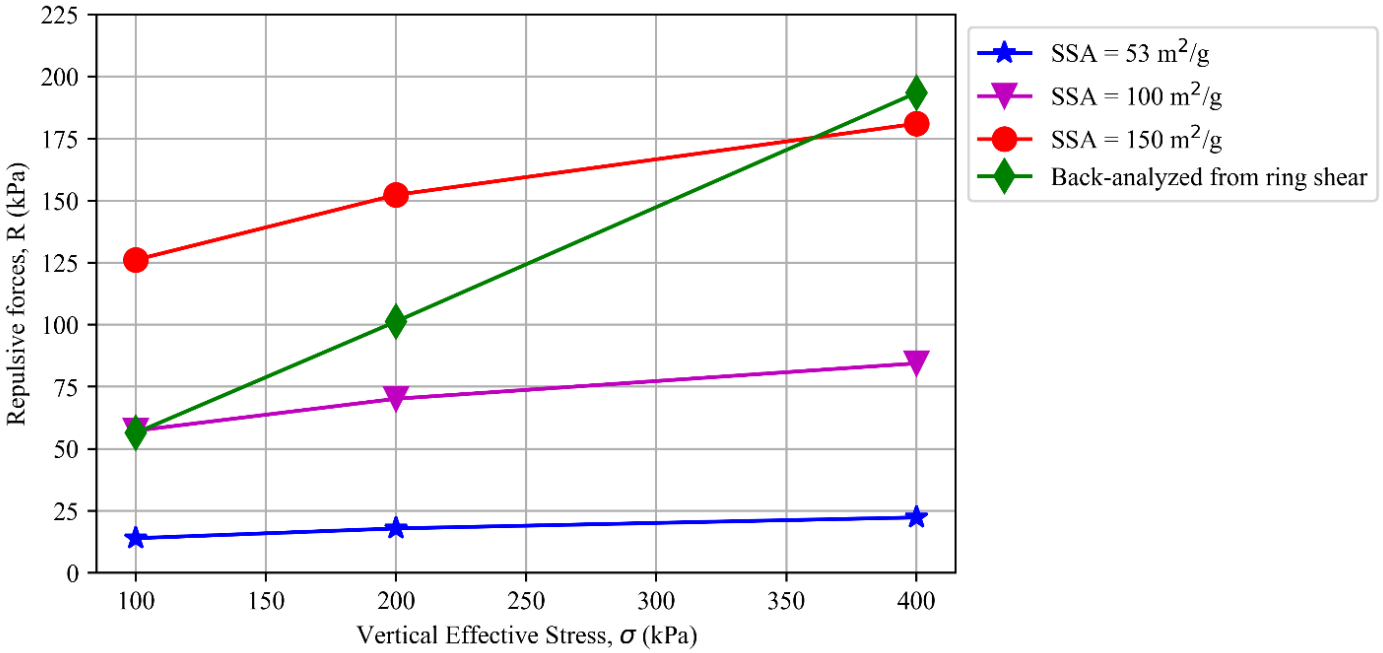

Figure 4.28: Comparison of repulsive stresses as predicted from osmotic pressure theory and back analyzed values from the ring shear testing.

The work presented in this thesis strongly supports the theory that increases in shear strength amongst GuCl treated montmorillonites are a *product* of interlayer collapse, DDL contraction, and subsequent alterations of the clay fabric. These three factors coalesce to interrupt the sliding

mechanism of shear associated with the montmorillonite mineral. The alteration of the shear mechanism in montmorillonites due to saline porewaters was hypothesized by Lupini et al. (1981) as a possible explanation for the results obtained by Kenney (1967). Lupini et al.'s statement appears to fit the current research, as it is believed that the mechanism of shear for Regina Clay shifts to a more transitional type of behaviour, resulting from larger effective particle sizes developing after GuCl treatment. Evidence for this statement has been provided by the eSEM, SEM, ring shear testing, and osmotic consolidation testing. The chemo-mechanical alteration in the shear mechanism of the soil appears to play a role in the demonstrated increase of the residual shear strength.

Chapter 5 Conclusion

5.1 Study Objectives

The goal of this research was to assess the feasibility of using guanidinium salts as a means of insitu strengthening for natural soils. This goal has been reached by completing two laboratory-scale objectives: 1) clearly identify the mechanism associated with guanidinium salt treatment at a mineralogical scale; and, 2) investigate and quantify potential implications that may be associated with full-scale use of this insitu strengthening technique.

Previous research investigating the use of the GDN^+ ion as an insitu strengthening technique has only been performed with synthetic clay products (Minder et al., 2016). Due to the complexity of ion exchange within natural soils, and the potential for interaction or competition of ions that exist in natural porewater, it seemed a prudent next step to investigate whether the findings of Minder et al. (2016) could be reproduced for natural soils.

5.2 Summary of Results from General Soil Characterisation

Regina Clay, Whitecourt Clay, Floral Till, and Battleford Till were the natural soils included in this study. Prior to investigating the effects of guanidinium salts, the baseline geotechnical and mineralogical properties of these four soils were determined. In addition to geotechnical characterization, synthetic porewater solutions were reverse engineered for all four soils.

Following this preliminary characterization, it was concluded that Regina Clay would be most heavily influenced by guanidinium treatments based on its high montmorillonite content, CEC, and activity. Several procedures that intended to assess the field-scale implications of guanidinium treatment required testing times in excess of two months, therefore due to time constraints, it was not feasible to perform these tests on all four soils. Due to Regina Clay's heightened sensitivity to guanidinium treatments, it was the only soil used in these testing procedures.

5.3 Summary of Results from Investigating the Mechanism

As previously stated, clearly defining the mechanism of guanidinium treatment for smectitic soils was one of two major focuses of this research. The following tasks were completed to fulfill this objective:

- Qualitative XRD;
- Batch ion exchange testing; and,
- SEM and eSEM.

The qualitative XRD analysis demonstrated a consistent collapse of the montmorillonite interlayer spacing for all four natural soils. The extent of interlayer collapse was determined to be independent of molar concentrations, within the range of 0.1 M to 1.0 M GuCl solutions. To assess the permanence of the interlayer collapse, several samples were re-exposed to a synthetic porewater solution that was representative of the soil's insitu groundwater. For all samples, re-exposure to their insitu groundwater did not produce any alterations in interlayer spacing. This observation indicates that the interlayer collapse could be considered permanent in naturally occurring conditions.

The batch ion exchange testing assessed the affinity and sorption efficiency of the guanidinium ion relative to a soil's CEC. Regina Clay was the only soil used in this testing procedure because it had the highest montmorillonite content. The sorption capacity and affinity were measured for GuCl solutions ranging from 0.1 to 0.5 M. The guanidinium ion proved capable of displacing divalent ions from bound water positions in a more efficient manner than other monovalent cations (Na^+ and K^+) and showed a sorption capacity of approximately 100% at concentrations of just 0.5 M.

High magnification SEM was performed on homo-ionized guanidinium Regina Clay samples to assess changes in soil fabric after being exposed to guanidinium salts. Images showed an increase in the average particle size and a higher degree of face-to-face aggregation (particle domain formation). The sheared surfaces of several Regina Clay samples were imaged in an eSEM to preserve moisture in the sample during imaging. Samples that were not subjected to GuCl treatments showed a high degree of particle orientation and slickensides. Images of treated

samples showed a much “rougher” shearing surface, with several rotund looking particles that indicated a change in clay fabric.

5.4 Summary of Quantified Effects and Assessment of Field-Scale Implications

The second objective of this research was to assess and quantify potential implications associated with full-scale use of this insitu soil strengthening technique. This objective was accomplished by completing the following tasks:

- Atterberg limit testing;
- Ring shear testing; and,
- Oedometric testing.

The Atterberg limit testing was performed using GuCl solutions across a wide range of concentrations to evaluate changes in plasticity. Regina Clay showed an initial increase in liquid limit at concentrations below 0.1 M. This finding was surprising but was attributed to macropores forming inside of the domains (evident in the SEM imaging). For concentrations in excess of 0.1 M, a rapid decline of the liquid limit occurred, as expected. The liquid limit test was repeated using a range of KCl solutions for Regina Clay, to observe whether the initial increase in liquid limit was consistent for a similar monovalent cationic solution. These results also showed an initial increase in the liquid limit. However, with increasing KCl concentration, the same lower bound liquid limit that was achieved using guanidinium salts could not be achieved. This finding supports the hypothesis that the guanidinium ion possesses a unique ability to displace other major cations due to its oddly shaped hydrated radius and that it is more effective in doing so than similar monovalent species (i.e., Na^+, K^+). The three other natural soils showed small initial increases in their liquid limits for concentrations below 0.5 M. Each small initial increased was followed by a gradual reduction for concentrations in excess of 0.5 M. Both of these observations were expected, as these three soils had low montmorillonite contents.

The ring shear testing consisted of several long-term tests intended to 1.) quantify increases in residual shear strength following treatment; and, 2.) assess the permanence of the insitu strengthening technique. The residual failure envelopes, categorized by the sample bath composition, in decreasing order were: 0.1 M GuCl (initially hydrated with synthetic porewater), 0.1 M GuCl (initially hydrated with DDI water), synthetic porewater, and DDI water. These tests

corresponded to residual failure envelopes of 8.5° (c’ = 8.2 kPa), 7.0° (c’ = 5.5 kPa), 5.0° (c’ = 2.5 kPa), and 4.3° (c’ = 2.5 kPa), respectively.

The difference in shear strength between the two treated samples can be attributed to the cations in the synthetic porewater solution. These cations would have caused a more aggregated structure prior to treatment (as shown by a comparison of the untreated samples), which likely magnified the effects of GuCl treatment. Based on these results, initially hydrating a sample with DDI water before GuCl treatment may serve as a conservative lower bound expectation for possible increases in shear strength.

The permanence of the GuCl treatment was confirmed by prolonged flushing of the sample bath with both DDI water and synthetic porewater. In both cases, the residual shear strength of the sample remained constant, even in the absence of a high salt content in the free porewater. This observation was a major finding, as the feasibility of this insitu strengthening technique relies on its permanence.

Oedometric testing evaluated changes in hydraulic conductivity, stiffness, and osmotic volume change. Regina Clay samples treated with a 0.1 M GuCl solution showed an increase in hydraulic conductivity of approximately half an order of magnitude for a variety of normal stresses approaching 1 MPa.

A comparison of the virgin compression index between samples initially hydrated in a synthetic porewater solution, 0.1 M GuCl solution, and 0.25 M GuCl solution demonstrated no loss in stiffness for the GuCl treated samples. However, samples that were initially hydrated in synthetic porewater prior to being leached with a 0.1 M GuCl solution showed a stiffer response and an apparent pre-consolidation pressure for the load step applied immediately after treatment. This observation was consistent with those made by Barbour (1987) and can likely be attributed to artificial aging. Subsequent loading caused the slope of the post-treatment NCL to converge upon the slope of the initial NCL; however, the NCL slope following treatment consistently remained 17% flatter. This 17% reduction in slope would normally be indicative of an increase in stiffness, but it was not considered to be significant given the magnitude of change.

Osmotic consolidation testing was performed in accordance with the method outlined by Barbour (1987) to 1.) assess the potential for volume change following GuCl treatment; and, 2.) indirectly assess changes in repulsive forces between clay particles. No volume change was measured for samples under normal stresses exceeding 45 kPa. A sample subjected to a 0.1 M GuCl solution at the 45 kPa load step (sample name: RC1) produced volumetric strains of less than 0.5%. Given that only small strains could be produced at extremely low normal stresses, it was concluded that for field-scale applications, no volume change will occur following GuCl treatment.

The change in repulsive stress was measured for Regina Clay samples subjected to GuCl solutions across a variety of load steps using Barbour's method (1987). As previously discussed, no volume change occurred for samples with a normal stress above 45 kPa. The lack of volume change is indicative of no change in the R-A stress state. For sample RC1, the change in volume corresponded to a 3.5 kPa change in the R-A stress state.

Using osmotic pressure theory, the repulsive forces between Regina Clay particles were determined in relation to Gouy Chapman theory (Barbour, 1987; Bolt, 1956; Sridharan & Jayadeva, 1983). The results of this analysis were sensitive to the assumed SSA of the soil; however, when comparing theoretical values to the indirectly measured values, and the back analyzed values measured from the ring shear testing, no agreement could be found. Furthermore, the slope of the line from the theoretical solution was vastly different than that of the back analyzed envelope.

The disconnection between the various methods used to calculate changes in the R-A stress state, coupled with the evidence from the SEM and eSEM, suggests that for the natural smectitic soil tested, the mechanism controlling the shear and volume change behaviours following GuCl treatment cannot be governed by DDL repulsion. There is strong evidence that suggests a chemo-mechanical alteration, stemming from a change in the clay fabric, contributes to the significant increase in shear strength following treatment. The overall mechanism governing the insitu treatment technique appears to be a combination of interlayer collapse, DDL contraction, and subsequent alterations of the clay fabric.

5.5 Future Research

The targeted problem for this insitu soil strengthening technique is slow-moving, deep seated landslides. The expansive nature and deep locations of the shear planes associated with these landslides make conventional geotechnical engineering solutions extremely difficult and expensive. The work presented in this thesis has shown that treating a natural, smectitic soil with guanidinium yields favourable engineering properties, such as a reduction in plasticity and increases in shear strength and permeability. Due to the difficult locations of these shear planes, the proposed delivery method of guanidinium treatment is via borehole. Figure 5.1 shows a conceptual drawing of how the insitu soil strengthening solution delivery may be implemented.

The technique requires a well characterized site with a defined shear plane location. Boreholes would be drilled to a sufficient depth such that they intersect with this shear plane. These boreholes would act as wells that are screened across various depths. The boreholes would be filled with a guanidinium solution, allowing the treatment process to occur via advection and diffusion. A low hydraulic conductivity is often associated with these types of highly plastic soils; therefore, diffusion is expected to dominate the delivery process. Success has been found using a similar technique to treat quick clay formations in Norway (Helle et al., 2016; Helle et al., 2017a, 2017b).

Future research should aim to complete field-scale trials of guanidinium treatment. The proof of concept for this treatment technique has been sufficiently developed in the laboratory via the work of Minder (2016), Pu (2017), and this thesis. Before this technique can be adopted as a viable treatment option, its effectiveness needs to be verified at full-scale.

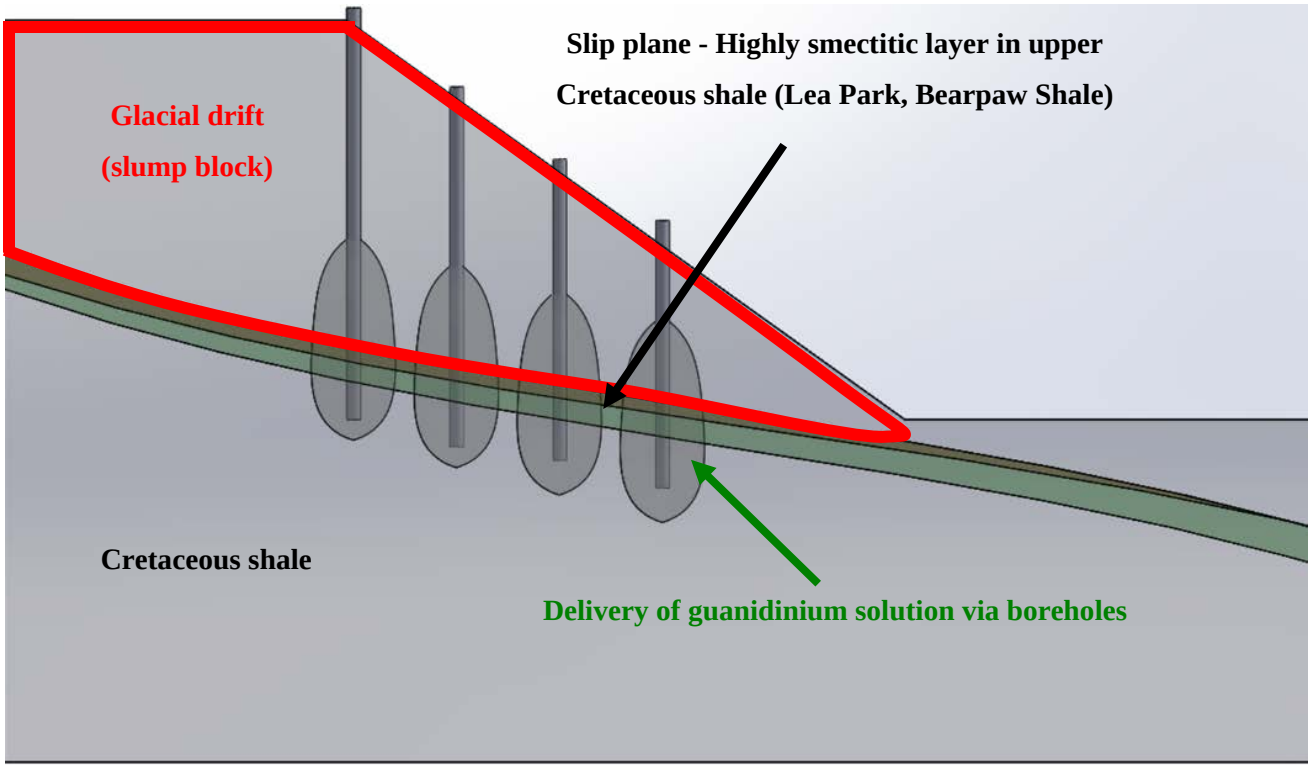

Figure 5.1: Conceptual image of the insitu soil strengthening technique.

References

Anson, R. W. W., & Hawkins, A. B. (1998). The effect of calcium ions in pore water on the residual shear strength of kaolinite and sodium montmorillonite. *Géotechnique*, *48*(6), 787–800.

Aylmore, L. A. G., & Quirk, J. P. (1959). Swelling of Clay-Water Systems. *Nature*, *183*, 1752–1753.

Balasubramonian, B. I. (1972). *Swelling of Compaction Shale*. University of Alberta.

Barbour, S. L. (1987). *Osmotic flow and volume change in clay soils*, 1–243.

Barbour, S. L., & Fredlund, D. G. (1989). Mechanisms of osmotic flow and volume change in clay soils. *Canadian Geotechnical Journal*, *26*(4), 551–562.

Benson, C. H., & Meer, S. R. (2009). Relative Abundance of Monovalent and Divalent Cations and the Impact of Desiccation on Geosynthetic Clay Liners. *Journal of Geotechnical and Environmental Engineering*, *135*(3), 349–358.

Bolt, G. H. (1956). Physico-chemical analysis of the compressibility of pure clays. *Geotechnique*, *6*(2), 86–93.

Bradley, W. F., Grim, R. E., & Clark, G. L. (1937). A Study of the Behavior of Montmorillonite upon Wetting, 216–222.

Brindley, G. W., & Brown, G. (1980). *Crystal structures of clay minerals and their X-ray identification* ([New ed.].). London: Mineralogical Society, Monograph 5.

Chandler, R. J., Skempton, A. W., & Muir Wood, A. M. (1975). The Design of Permanent Cutting Slopes in Stiff Fissured Clays. *Geotechnique*, *25*(2), 425–427.

Chapman, D. L. (1913). A contribution to the theory of electrocapillarity. *The London, Edinburgh, and Dublin Philosophical Magazine and Journal of Science*, *25*(148), 475–481.

Chatterji, P. K., & Morgenstern, N. R. (1990). Modified shear strength formulation for swelling clay soils. In *ASTM Special Technical Publication* (pp. 118–135).

Chattopadhyay, P. K. (1972). *Residual Shear Strength of Some Pure Clay Minerals*. Univsersity of Alberta.

Christiansen, E. A. (1971). Tills in Southern Saskatchewan, Canada. In *Till; a Symposium* (pp. 167–183). Ohio State Univ. Press, [Columbus].

Christiansen, E. A. (1983). The Denholm landslide, Saskatchewan. Part 1: geology. *Canadian Geotechnical Journal*, *20*(2), 197–207.

Cokca, E., & Birand, A. (1993). Determination of Cation Exchange Capacity of Clayey Soils by the methylene blue test. *Geo-Technical Testing Journal*, *16*(4), 518–524.

Cruden, D.M.,Varnes, D.J.,1996, Landslide Types and Processes, Transportation Research Board, U.S. National Academy of Sciences, Special Report, 247: 36-75

Di Maio, C. (1996). The influence of pore fluid composition on the residual shear strength of some natural clayey soils. *VII International Symposium on Landslides*.

Di Maio, C., Santoli, L., & Schiavone, P. (2004). Volume change behaviour of clays: The influence of mineral composition, pore fluid composition and stress state. *Mechanics of Materials*, *36*(5–6), 435–451.

Drever, J. I. (1973). The Preparation for X-ray of Oriented Specimens Clay Mineral Diffraction Analysis Peel Technique by a Filter-Membrane. *American Mineralogist*, *58*, 553–554.

Eckel, B. F., Sauer, E. K., & Christiansen, E. A. (1987). The Petrofka landslide, Saskatchewan. *Canadian Geotechnical Journal*, *24*(1), 81–99.

Eide Helle, T., Aagaard, ; Per, & Nordal, S. (2017). In Situ Improvement of Highly Sensitive Clays by Potassium Chloride Migration.

Fredlund, D. G. (1975). *Engineering properties of expansive clays*. Saskatoon, Sask.: Transportation and Geotechnical Group, Department of Civil Engineering, University of Saskatchewan.

Fredlund, D. G., & Morgenstern, N. R. (1976). Constitutive Relations for volume change in unsaturated soils. *Canadian Geotechnical Journal*, *13*(3), 261–276.

Gouy, M. (1910). Sur la constitution de la charge électrique à la surface d'un électrolyte. *J. Phys. Theor. Appl*, *9*(1).

Helle, T., Aagaard, P., & Nordal, S. (2017). In situ improvement of highly sensitive clays by potassium chloride migration. *Journal of Geotechnical and Geoenvironmental Engineering*, *143*(10).

Helle, T. E., Nordal, S., Aagaard, P., & Lied, O. K. (2016). Long-term effect of potassium chloride treatment on improving the soil behavior of highly sensitive clay — Ulvensplitten, Norway. *Canadian Geotechnical Journal*, *53*(3), 410–422.

K. U., & Ulrich, A. C. (2012). Evaluating methods for quantifying cation exchange in mildly calcareous sediments in Northern Alberta. *Applied Geochemistry*, *27*, 2511–2523.

Horn, H. M., & Deere, D. U. (1962). Frictional Characteristics of Minerals. *Géotechnique*, *12*(4), 319–335.

Jo, H. Y., Benson, C. H., & Edil, T. B. (2004). Hydraulic conductivity and cation exchange in

non-prehydrated and prehydrated bentonite permeated with weak inorganic salt solutions. *Clays and Clay Minerals*, *52*(6), 661–679.

Jo, H. Y., Benson, C. H., Shackelford, C. D., Lee, J. M., & Edil, T. B. (2005). Long-term hydraulic conductivity of a geosynthetic clay liner permeated with inorganic salt solutions. *Journal of Geotechnical and Geoenvironmental Engineering*, *131*(4), 405–417.

Jo, H. Y., Katsumi, T., Benson, C. H., & Edil, T. B. (2001). Hydraulic conductivity and swelling of nonprehydrated GCLS permeated with single-species salt solutions. *Journal of Geotechnical and geoenvironmetal Engineering*, *127*(7), 557–567.

Kaufhold, S. (2006). Comparison of methods for the determination of the layer charge density (LCD) of montmorillonites. *Applied Clay Science*, *34*(1–4), 14–21.

Kenney, T. C. (1967). The influence of mineral composition on the residual strength of natural soils. In *Geotechnical Conference, Oslo, 1967, Proceedings, Vol.1* (pp. 123–129).

Kjellander, R., Marčelja, S., Pashley, R. M., & Quirk, J. P. (1990). A theoretical and experimental study of forces between charged mica surfaces in aqueous cacl2 solutions. *The Journal of Chemical Physics*, *92*(7), 4399–4407.

Kolstad, D. C., Benson, C. H., & Edil, T. B. (2004). Hydraulic conductivity and swell of nonprehydrated geosynthetic clay liners permeated with multispecies inorganic solutions. *Journal of Geotechnical and Geoenvironmental Engineering*, *130*(12), 1236–1249.

Koumoto, T., & Houlsby, G. T. (2001). Theory and practice of the fall cone test. *Géotechnique*, *51*(8), 701–712.

Laird, D. A. (1987). *Layer charge and crystalline swelling of expanding 2:1 phyllosilicates*. Iowa State University.

Laird, D. A. (2006). Influence of layer charge on swelling of smectites. *Applied Clay Science*, *34*(1–4), 74–87.

Laird, D. A., & Shang, C. (1997). Relationship between cation exchange selectivity and crystalline swelling in expanding 2:1 phyllosilicates. *Clays and Clay Minerals*, *45*(5), 681–689.

Lambe, T. W. (1958). The Engineering Behaviour of Compacted Clay. *Journal of the Soil Mechanics and Foundations Division*, *84*(2), 1–35.

Lambe, T. W. (1960). A Mechanistic Picture of Shear Strength in Clay. In *Research Conference on Shear Strength of Cohesive Soils* (pp. 555–580). Boulder, Colorado.

Lupini, J. F., Skinner, A. E., & Vaughan, P. R. (1981). The drained residual strength of cohesive soils. *Géotechnique*, *31*(2), 181–213.

Mackenzie, R. C., & Mitchell, B. D. (1966). Clay mineralogy. *Earth-Science Reviews*, *2*, 47–91.

Maes, A., & Cremers, A. (1977). Charge Density Effects in Ion Exchange.

Maio, C. Di. (1996). Exposure of bentinite to salt solution: osmotic and mechnical effects. *Géotechnique*, *48*(3), 433–436.

Maio, C. Di, Hueckel, T., & Loret, B. (Eds.). (2002). *Chemo-Mechanical Coupling in Clays from Nano-Scale to Engineering Applications*.

Marcus, Y. (2012). The guanidinium ion. *Journal of Chemical Thermodynamics*, *48*, 70–74. Https://doi.org/10.1016/j.jct.2011.11.031

Marshall, C. E. (1949). *The colloid chemistry of the silicate minerals.* New York: Academic Press.

Mesri, G., & Abdel-Ghaffar, M. E. M. (1995). Cohesion intercept in effective stress-stability analysis. *Journal of Geotechnical Engineering*, *121*(1), 90–91.

Mesri, G., & Olson, R. E. (1971). Consolidation Characteristics of Montmorillonite. *Geotechnique*, *21*(4), 341–352.

Mesri, G., & Olson, R. E. (1971). Mechanisms Controlling the Permeability of Clays. *Clays and Clay Minerals*, *19*, 151–158.

Minder, P. (2016). *Applications of Chemical Modification of Smectite Clays in Geotechnical Problems*. ETH Zurich.

Minder, P., Puzrin, A. M., & Plötze, M. (2016). Enhanced delivery of chemical agents in soil improvement applications. *Géotechnique*, (6), 469–480.

Mitchell, J. K., & Soga, K. (2005). *Fundamentals of Soil Behavior*. *Soil Science Society of America Journal* (3rd ed..). Hoboken, N.J.: John Wiley & Sons. X

Mitchell, W. R. (1987). Microbial degradation of guanidinium ion. *Chemosphere*, *16*(5), 1071–1086.

Moore, M. D., & Reynolds, C. R. (1989). *X-ray diffraction and the identification and analysis of clay minerals*. Oxford [England] ; New York: Oxford University Press.

Moore, R. (1991). The chemical and mineralogical controls upon the residual strength of pure and natural clays. *Géotechnique*, *41*(1), 35–47.

Norrish, K. (1954a). Manner of Swelling of Montmorillonite. *Nature*, *173*(4397), 256–257.

Norrish, K. (1954b). Swelling of montmorillonite, *3861*(03), 3–7.

Norrish, K., Quirk, J. P., Geometry, R., & Analysis, G. (1954). Crystalline swelling of

montmorillonite: Use of electrolytes to control swelling. In *Nature* (Vol. 173, pp. 255–256).

Osicki, R., Fleming, I., & Haug, M. (2008). A Simple Compatibility Testing Protocol for Bentonite-Based Barrier Systems. In *Advances in Geosynthetic Clay Liner Technology: 2nd Symposium* (Vol. 1, pp. 31-31–10).

Petrov, R. J., & Rowe, R. K. (1997). Geosynthetic clay liner (GCL) - chemical compatibility by hydraulic conductivity testing and factors impacting its performance. *Canadian Geotechnical Journal*, *34*(6), 863–885.

Plötze, M., & Kahr, G. (2008). Diagnostic intercalation in clay minerals - use of Guanidine carbonate. In *Mineralogia Special Papers* (pp. 1896–2203). Warsaw.

Puppala, A. J., Pedarla, A., Pino, A., & Hoyos, L. R. (2017). Diffused Double-Layer Swell Prediction Model to Better Characterize Natural Expansive Clays. *Journal of Engineering Mechanics*, *143*(9), 04017069.

Ross, C. S. (1945). Minerals and Mineral Relationships of the Clay Minerals. *Journal of the American Ceramic Society*, *28*(7), 173–183.

Santamarina, J. C., Klein, K. A., Wang, Y. H., & Prencke, E. (2002). Specific surface: determination and relevance. *Canadian Geotechnical Journal*, *39*(1), 233–241.

Sauer, Karl, E. (1984). A landslide in clay shale in the north saskatchewan river valley, canada. *Engineering Geology*, *20*, 279–300.

Schanz, T., & Tripathy, S. (2009a). Swelling pressure of a divalent-rich bentonite: Diffuse double-layer theory revisited. *Water Resources Research*, *45*(2).

Schanz, T., & Tripathy, S. (2009b). Swelling pressure of a divalent-rich bentonite: Diffuse double-layer theory revisited. *Water Resources Research*, *45*(2), 1–9.

Shainberg, I. (2006). Charge Density and Na-K-Ca Exchange on Smectites1. *Clays and Clay Minerals*, *35*(1), 68–73.

Skempton, A. W. (1964). Long-Term Stability of Clay Slopes. *Géotechnique*, *14*(2), 77–102.

Skempton, A. W. (1985). Residual strength of clays in landslides, folded strata and the laboratory. *Géotechnique*, *35*(1), 3–18.

Sparks, D. L. (1999). Soil Physical Chemistry. In *Soil Physical Chemistry* (2nd ed., pp. 1–37). Boca Raton: CRC Press.

Sposito, G. (2004). *The surface chemistry of natural particles*. Oxford ; New York: Oxford University Press.

Sridharan, A. (1991). *Engineering Behaviour of Fine Grained Soils*. *Indian Geotechnical*

Journal (Vol. 21). Retrieved from http://www.iitg.ac.in/amurali/IGJ/IGS Annual Lectures/1990 Prof. A. Sridharan - IGS Annual Lecture.PDF

Sridharan, A., Anson, R. W. W., & Hawkins, A. B. (2002). Discussion: The effect of calcium ions in pore water on the residual shear strength of kaolinite and sodium montmorillonite. *Geotechnique*, *48*(5), 379–381.

Sridharan, A., & Jayadeva, M. S. (1983). Double layer theory and compressibility of clays. *Geotechnique*, *33*(4), 461–462.

Sridharan, A., & Prakash, K. (1999). Influence of clay mineralogy and pore-medium chemistry on clay sediment formation. *Canadian Geotechnical Journal*, *36*(5), 961–966.

Sridharan, A., & Rao, G. V. (1973). Mechanisms controlling volume change of saturated clays and the role of the effective stress concept. *Geotechnique, 23*(3), 359–382.

Sridharan, A., Rao, S., & Murthy, N. (1986). Compressibility behaviour of homoionized bentonites. *Geotechnique, 36*(4), 551–564. Https://doi.org/10.1680/geot.1987.37.4.533

Sridharan, A., & Venkatappa Rao, G. (1979). Shear strength behaviour of saturated clays and the role of the effective stress concept. *Geotechnique, 29*(2), 177–193.

Stern, O. (1924). Zur theorie der elektrolytischen doppelschicht. *Zeitschrift Für Elektrochemie Und Angewandte Physikalische Chemie*, *30*(21-22), 508–516.

Stul, M. S., & Cremers, A. (1979). *Layer charge-cation-exchange capacity relationships in montmorillonite*. *Clays and Clay Minerals* (Vol. 27).

Terzaghi, K. (1923). “Die Berechnungder Durchlassigkeitsziffer des Tones aus dem Verlauf der hydrodynamischen Spannungserscheinungen” (”Calculation of the porosity index of clay from hydrodynamic tension conditions“). *Mathematish-Naturwissenschaftliche*, 125–138.

Terzaghi, K., Peck, R. B., & Mesri, G. (1995). *Soil Mechanics in Engineering Practice*. John Wiley, New York, NY (United States).

Tiwari, B., Tuladhar, G. R., & Marui, H. (2005). Variation in Residual Shear Strength of the Soil with the Salinity of Pore Fluid. *Journal of Geotechnical and Geoenvironmental Engineering*, *131*(12), 1445–1456.

Tripathy, S., Sridharan, A., & Schanz, T. (2004). Swelling pressures of compacted bentonites from diffuse double layer theory. *Canadian Geotechnical Journal*, *41*(3), 437–450.

Van Olphen, H. (1977). *An Introduction to Clay Colloid Chemistry* (2nd Edition). New York: Wiley.

Yukselen, Y., & Kaya, A. (2008). Suitability of the methylene blue test for surface area, cation exchange capacity and swell potential determination of clayey soils. *Engineering Geology*,

APPENDIX SYNTHETIC POREWATER CONSTITUENTS

Table A.1**:** Regina Clay Synthetic Porewater Constituents

Proposed Chemicals	(mmol/L)	Molar Mass (g/mol)	Total Weight (g/L)
NaBr	0.014	102.894	0.001
$SrCl_2.6H_2O$	0.071	266.620	0.019
$CuSO_4.5H_2O$	0.014	249.680	0.003
K_2SO_4	0.014	174.259	0.002
$ZnSO_4.7H_2O$	0.123	287.560	0.035
$NaNO_3$	1.036	84.995	0.088
$NaHCO_3$	1.474	84.007	0.192
$CaCl_2.2H_2O$	0.661	147.010	0.097
Na_2SO_4	14.787	142.040	2.043
$MgSO_4$	20.435	120.366	2.460
$CaSO_4.2H_2O$	12.180	172.164	2.097

Table A.2: Whitecourt Clay Synthetic Porewater Constituents

Proposed Chemicals	(mmol/L)	Molar Mass (g/mol)	Total Weight (g/L)
$SrCl_2.6H_2O$	0.021	266.620	0.006
$NaHCO_3$	1.873	84.007	0.245
Na_2S0_4	2.286	142.040	0.250
$MgSO_4$	2.687	120.366	0.323
K_2SO_4	0.199	174.259	0.035
$CaCl_2.2H_2O$	0.160	147.010	0.024
$CaSO_4.2H_2O$	4.595	172.164	0.791

Table A.3: Floral Till Synthetic Porewater Constituents

Proposed Chemicals	(mmol/L)	Molar Mass (g/mol)	Total Weight (g/L)
NaBr	0.013	102.894	0.001
K_2SO_4	0.403	174.259	0.070
$MgSO_4$	14.071	120.366	1.694
$MnSO_4$. H_2O	0.009	169.020	0.002
$ZnSO_4$.7 H_2O	0.042	287.650	0.012
$SrCl_2$.6 H_2O	0.032	266.620	0.009
Na_3PO_4	0.033	163.940	0.006
$NaHCO_3$	1.932	84.007	0.302
$NaNO_3$	0.046	84.995	0.004
Na_2SO_4	3.571	142.040	0.389
$CaCl_2$	1.235	110.980	0.137
$CaSO_4$.2 H_2O	10.654	172.164	1.834

Table A.4: Battleford Till Synthetic Porewater Constituents

Proposed Chemicals	(mmol/L)	Molar Mass (g/mol)	Total Weight (g/L)
$SrCl_2.6H_2O$	0.008	266.620	0.002
$NaHCO_3$	2.059	84.007	0.293
$NaNO_3$	0.035	84.995	0.003
Na_2SO_4	0.658	142.040	0.000
K_2SO_4	0.132	174.259	0.023
$MgSO_4$	8.684	120.366	1.045
$CaCl_2.2H_2O$	1.399	147.010	0.206
$CaSO_4$.2 H_2O	2.760	172.164	0.475